

Aus dem Max-Planck-Institut für Kolloid- und Grenzflächenforschung
in Zusammenarbeit mit der Medizinischen Fakultät Charité – Universitätsmedizin Berlin

DISSERTATION

Protective potential and immunological evaluation
of synthetic *Plasmodium* GPI glycoconjugate vaccines
against experimental cerebral malaria

zur Erlangung des akademischen Grades

Doctor medicinae (Dr. med.)

vorgelegt der Medizinischen Fakultät

Charité – Universitätsmedizin Berlin

von

Fridolin Steinbeis

aus München

Datum der Promotion: 25.06.2017

This thesis was performed under the supervision of Professor Dr. Peter H. Seeberger and Professor Dr. Bernd Lepenies at the Max Planck Institute of Colloids and Interfaces at the Department of Biomolecular Systems and Professor Dr. Norbert Suttrop from Charité – Universitätsmedizin Berlin between November 2014 and November 2015.

Acknowledgements

I express my deepest gratitude to Prof. Dr. Peter Seeberger and Prof. Dr. Bernd Lepenies for their excellent support, their scientific guidance and supervision throughout the last year. I am especially grateful for the striking openness and the friendly reception of the Glycoimmunology group where I performed my Doctor medicinae (Dr. med.) at the Biomolecular Systems Department. I also want to thank Prof. Dr. med. Norbert Suttorp from Charité – Universitätsmedizin Berlin for providing help and supervising me within the last year.

I especially want to thank my colleagues and friends from the Glycoimmunology-, Vaccines- and GPI-group for their cordial welcome and the pleasant working environment, the scientific support and for plentiful fruitful discussions. I am especially grateful for the patient help from Timo Johannssen, who was a great mentor and valued support during the final experiments. I also want to thank Ankita Malik, Maurice Grube and Dr. Daniel Varón Silva for their hard and persistent work on the GPI synthesis and characterization. Further, I would like to thank Dr. Maria Antonietta Carillo, Dr. Benjamin Schumann, Dr. Sharavathi G. Parameswarappa and Dr. Clane L. Pereira for sharing their profound knowledge and performing GPI conjugation to CRM₁₉₇. I am also grateful for the support from Uwe Vogel and Annette Wahlbrink, the excellent care taking of the animals by Susanne Eisenschmidt and the great help and advice from Jonnel Anthony Jaurigue, Dr. Naeem Khan, Stephanie Zimmermann and Dr. Julia Hütter.

Finally, I devote my warmest thanks to my lovely companion Marie-Laure for her endless support, unconditional help and indispensable patience and to my marvelous daughter Emilia, for enriching my life with her cheerful nature.

Table of contents

Table of contents	4
List of abbreviations.....	7
Abstract	9
Zusammenfassung.....	11
1 Introduction.....	13
1.1 The immune system.....	13
1.1.1 Innate immunity	13
1.1.2 Adaptive immunity.....	14
1.1.3 Innate control of adaptive immunity	15
1.2 Malaria.....	15
1.2.1 Malaria epidemiology	16
1.2.2 Malaria pathogenesis.....	17
1.2.3 Cerebral malaria	18
1.2.4 Murine model of cerebral malaria.....	20
1.3 The role of glycosylphosphatidylinositol in malaria pathogenesis	20
1.4 Vaccines.....	22
1.4.1 Malaria eradication and the importance of anti-malarial vaccines	24
1.4.2 Carbohydrate-based vaccines	25
1.4.3 Synthetic GPI glycoconjugate vaccines	25
2 Aim	27
3 Materials and methods	29
3.1 Materials	29
3.1.1 Instruments	29
3.1.2 Consumables	30
3.1.3 Buffers and medium	31

3.1.4	Antibodies	32
3.1.4.1	Glycan array	32
3.1.4.2	Flow cytometry	32
3.1.4.3	ELISpot	33
3.1.4.4	Cytometric bead array	33
3.1.5	Kits, reagents and chemicals	34
3.1.6	GPI glycans	35
3.1.7	Mice and parasite strains	36
3.1.8	Software	36
3.2	Methods	36
3.2.1	Study design	36
3.2.2	GPI synthesis and conjugation	38
3.2.3	Animal experiments	39
3.2.4	Immunization	39
3.2.5	Serum collection.....	39
3.2.6	<i>Plasmodium berghei</i> ANKA stabilates	40
3.2.7	<i>Plasmodium berghei</i> ANKA infection	40
3.2.8	Parasitemia	40
3.2.9	Weight and score	40
3.2.10	Glycan array printing and development	41
3.2.11	Flow cytometry	42
3.2.12	ELISpot	43
3.2.13	Cytometric bead array	44
3.2.14	Statistical analysis	44
4	Results.....	45
4.1	GPI synthesis, conjugation to CRM ₁₉₇ and glycoconjugate characterization	45
4.2	Immunogenicity of GPI-CRM ₁₉₇ conjugates 1-6	48

4.3	Protection of GPI-CRM ₁₉₇ vaccinated mice from ECM	54
4.4	Vaccine-specific T cell response	58
4.5	Spleen cell composition.....	60
4.5.1	T cell frequency and activation	60
4.5.2	Regulatory T cells	60
4.5.3	Macrophage and dendritic cell frequency and cellular activation.....	61
4.6	Serum cytokine levels.....	61
4.7	Brain CD8 ⁺ T cell sequestration	66
5	Discussion	68
5.1	Immunogenicity.....	70
5.2	Immune cell modulation and cytokines.....	71
5.3	Brain CD8 ⁺ T cell sequestration.....	74
5.4	GPI structure-activity relationship.....	75
6	Conclusion	77
7	Bibliography	78
	Curriculum vitae.....	91
	Declaration of academic honesty	95

List of abbreviations

Ab	Antibody
AEC	3-amino-9-ethylcarbazole
APC	Allophycocyanin
CBB	Coomassie brilliant blue
CFA	Complete Freund's adjuvant
CLRs	C-type lectin receptors
CM	Cerebral malaria
CRM ₁₉₇	Cross-reacting material
CRM ₁₉₇ -Gal	Galactose-conjugated CRM ₁₉₇
DC	Dendritic cell
dH ₂ O	Deionized water
ECM	Experimental cerebral malaria
EDTA	Ethylenediaminetetraacetic acid
FCS	Fetal calf serum
FITC	Fluorescein isothiocyanate
GlcN	Glucosamine
GPI	Glycosylphosphatidylinositol
GPI1-6	GPI-CRM₁₉₇ glycoconjugate 1-6
GPI-Man ₃	GPI containing 3 mannoses
GPI-Man ₄	GPI containing 4 mannoses
GrB	Granzyme B
h	Hours
HRP	Horseradish peroxidase
i.p.	Intraperitoneal
ICAM-1	Intercellular adhesion molecule 1
IFN	Interferon
IL	Interleukin
IVC	Individually ventilated cage
JNK	c-Jun N-terminal kinases
KLH	Keyhole limpet hemocyanin
MALDI	Matrix-assisted laser desorption/ionization
MHC	Major histocompatibility complex
MyD88	Myeloid differentiation primary response gene 88
NF-κB	Nuclear factor kappa-light-chain-enhancer of activated B cells

NK cell	Natural killer cell
NKT cell	Natural killer T cell
NLRs	Nucleotide-binding oligomerization domain-like receptor
NO	Nitric oxide
p.i.	<i>Post</i> infection
p38	P38 mitogen-activated protein kinases
PAMP	Pathogen-associated molecular pattern
PbA	<i>Plasmodium berghei</i> ANKA
PBS	Phosphate buffered saline
PBS-T	PBS with Tween 20
PE	Phycoerythrin
PerCP	Peridinin chlorophyll
PEthN	Phosphoethanolamine
PfEMP-1	<i>Plasmodium falciparum</i> erythrocyte membrane protein 1
PI	Phosphoinositol
pRBC	<i>Plasmodium</i> infected red blood cells
PRR	Pattern recognition receptor
RLRs	Retinoid acid-inducible gene-1-like receptor
RPMI	Roswell Park Memorial Institute medium
RBC	Red blood cell
RT	Room temperature
SBAP	Succinimidyl 3-(bromoacetamido)propionate
SDS-PAGE	Sodium dodecyl sulfate polyacrylamide gel electrophoresis
sfu	Spot forming unit
SPF	Specific-pathogen-free
TCEP	Tris(2-carboxyethyl)phosphine
TCR	T cell receptor
TLR	Toll-like receptor
TNF	Tumor necrosis factor
T _{reg}	Regulatory T cells
Tris	Tris(hydroxymethyl)aminomethane
VCAM-1	Vascular cell adhesion molecule 1

Abstract

Background: Cerebral malaria is the most severe manifestation of *Plasmodium falciparum* malaria. Sensing of *Plasmodium*-specific pathogen-associated molecular patterns such as glycosylphosphatidylinositol (GPI) by the host pattern recognition receptors leads to the induction of pro-inflammatory pathways, and has been shown to be a major contributor to cerebral malaria pathogenesis. Carbohydrate-based vaccines have widely been applied and successfully prevented disease and death in recent decades. An antitoxic GPI glycoconjugate vaccine therefore represents a promising approach to preventing cerebral malaria pathogenesis.

Method: Six structurally distinct GPI glycans were synthesized and conjugated to CRM₁₉₇. GPI1 and GPI2 both containing Man₃-GlcN, with PEthN attached to GPI2; GPI3 and GPI4 core structures containing Man₄-GlcN, with PEthN attached to GPI4; and GPI5 (Man₃-GlcN) and GPI6 (Man₄-GlcN) both containing PEthN and PI. Glycoconjugates were tested for immunogenicity and efficacy in C57BL/6JRj mice susceptible to experimental cerebral malaria (ECM). Mice were immunized three times intraperitoneally at 14-day intervals and were finally challenged with 1x10⁶ erythrocytes infected with *P. berghei* ANKA (PbA). Serum samples were obtained before immunizations to determine anti-GPI antibody level. Prior to onset of ECM (day 6 *post* infection), 5 mice per group were sacrificed to investigate spleen cell composition, brain T cell sequestration and vaccine-specific T cell re-stimulation. The remaining 10 mice per group were used for survival studies.

Results: Mice immunized with GPI2, GPI4, GPI5 and GPI6 developed significantly increased anti-GPI antibodies compared to control mice. Only a slight increase was observed in mice immunized with GPI1 and GPI3. Control mice succumbed to experimental cerebral malaria in 100% of cases, whereas all GPI-CRM₁₉₇-immunized mice displayed an improved survival. In particular, GPI5-vaccinated mice were significantly protected against PbA-induced encephalopathy with 40% survival. Immunological characterization of spleen cell population and serum cytokines did not reveal significant differences between GPI-CRM₁₉₇-vaccinated groups. However, distinct trends were observed, with GPI5 showing decreased cellular activation and reduced levels of serum cytokines TNF- α , IFN- γ and IL-6.

Conclusion: In this study, the efficacy and immunogenicity of structurally distinct GPI glycoconjugate vaccines was investigated. For the first time, the approved non-toxic mutant of

diphtheria toxin CRM₁₉₇ and alum were applied in this glycoconjugate formulation. A structure-activity relationship of different synthetic GPIs with respect to immunogenicity by glycan array analysis was established. Further, the effectiveness of the GPI-antitoxic vaccine approach could be reproduced with a diminished pro-inflammatory immune response against *Plasmodium* GPI, preventing disease pathology and death in some of the glycoconjugates tested. In conclusion, this study adds to current evidence that a GPI-antitoxic vaccine provides protection against *Plasmodium* GPI-induced ECM.

Abbreviations: PEthN=phosphoethanolamine, GlcN=glucosamine, PI=phosphoinositol, Man₃=GPI structure containing a three-mannose chain, Man₄=GPI structure containing a four-mannose chain.

Zusammenfassung

Hintergrund: Die zerebrale Malaria gehört zu den schwersten Verlaufsformen der durch *Plasmodium falciparum* verursachten Malaria tropica. Die Erkennung von pathogen-assoziierten molekularen Mustern, wie beispielsweise parasitäres Glykosylphosphatidylinositol (GPI) durch Mustererkennungsrezeptoren, führt zur Induktion einer proinflammatorischen Reaktion des Wirtes. Dieser konnte eine entscheidende Rolle in der Pathogenese der zerebralen Malaria nachgewiesen werden. Kohlenhydrat-basierte Impfstoffe sind ein essentieller Bestandteil der aktuell zugelassenen Vakzine und spielen eine wichtige Rolle in der Prävention von Infektionskrankheiten. Ein antitoxischer GPI-Glykokonjugat-Impfstoff ist daher ein vielversprechender Ansatz zur Prävention der zerebralen Malaria.

Methode: Sechs strukturell verschiedene GPI-Glykane wurden synthetisiert und an CRM₁₉₇ konjugiert: GPI1 und GPI2 jeweils basierend auf Man₃-GlcN, mit PEthN zusätzlich an GPI2 gebunden; GPI3 und GPI4 basierend auf Man₄-GlcN, mit PEthN an GPI4 gebunden; sowie GPI5 (Man₃-GlcN) und GPI6 (Man₄-GlcN) jeweils mit PEthN und PI versehen. Alle Glykokonjugate wurden an für die experimentelle zerebrale Malaria (ECM) empfänglichen C57BL/6JRj Mäusen hinsichtlich Immunogenität und Wirksamkeit getestet. Die Immunisierung wurde intraperitoneal in 14-tägigen Abständen appliziert und den Versuchstieren anschließend 1×10^6 *P. berghei* ANKA (PbA) infizierte Erythrozyten injiziert. Serumproben wurden vor den Immunisierungen entnommen. 5 Mäuse wurden zur detaillierten Analyse von Milzzellpopulationen, zerebraler T-Zell-Sequestrierung und Impfstoff-spezifischen T-Zell Re-stimulation vor Auftreten ECM-spezifischer Symptome (Tag 6 *post infectionem*) pro Gruppe verwendet. Mit den verbleibenden 10 Mäusen wurde die Wirksamkeit der Impfstoffe mittels Überlebensstudien durchgeführt.

Ergebnisse: GPI2, GPI4, GPI5 und GPI6 immunisierte Mäuse entwickelten signifikant höhere anti-GPI-Antikörper im Vergleich zu Kontrolltieren. Für GPI1 und GPI3 konnte nur ein leichter Anstieg beobachtet werden. Insgesamt war die Prävalenz der ECM bei den Kontrollmäusen 100%, wohingegen alle GPI-CRM₁₉₇-immunisierten Mäuse eine verbesserte Überlebensrate aufwiesen. Insbesondere konnte bei GPI5 geimpften Mäusen ein signifikanter Schutz gegen PbA induzierte Enzephalopathie festgestellt werden. Die immunologische Charakterisierung von Milz-Zellpopulation und Serum-Zytokinen zeigte keine signifikanten Unterschiede zwischen den GPI-CRM₁₉₇ geimpften Gruppen. Es konnten jedoch Tendenzen beobachtet werden, wobei GPI5

immunisierte Mäuse eine verringerte Zellaktivierung sowie ebenfalls verringerte TNF- α , IFN- γ und IL-6 Spiegel im Serum aufwiesen.

Diskussion: In dieser Studie konnte die Wirksamkeit und der Wirkmechanismus eines GPI-Glykokonjugat-Impfstoffes weiter untersucht werden. Zum ersten Mal wurden das zugelassene Trägerprotein CRM₁₉₇ und Alum als Adjuvans verwendet. Es ließ sich eine Struktur-Funktionsbeziehung verschiedener synthetischer GPI-Konstrukte in Bezug auf die Immunogenität mittels Glycan Array-Analyse herstellen. Ferner konnte die anti-inflammatorische Wirksamkeit antitoxischer GPI-Impfstoffe reproduziert, sowie ein daraus resultierendes verbessertes Überleben in ECM-empfindlichen Mäusen festgestellt werden. Zusammenfassend lässt sich herausstellen, dass der Nachweis eines partiellen Impfschutzes gegen *Plasmodium* GPI induzierte ECM durch synthetische GPI-Vakzine gelungen ist.

Abkürzungen: PEthN=Phosphoethanolamin, Glc=Glucosamin, PI=Phosphoinositol, Man₃=GPI Struktur mit drei Mannosezucker, Man₄=GPI Struktur mit vier Mannosezucker.

1 Introduction

1.1 The immune system

The mammalian immune system is essential for the physical integrity to fight pathogens and restore homeostasis. It comprises a complex interaction of cellular and humoral components to protect against pathogens, including bacteria, toxins, viruses, fungi and parasites as well as neoplasms. Innate immunity includes the immediate response of the host towards invading pathogens. It aims to prevent pathogen penetration through physical and chemical barriers and when overcome, rapidly recognizes pathogen-associated patterns and instigates the adaptive immune response. Phagocytosis of invading pathogens is accomplished by monocytes/macrophages and granulocytes (neutrophils), whereas antigen-presenting cells (APCs) such as dendritic cells (DCs) initialize the adaptive immune response after antigen encounter (1). The innate humoral response includes various cytokines and the complement system which tightly regulate cellular activation, thereby regulating the adaptive immune response (2). Adaptive immunity launches the specific response to the invading pathogens (or neoplasms) and shapes cellular memory. T and B lymphocytes mediate a precise immunological response, where $CD4^+$ and $CD8^+$ T cells shape the cellular defense and plasma cells provide specific antibodies for humoral immunity. Further, induced immunological memory allows for a rapid and specific response in case of re-exposure to a familiar pathogen (3).

1.1.1 Innate immunity

Crossing the first barriers of innate protection such as epithelium, antimicrobial lysozyme and defensins, innate sensing of conserved pathogen-associated molecular patterns (PAMPs) by pattern recognition receptors (PRRs) induces phagocytosis for immediate antigen clearance and initiates the adaptive immune response (1, 4, 5). Similar to PAMPs, endogenous danger-associated molecular patterns (DAMPs) are also detected by PRRs. Activated PRR-expressing cells such as epithelial cells, resident DCs, macrophages and mast cells, initiate a local immune response by cytokine and chemokine secretion, attracting monocytes and granulocytes (neutrophils, basophils, eosinophils) (4). Different classes of PRRs expressed by epithelial cells and antigen-presenting cells (APCs) have been identified, the most important ones including toll-like receptors (TLRs), nucleotide-binding oligomerization domain-like receptors (NLRs), retinoid acid-inducible gene-1-like receptors (RLRs) and C-type lectin receptors (CLRs) (1, 4, 5). Targeted recognition of PAMPs by different classes of PRR as well as

tissue and cell-specific expression of PRRs enables a subtle coordinated adaptive immune response. Further, different DC subsets have been identified to play a key role in T cell differentiation into T_H1, T_H2, T_H17 or regulatory T cells (T_{reg}) (4).

TLR sensing of PAMPs at the cell surface (TLR1, TLR2, TLR4, TLR5 and TLR6), endosome and lysosome (TLR3, TLR7, TLR8 and TLR9) initiates transcriptional upregulation of genes encoding pro-inflammatory cytokines and type I interferons (IFN). TLR2 and TLR4 are both involved in *Plasmodium* glycosylphosphatidylinositol (GPI) recognition to initiate a pro-inflammatory immune response (6). Generally, TLR signaling varies according to the cytoplasmic Toll/IL-1R homology (TIR) domain-containing adaptors including myeloid differentiation primary response gene 88 (MyD88), TIR domain-containing adaptor inducing IFN- β (TRIF), MyD88 adapter-like (Mal)/TIRAP, TRIF-related adaptor molecule (TRAM) and sterile-alpha and armadillo motif-containing protein (SARM) (5). Mal/TIRAP is essential for MyD88-dependent signaling of TLR2 and TLR4 (7). TLR signaling finally activates transcription factors nuclear factor kappa-light-chain-enhancer of activated B-cells (NF- κ B), activator protein 1 (AP-1) and interferon regulatory factors (IRF) in the nucleus and induces expression of pro-inflammatory cytokines and type I interferons (5). As the role of RLR, CLR and NLR sensing and signaling of GPI is yet unknown, they will not be elaborated in detail.

1.1.2 Adaptive immunity

Adaptive immunity, including both B and T cell defense and the humoral antibody response, commences delayed in time after infection but confers antigen-specific immunity and immunological memory (1, 4). Hematopoietic progenitor cells in the bone marrow differentiate into B and T lymphocytes, T cell precursors populate the thymus, whereas B cells remain in the bone marrow for differentiation and are finally released into the circulatory system as naïve B and T lymphocytes (3). The diverse repertoire of B cell-surface-bound immunoglobulins (also known as B cell receptors) and T cell receptors (TCR) is attempted by somatic recombination in progenitor B and T cells. Variable, diversity and joining gene segments (VDJ) are recombined in the variable region of light- (VJ) and heavy chains (VDJ) in order to maintain a high diversity of specific immunoglobulins (3). Secondary modifications such as somatic hypermutation, class-switch recombination and gene conversion further add to receptor repertoire diversity in B cells (3). Taken together, a highly diverse receptor repertoire allows for high affinity antigen binding and elimination through clonal expansion of selected lymphocyte populations (1).

1.1.3 Innate control of adaptive immunity

Antigen presentation by DCs establishes an important link between innate and adaptive immunity. Pathogen uptake by DCs induces cellular maturation and migration towards the regional draining lymph nodes to enable antigen presentation to naïve T cells (8). T cell differentiation requires T cell receptor (TCR) recognition of major histocompatibility complex (MHC) presented peptides, co-stimulatory CD28/CD80 or CD86 interaction and cytokine signaling (1). Missing co-stimulatory signals in the case of self-antigens lead to T cell anergy and tolerance (1). Dysfunctional tolerogenesis, however, induces auto-immunity against self-antigens (9).

In brief, the following examples highlight the crucial effect of antigen-presenting DC sub-population and cytokines on T effector differentiation: Extracellular fungal and bacterial carbohydrates are detected by CLRs dectin-1 and dectin-2 of CD1c⁺CD11b⁺ DCs and together with IL-23 induce T_H17 cell differentiation to avert infection. Sensing of viruses by CD141^{hi}CLEC9A⁺ DCs together with IL-6, IL-1 β and Type I interferons leads to CD8⁺ cytotoxic T cell (CTL) differentiation to fight viral infections (10, 11). Detection of intracellular bacteria or protozoa by CD207⁺CD103⁺ DCs leads to IL-12 production and T_H1 cell activation and CD301b⁺CD11b⁺ DCs are necessary to induce a T_H2 cell response in the case of helminths infection in mice (4).

1.2 Malaria

Malaria disease is caused by an apicomplexan parasite of the genus *Plasmodium* (12). More than 100 species infecting mammals exist, with *P. falciparum*, *P. vivax*, *P. ovale* and *P. malariae* naturally infecting humans and *P. knowlesi*, a primate parasite, causing zoonotic malaria infection (13).

Plasmodium life cycle starts with the transmission of sporozoites from the anopheline mosquito salivary gland to the mammalian host. Sporozoites infect hepatocytes and develop within 7 days into merozoites (see Fig. 1, *Liver stage*). Merozoites are subsequently released into the blood stream, where they undergo asexual replication. Repeated cycles of merozoite invasion and schizogony lead to an exponential growth of the parasite during blood stage infection. A small fraction of merozoites eventually develop into intracellular gametocytes (Fig. 1, *Blood stage*). When taken up by a female mosquito of the genus *Anopheles*, they develop into extracellular male and female gametes in the midgut to form zygotes that finally develop into ookinetes.

Motile ookinetes form oocysts that finally develop into the infectious sporozoites that migrate into the mosquito salivary glands, completing the parasite life cycle (Fig. 1, *Mosquito stage*) (14-16). *P. vivax* and *P. ovale* are both able to develop dormant liver stages (hypnozoites) that can persist and cause disease relapse after parasite clearance.

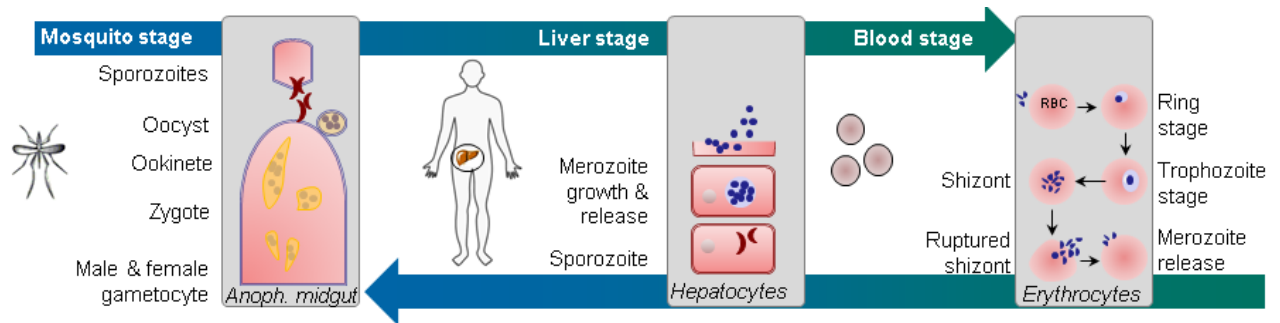


Figure 1: Plasmodium life cycle

Plasmodium life cycle starts with the uptake of male and female gametocytes from an infected host by the female anopheles mosquito. Within the mosquito midgut, extracellular gametocytes develop to form zygotes that develop into ookinetes. Motile ookinetes form oocysts that develop into sporozoites that migrate into the mosquito salivary glands and are injected into the host within the next blood meal. In the host, sporozoites travel to the liver and develop in hepatocytes to merozoites within 7 days. Merozoites are released into the blood stream, where they undergo asexual replication within red blood cells (RBC). Merozoites undergo schizogony and intracellular gametocytes develop in small fractions ready for transmission to a female anopheles mosquito (14-16).

1.2.1 Malaria epidemiology

Due to increased efforts in vector control, bed nets coverage and access to effective antimalarial treatment, malaria incidence and mortality have decreased by 30% and 47% worldwide respectively, since the beginning of this century (17). However, malaria remains a major global health challenge, with an estimated 198 million cases of disease and 548,000 deaths, 453,000 of these occurring in children under the age of 5 years in 2013 (17, 18).

Malaria disease burden is restricted to tropical and sub-tropical countries, most of them being developing countries. With 80% of cases and 90% of worldwide deaths, malaria burden was highest in the WHO African Region in 2013 (17). Even though philanthropic and public research funding has increased over the past decade, a research gap exists, evidenced by a low level of research funding despite a high disease burden (19).

1.2.2 Malaria pathogenesis

Malaria disease severity ranges from severe malaria to asymptomatic infection and depends amongst other factors on the hosts' balance of pro-inflammatory and regulatory reactions towards the parasite and its products (12, 20-22). The pivotal role of the immune response is highlighted by the fact that malaria incidence and deaths are highly skewed to immunologically naïve children under the age of 5 years, whereas naturally acquired immunity against malaria occurs in adults after repetitive infections with *Plasmodium* species (18, 23). *Plasmodium* species is another determining factor of disease severity, with *P. falciparum*, mostly prevalent in sub-Saharan Africa, accounting for the high proportion of death and disability in this region. As already hypothesized by Marchiafava and Bignami in 1892, sequestration of *P. falciparum*-infected red blood cells via *P. falciparum* erythrocyte membrane protein-1 (PfEMP-1) is fundamental to malaria disease pathogenesis, causing severe malaria conditions such as cerebral malaria, renal impairment and pulmonary edema (24-27).

Innate sensing of *Plasmodium* PAMPs such as GPI, hemozoin and nucleic acid motifs (DNA or RNA) by hosts PRRs leads to the induction of pro-inflammatory pathways (14). TLR activation by *Plasmodium* GPI and downstream transcriptional effects will be described in detail in chapter 1.3. Hemozoin, the crystalline disposal product of digested hemoglobin, as well as *Plasmodium* DNA and RNA, have been shown to signal through endosomal TLR9 activating NF- κ B, NOD-LRR- and pyrin domain-containing 3 (NLPR3) and IFN-inducible protein absent in melanoma 2 (AIM2) initiating inflammasome assembly (14). An important role of CLR such as DCIR and Clec9a has further been confirmed recently (28, 29), and endogenous DAMPs such as urate crystals and heme have been reported to contribute to innate immune activation during malaria infection (14). The role of DCs in malaria infection remains controversial, their ability to present *Plasmodium* antigens and induce an adaptive immune response remains however a matter of fact (30, 31). Activation of CD8⁺ and CD4⁺ T cells by DC MHC I cross-presentation and MHC II antigen presentation leads either to a cytotoxic T cell response or T helper cell-induced phagocytosis by activated macrophages, both promoting pathogen clearance (32). Adaptive immunity in malaria disease has further proven to be essential for parasite clearance and tolerance. CD4⁺ and CD8⁺ T lymphocytes were shown to reduce sporozoite load in hepatocytes (33). Further, antibodies directed against blood stage antigens are associated with protection and merozoite-antigen-specific T_H1 and T_H2 cells develop in immune individuals (33). Humoral protection is conferred via antibody binding and increased clearance of infected red blood cells

(pRBC), antibody opsonization and cellular killing and blockade of merozoite infection of red blood cells (RBC) (20).

Thus, a balanced immune response is essential for protection against malaria and the prevention of immunopathology. The following sequence of events has been suggested to trigger cerebral malaria pathogenesis. *Plasmodium*-infected RBCs sequester and accumulate in the microvasculature. Intravascular cell infiltrates (including activated leukocytes, natural killer and natural killer T cells, macrophages and DCs) accumulate and trigger local tissue inflammation, which leads to disruption of blood flow and blood clotting. Attracted platelets and pro-inflammatory cytokines mediate an upregulation of cell adhesion molecules, which again increases leukocyte binding and pRBC sequestration. The presence of CD8⁺ T cells in particular leads to endothelial damage and extravasation, contributing to severe malaria conditions (see Fig. 2) (12, 20).

1.2.3 Cerebral malaria

Cerebral malaria is the most severe manifestation of *P. falciparum* malaria. Impaired consciousness (score ≤ 2 by Blantyre Coma Scale for children or < 11 Glasgow Coma Scale for adults) and a positive parasitemia excluding any other causes of cerebral maladies clinically define this syndrome (34). Cerebral malaria occurs in 1% of *P. falciparum*-infected individuals, 90% of these being children in the WHO African region (17). Despite effective anti-malarial treatment, case fatality rates for cerebral malaria remain high, with 8.5-20%, accounting for a high burden of disease (35-38).

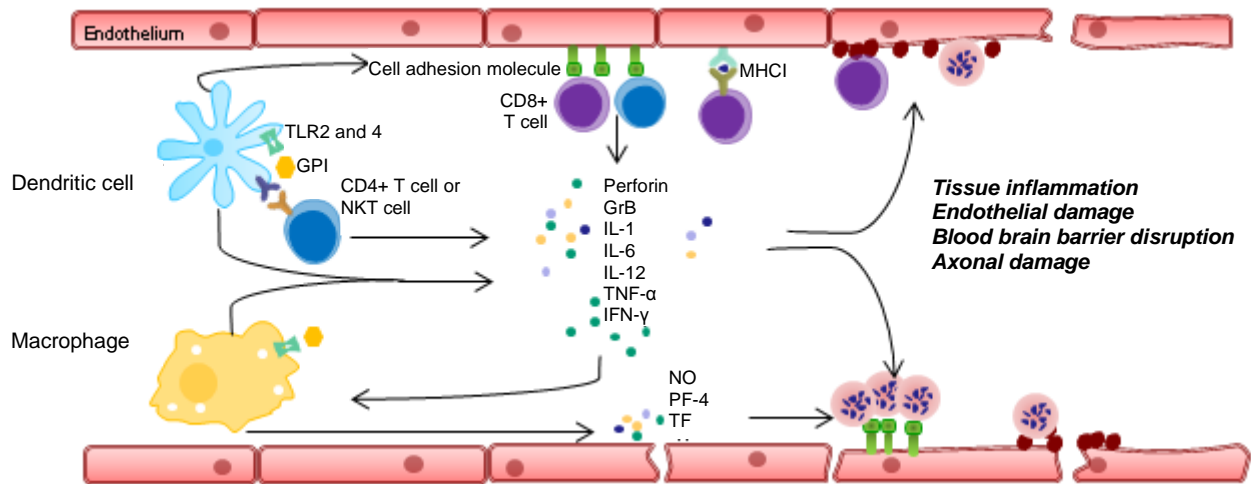


Figure 2: Plasmodium GPI mediated pathogenesis during blood stage infection

During blood stage infection, *Plasmodium* parasites and pro-inflammatory anti-malarial immune mechanisms lead to cerebral malaria pathogenesis. Plasmodium GPIs are strong pro-inflammatory mediators that are recognized by dendritic cells and macrophages via TLR2/1 and TLR2/6 and TLR4. Induction of NF-κB leads to transcription of TNF-α, IL-6 and IL-1 genes. Uptake of infected RBC and MHCII/CD1d presentation activates CD4⁺ T cells and NKT cells that secrete, amongst others, cytokines IL-12 and IFN-γ. IFN-γ-activated macrophages further amplify pro-inflammatory cytokine level and secrete nitric oxide (NO), tissue factor (TF) and platelet factor-4 (PF-4), contributing to endothelial damage. Expression of adhesion molecules such as ICAM-1 or CD36 is upregulated via IL-1 and activated macrophages and leads to increased binding of PfEMP-1 and leukocytes. CD8⁺ T cell sequestration and release of perforin and granzyme B (GrB) together with other pro-inflammatory cytokines contributes to endothelial damage. Platelet binding to endothelial cells increases leukocyte adhesion and binding of infected RBCs. Overarching pro-inflammatory reactions lead to endothelial damage, break-down of the blood brain barrier and finally to axonal damage with severe neurological complications (39-42).

Cerebral malaria develops as an immunologically mediated encephalitis against the sequestered parasite and activated brain endothelial cells. Sequestration of pRBC as well as the immunological response against the parasite (cellular and humoral) are key events in the pathogenesis of cerebral malaria (43-46). Binding of PfEMP-1 to vascular adhesion molecules (such as ICAM-1, VCAM-1, CD36, CD31 and CSA in the placenta), as well as cross-presentation of *Plasmodium* antigens by endothelial cells mediate local tissue inflammation and attracts pro-inflammatory cell populations (45, 47-52). The level of pRBC sequestration in the brain has been shown to correlate with impaired consciousness due to brain swelling in children with cerebral malaria (53, 54). Finally, pRBC sequestration, tissue inflammation, blood brain barrier breakdown and brain edema lead to hypoxia, which results in axonal damage and neurological sequelae.

Cellular and humoral mediators of the pro-inflammatory response during cerebral malaria have been extensively studied and a role for lymphoid cells (CD8⁺ and CD4⁺ T cells, NK and NKT

cells) and myeloid cells (monocytes, dendritic cells, neutrophils) as well as pro-inflammatory cytokines (IL-1 β , IL6, IL-8, IL-12p70, TNF- α , INF- γ) has been described in population studies as well as in the murine model of ECM (Fig. 2) (45, 55-58).

1.2.4 Murine model of cerebral malaria

Plasmodium species infecting murine rodents are *P. berghei*, *P. chabaudi*, *P. vinckei* and *P. yoelii* that are commonly used for mechanistical studies in the murine model of malaria. The murine model of cerebral malaria has been paramount in improving our understanding of the pathogenesis of cerebral malaria. Despite differences between murine and human hosts and a lively academic discourse (59), correlations of the main pathological findings between humans and mice have been shown in multiple studies (60, 61).

P. berghei ANKA infection of C57BL/6 and CBA mice leads to cerebral pathology. Neurological symptoms become apparent from day 6 *post* infection and develop from ataxia to coma and death (61). A pathogenic mechanism similar to that found in the human host is suggested in mice, starting with the activation of endothelial cells and upregulation of cell adhesion molecules (ICAM-1, VCAM-1, CD36, CD31). This pathway further progresses to activation of CD4⁺ and CD8⁺ T lymphocytes, NKT cells and myeloid cells that finally secrete pro-inflammatory cytokines resulting in a systemic inflammatory reaction responsible for disease pathology (62-68).

Other mouse strains (CBA/ca, DBA/2) or *Plasmodium* species (lethal *P. yoelii* 17XL, *P. berghei* K173) have also been shown to induce ECM. As they lack key features of human cerebral malaria (*i.e.* sequestration of pRBC), they were not taken into account in the present study.

1.3 The role of glycosylphosphatidylinositol in malaria pathogenesis

Glycosylphosphatidylinositol (GPI) glycolipids serve as protein anchors on eukaryotic cell surfaces and are highly expressed by protozoan parasites such as *Plasmodium*, *Trypanosoma*, *Leishmania* and *Toxoplasma* species (Fig. 3A and B) (69). GPI expression by protozoan parasites is 100 times higher than in mammalian cells and accounts for 90% of glycosylated proteins (69, 70). Both free

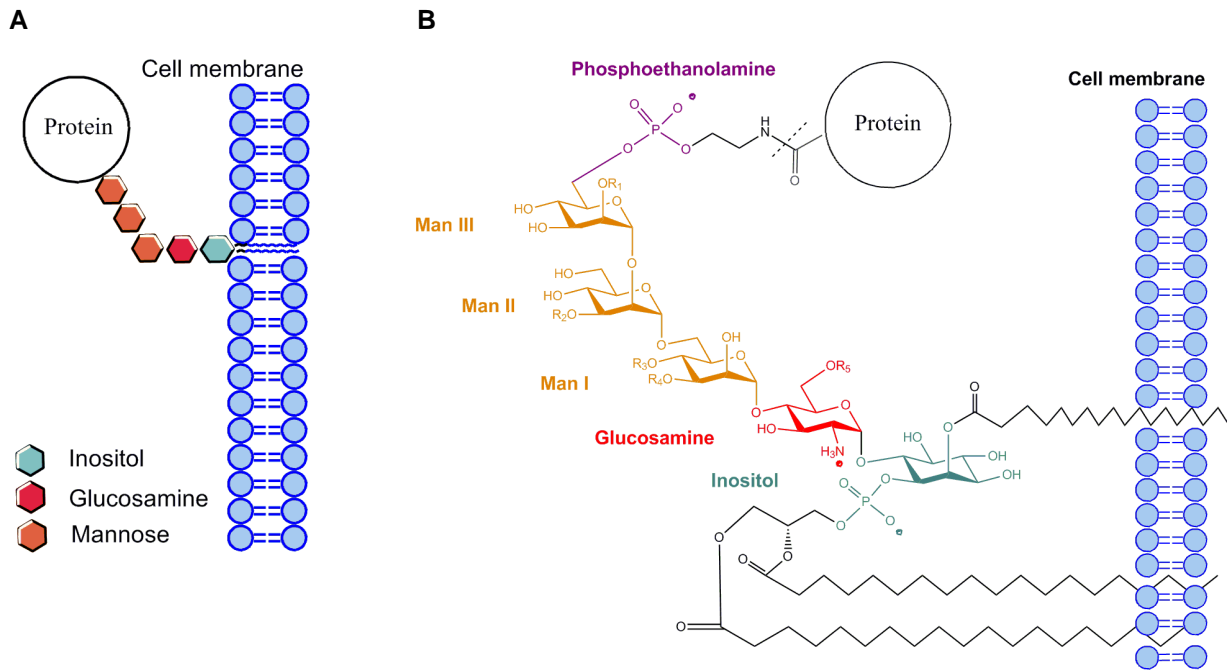


Figure 3: Chemical core structure of Glycosylphosphatidylinositol (GPI)

(A) Schematic representation of GPI-anchored protein on a cell membrane. (B) Common core structure of GPI, with captions R1-R5 varying according to origin (for *P. falciparum* see Fig. 4 A and B).

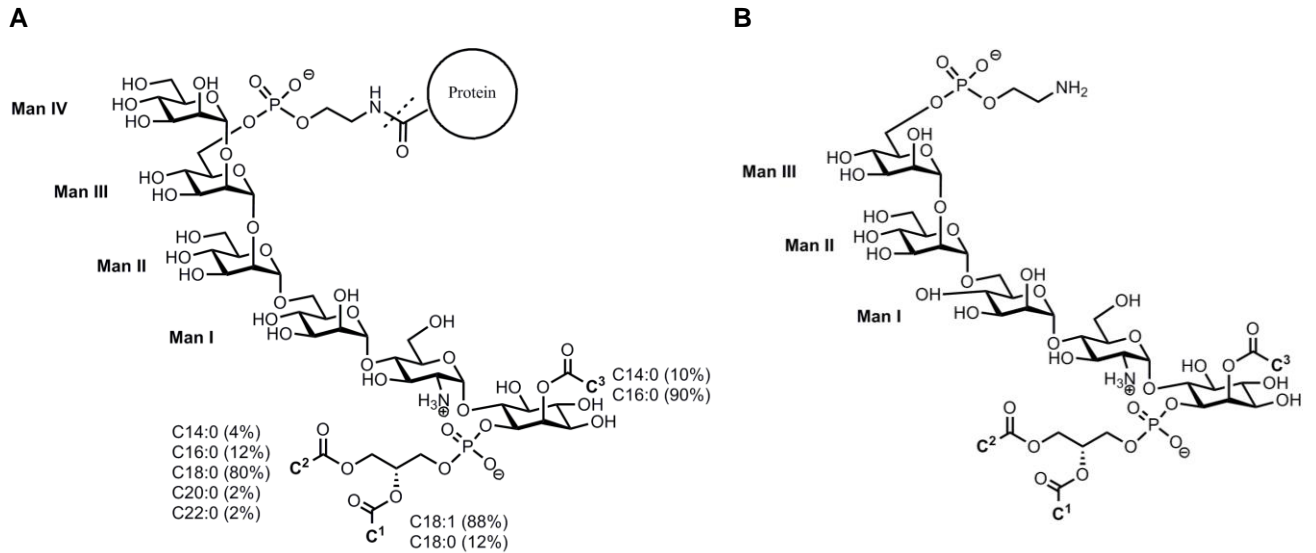


Figure 4: Chemical structure of *Plasmodium falciparum* Glycosylphosphatidylinositol (GPI)

(A) *P. falciparum* Man₄ (with Man IV at R1) GPI structure, anchoring proteins. (B) Free Man₃ (without Man IV at R1) GPI is also present during asexual blood stage development in *P. falciparum*. A fatty acid ester is present at C3 (palmitate or myristate) and diacylglycerol moiety at C1 and C2 containing mainly C18:0, C18:1 and C16:0 and less frequently C14:0, C20:0 and C22:0. (Figures obtained and modified from Dr. Daniel Varón Silva)

Man₃ GPI (containing three mannoses) and protein-linked Man₄ GPI (containing four mannoses) have been shown to be present in *P. falciparum* (Fig. 4 A and B). The proportion of Man₃ to protein-linked Man₄ GPIs is comparably high with a ratio of 5:1 in *P. falciparum* (71).

GPIs share a common core structure, containing three mannoses, one glucosamine and one inositol (NH₂(CH₂)₂OPO₃H-6Man α 1 \rightarrow 2Man α 1 \rightarrow 6Man α 1 \rightarrow 4GlcN α 1 \rightarrow 6myo-Inol1-OPO₃H-Lipid) with diverging attachments for different species (Fig. 3 A and B) (72, 73). *P. falciparum* GPI contains one additional terminal mannose and a saturated fatty-acyl group at C2 of myo-inositol (Fig. 4 A) (73).

As previously described, an excessive pro-inflammatory response against *Plasmodium* parasites and its waste products is associated with severe malaria conditions such as cerebral malaria (see 1.1.2 and 1.1.3). *P. falciparum* GPI acts as a malaria parasite-associated molecular pattern that induces a strong pro-inflammatory response, which is thought to contribute to disease pathology (40, 41, 74). *In vitro* studies could demonstrate that the induction of the pro-inflammatory response of *P. falciparum* GPI is mediated *via* TLR2 (TLR2/1 > TLR2/6) and to a lesser extent TLR4 signaling. Pro-inflammatory cytokines TNF- α , IL-12, IL-6 and NO rely on NF- κ B and JNK pathways that are regulated *via* TLR signaling (39, 42). Likewise, cell adhesion molecules (ICAM-1, VCAM-1) are upregulated by NF- κ B signaling, which is further increased in the presence of TNF- α and IL-1 (6, 40, 74). Taken together, GPI induces the transcription of key pro-inflammatory cytokine genes and leads to upregulation of adhesion molecules, contributing to CM pathogenesis (Fig. 2).

The importance of this pro-inflammatory cascade elicited by *Plasmodium* GPI is further highlighted by the fact that polymorphisms of TLR2, TLR4 and Mal/TIRAP impact susceptibility to severe malaria (75-77). As previously mentioned, TLR2 and TLR4 are involved in GPI sensing, consequently dysfunctional signaling might impact GPI-induced inflammation and render those individuals less susceptible to CM. Furthermore, polymorphisms of Mal/TIRAP, essential for TLR2 and TLR4 MyD88-dependent signaling, might influence the GPI-mediated pro-inflammatory innate immune response.

1.4 Vaccines

Since the discovery of the protective potential of vaccines by Edward Jenner in 1796, vaccines have played an essential role in disease prevention and elimination (78). Over the past century, a

variety of new vaccines has been developed, that can be grouped into live attenuated and inactivated subunit vaccines, the latter including protein, carbohydrate and glycoconjugate-based vaccines (79). In general, the processing of vaccine antigens by the immune system corresponds to pathogen encounter as described in 1.1.1 and 1.1.2. In brief, innate sensing of immunized antigens by antigen-presenting cells (APC) leads to maturation and migration towards secondary lymph nodes, where B cells undergo differentiation into plasma cells with the help of antigen-specific T cells. Co-stimulatory signals lead to clonal B cell expansion and differentiation into plasma cells, with high affinity antibodies against the vaccine antigen. Finally, plasma cells migrate to the bone marrow, where stromal cells provide survival signals to guarantee long term protection (80). Once inoculated, live attenuated vaccines replicate and spread throughout the body, thus triggering an innate immune response at multiple sites and being detected by various different PAMPs (80). This leads to an efficacious cellular and humoral response that confers long-term protection (79). In contrast, inactivated vaccines evoke a locally limited immune response that require adjuvants to enhance immunogenicity and booster vaccinations to guarantee long-term protective immunity (79).

Adjuvants, though mechanistically sparsely investigated, essentially enable longer antigen presentation through emulsification and act as an activation signal to induce the expression of genes encoding pro-inflammatory cytokines and receptors (79, 80). The most commonly licensed adjuvant, alum (aluminum phosphate or aluminum hydroxide) is based on mineral salts, induces inflammasome activation in DC, enhances antibody production by B cells, enables a T_H2 response and adsorbs antigens at its surface for prolonged presentation to APCs (79, 81). The oil-in-water emulsions MF59 (Novartis) and AS03 (GlaxoSmithKline) (squalene, polysorbate 80, sorbitan trioleate or α -tocopherol), both used in influenza vaccines, improve antigen uptake by APCs and induce activation of various genes associated with inflammation (79, 81). TLR signaling adjuvant AS04 (GlaxoSmithKline) (aluminum hydroxide, monophosphoryl lipid A) has been shown to elicit a T_H1 immune response (79). Finally, AS01 (GlaxoSmithKline) (liposome, monophosphoryl lipid A, saponin QS-21 Stimulon[®]), licensed in 2015 (RTS,S, Mosquirix[™]), enhances inflammasome activation in DCs and macrophages, antibody production and antigen-specific T cell responses (T_H1 and T_H2) (82).

Protective immunity relies both on B cell-mediated availability of neutralizing antibodies (*inter alia* hepatitis, yellow fever, diphtheria, tetanus, influenza, rotavirus, rabies, pneumococcal- and meningococcal bacteria) and on antigen-specific T cells (*inter alia* varicella, influenza, pneumococcal- and meningococcal bacteria) (79, 83). Importantly, vaccine-activated DCs steer

the type of response (*i.e.* T_H1 or T_H2 by CD11c⁺CD11b⁺CD8α⁻ or CD11c⁺CD11b⁻CD8α⁺, respectively) and are key to clonal expansion and memory of T and B cells (79).

1.4.1 Malaria eradication and the importance of anti-malarial vaccines

In the wake of the WHO *Global Technical Strategy for Malaria 2016–2030* agenda to accomplish malaria eradication by 2030, the role of disease prevention becomes a prerequisite (84). This technical report is complemented by the Roll Back Malaria Partnerships *Action and Investment to defeat Malaria 2016–2030 (AIM) – for a malaria-free world* and the *Malaria Eradication Research Agenda (malERA)* initiative, that calls for development of new innovative vaccines (85, 86).

Vector control and antimalarial treatment are fundamental pillars to prevent malaria progression and control disease transmission. Four main groups of insecticides are currently used, including organochlorines, organophosphates, carbamates and pyrethroids. Anopheline resistance to most available insecticides, especially the commonly used pyrethroids applied in insecticide-treated nets (ITNs), threatens the current decline in malaria incidence (87). Antimalarial drug resistance is equally fraught with problems. Antimalarial treatment varies according to *Plasmodium* species, transmission frequency and drug sensibility. Artemisinin-based combination therapy (ACT) is recommended as the first line treatment for uncomplicated *P. falciparum* and *P. vivax* infection. chloroquine (CQ) is the first-line treatment of *P. vivax* (when sensitive), *P. ovale* and *P. malariae*. Primaquine is applied for both *P. vivax* and *P. ovale* to clear dormant liver stages (88). However, resistance against all currently used antimalarial drugs, especially emerging artemisinin resistance in *P. falciparum*, threatens the successes of decreased malaria incidence and mortality and hampers the progress of malaria elimination (89). Even though drug resistance is mechanistically poorly understood, single nucleotide polymorphisms (SNPs) of transport proteins such as pfmdr1, pfcert, pfmrp1, pfatp4 have been shown to influence sensitivity of currently used antimalarial drugs (90). Increasing mechanisms of parasite and vector resistance against treatment and control options render antimalarial vaccines a third, indispensable pillar of malaria eradication. Especially antimalarial vaccines, targeting conserved pathogen structures with a low potential for genetic variability could therefore be of major importance in the future.

To prevent malaria disease and transmission, traditional vaccine approaches have so far focused on either inducing sterile immunity by targeting sporozoite stages (pre-erythrocytic vaccines), preventing asexual replication of merozoites in RBC (blood-stage vaccines) or targeting sexual

replication in the anopheline midgut to block transmission to the human host (transmission blocking vaccines) (91-95). Most anti-malarial vaccine candidates are based on recombinant protein antigens present in the different stages of the *Plasmodium* life cycle. Additionally, virally vectored DNA vaccines as well as attenuated or genetically modified parasite vaccines have been successfully tested (96-98). To date, the only approved vaccine that has been evaluated in large-scale phase III clinical trials is the RTS,S/AS01 vaccine (PATH Malaria Vaccine Initiative and GlaxoSmithKline Biologicals) that induces 43% protection after 12 months from prime-immunization and 16% long-term protection after 48 months in immunized individuals (91-93, 99). Even though progress has been made over recent decades, major improvements of RTS,S (*i.e.* a genotype-specific circumsporozoite protein sequence for enhanced efficacy as recently suggested by Neafsey *et al.* (100)), and further investigation in clinical and promising pre-clinical vaccines is needed.

1.4.2 Carbohydrate-based vaccines

Carbohydrate-based vaccine development started in the early 1920s, when Heidelberger and Avery detected the immunogenic capsular polysaccharides of *Streptococcus pneumoniae* (101). It was soon recognized that polysaccharide epitopes are naturally thymus-independent antigens and conjugation to immunogenic carrier proteins was necessary to enhance immunogenicity and induce B and T cell memory (102, 103). With this discovery, a new generation of highly effective glycoconjugate vaccines was generated, including vaccines against *Neisseria meningitides*, *Haemophilus influenzae type b* and *Streptococcus pneumoniae* (104). Denatured bacterial toxoids such as diphtheria toxoid (DT), tetanus toxoid (TT), nontoxic cross-reactive material of diphtheria toxin (CRM₁₉₇) and *N. meningitides* derived outer membrane protein complex (OMPC) have been used as carrier proteins in human glycoconjugate vaccines (104). Consequently, glycoconjugate vaccines were able to elicit a CD4⁺ T cell response *via* MHCII presentation of the peptides by antigen-presenting cells, which subsequently enabled B cell maturation and isotype switching (105).

1.4.3 Synthetic GPI glycoconjugate vaccines

In addition to the traditional protein-based vaccines, carbohydrate-based vaccines have shown to be highly effective in preventing diseases caused by *Neisseria meningitides*, *Streptococcus pneumoniae*, *Haemophilus influenzae type b* and *Salmonella typhi* (105). Usually, capsular

polysaccharides are purified from pathogens and conjugated to a carrier protein to elicit an adaptive immune response *via* CD4⁺ T cell activation (83). With advancements in carbohydrate synthesis, especially automated oligosaccharide solid-phase synthesis, synthetic carbohydrate-based vaccines are already being clinically applied and positively pre-clinically tested (106, 107).

As outlined above (section 1.2), *P. falciparum* GPI was shown to act as a malaria parasite-associated molecular pattern that mediates a strong pro-inflammatory response and contributes to severe malarial conditions such as CM. It has been reported that *Plasmodium* GPI acts as an immunogenic epitope in humans and evokes an age-dependent antibody response that correlates with immunity to severe malaria (71). Anti-GPI antibody levels in children with severe malaria were shown to recognize predominantly Man₃- and Man₄-GPIs, closely related to the naturally occurring epitope (108). Further, a structure-dependent recognition of synthetic GPI was established, with GPIs containing less than 5 carbohydrate subunits not being detected by antibodies derived from malaria-infected individuals (109). Interestingly, individual sera were shown to recognize only GPIs containing phosphoethanolamine at the third mannose residue (109). Also, immunization with synthetic Man₄-GPI conjugated to the carrier protein keyhole limpet haemocyanin (KLH) and emulsified in complete Freund's adjuvant (CFA) showed protection from experimental cerebral malaria, pulmonary edema and acidosis in C57BL/6 mice (110). KLH is frequently used as an experimental carrier protein due to its large size, high loading potential and excellent immunogenicity, however, it is not approved for human use. Similarly, CFA, a highly efficacious water-in-oil emulsion-based adjuvant containing mycobacterium antigen, is not approved either due to its toxicity.

The GPI-antitoxic vaccine approach was adopted in this study, employing a licensed adjuvant and carrier protein combined with structural modifications of synthetic GPI in view of a potential use of an optimized glycoconjugate vaccine in humans in the future.

2 Aim

GPIs are highly expressed by protozoan parasites. In *Plasmodium*, high numbers of both free Man₃ and protein anchored Man₄ GPIs were shown to be released during asexual parasite replication. Malaria GPIs are one factor contributing to severe malaria pathogenesis.

The ability of *Plasmodium* GPI to induce an excessive pro-inflammatory response through PRR recognition and signaling was demonstrated in the murine model of malaria (40, 74, 110). Further, anti-GPI antibody levels in malaria-exposed individuals correlate with protection against severe malaria disease (109, 111, 112). These findings have led to the hypothesis that immunization with a GPI glycoconjugate vaccine might protect from severe malaria conditions, especially cerebral malaria. In a proof-of-concept study, synthetic *Plasmodium* Man₄ GPI conjugated to KLH and emulsified in complete Freund's adjuvant (CFA) has proven to be protective in ECM-susceptible mice (110). However, neither KLH nor CFA are approved for use in human vaccines.

In the present study, the approved non-toxic mutant of diphtheria toxin, CRM₁₉₇, was applied as carrier protein and formulated with alum as adjuvant for the first time to test the protective potential of different synthetic GPI glycoconjugates in the murine model of cerebral malaria. Unlike previously, GPIs were conjugated from phosphoinositol or glucosamine and not from ManIII. Hypothetically, this approach allows for the naturally occurring presentation of free, protein unbound Man₃ GPIs. Further, GPI structures synthesized varied according to their length (Man₃ and Man₄) and presence of functional groups (phosphoethanolamine, inositol), to gain further insights into immunogenicity, immunodominant epitopes and their role in protection. Diverging GPI-CRM₁₉₇ glycoconjugates were first tested in C57BL/6 mice for efficacy and safety. Survival, clinical scoring and parasitemia of immunized and PbA-infected mice were applied to highlight the protective potential of GPI vaccination. Immunogenicity of the GPI glycoconjugate vaccines and cross-reactivity of induced antibody responses were then assessed by glycan array analysis. The cellular immune response and serum cytokine levels were investigated after immunizations on day 6 *post Plasmodium* challenge to evaluate potential cell-mediated protective effects. Key lymphoid and myeloid cell population derived from sacrificed mouse spleens were quantified by flow cytometry, and cellular activation were analyzed. Serum levels of ECM-inducing (and protecting) cytokines were assessed by cytometric bead array prior to and *post* PbA infection. Vaccine-specific T cell responses were investigated *ex-vivo* via ELISpot. And brain homogenates were used to determine CD8⁺ T cell sequestration measured by flow cytometry.

To the best of my knowledge, this is the first experimental approach investigating a structure-activity relationship of different anti-toxic GPI glycoconjugate vaccines against severe malaria conditions using CRM₁₉₇ as carrier protein and alum as an adjuvant.

3 Materials and methods

3.1 Materials

3.1.1 Instruments

Instrument	Name	Manufacturer
Autoclave	Laboclav	SHP Steriltechnik AG, Detzel Schloss, Germany
Automatic cell counter	EVE®	NanoEnTek, Seoul, Korea
Cell counter	Tamaco®	Taichung, Taiwan
Centrifuge	5810R	Eppendorf, Wesseling-Berzdorf, Germany
ELISpot reader	Bioreader®5000-α	BioSys, Karben, Germany
Flow cytometer	FACSCanto™ II	BD Pharmingen, Heidelberg, Germany
Fluorescent scanner	Axon GenePix® 4300A	Molecular Devices, Sunnyvale, CA, US
Heating block	Thermomixer comfort	Eppendorf, Wesseling-Berzdorf, Germany
Incubator	Binder C150	Binder, Tuttlingen, Germany
Magnetic stirrer	MR Hei-Tec	Heidolph, Schwabach, Germany
Microarray printer	SciFlexarrayer	Scienion, Berlin, Germany
Microcentrifuge	5417R	Eppendorf, Wesseling-Berzdorf, Germany
Microscope	Olympus CX31	Olympus, Hamburg, Germany
Multichannel pipette	Transferpette® S-8	Brand, Wertheim, Germany
Multistep pipette	Multipette® stream	Eppendorf, Wesseling-Berzdorf, Germany
pH meter		Mettler Toledo, Columbus, OH, US
Pipettes	Research plus	Eppendorf, Wesseling-Berzdorf, Germany
Sterile bench	Herasafe KS	Thermo Scientific, Bonn, Germany
Vortexer	Vortex-Genie® 2	Scientific Industries, Bohemia, NY, US
Water bath		Memmert, Schwabach, Germany
Water deionizer	Milli-Q®	Merck-Millipore, Darmstadt, Germany

3.1.2 Consumables

Instrument	Name	Manufacturer
3D-Maleimide slides		PolyAn, Berlin, Germany
Cell counting slide	EVE®	NanoEnTek, Seoul, Korea
Cell culture plates	Brandplates®	Brand, Wertheim, Germany
Cell culture plates (V-bottom)	Cellstar®	Greiner bio-one, Frickenhausen, Germany
Cell strainer (40 µm)	Falcon®	Corning, NY, US
Combitips (1 mL, 2.5 mL)		Eppendorf, Wesseling-Berzdorf, Germany
ELISpot plates (96 well)	MultiScreen® HTS	Millipore, Bedford, MA, US
FACS tubes		Sarstedt, Nümbrecht, Germany
Falcon tubes	Corning®	Corning, NY, US
Lancet	Solofix®	B. Braun, Melsungen, Germany
Microscope slide		Marienfeld, Lauda-Königshofen, Germany
Needles (27G x ½")	Fine-Ject®	Henke Sass Wolf, Tuttlingen, Germany
Pasteur pipettes (150 mm)		Roth, Karlsruhe, Germany
Petri dishes (50 mm)	Corning®	Corning, NY, US
Pipette tips	DeckWorks™	Corning, NY, US
Safe-lock tubes	Eppendorf tubes®	Eppendorf, Wesseling-Berzdorf, Germany
Syringes (1 mL, 5 mL)	Omifix®	B. Braun, Melsungen, Germany

3.1.3 Buffers and medium

Buffer	Composition
2-mercaptoethanol	0.1% (v/v) 2-mercaptoethanol in 1x PBS
Complete RPMI	RPMI 1640, 10% FCS, 5 mM L-glutamine, 5 mM penicillin/streptomycin
Davidson solution	111 mL/L 100% acetic acid, 347 mL/L deionized water, 320 mL/L 99% ethanol, 222 mL/L 10% formaldehyde in 1x PBS
ELISpot coating buffer	1x PBS (cell culture grade)
ELISpot dilution buffer	10% FCS 1x PBS
ELISpot wash buffer I	0.05% tween in 1x PBS
ELISpot wash buffer II	1x PBS
Erythrocyte lysis buffer	10% 100 mM Tris, 90% 160 mM ammonium chloride, pH 7.4
FACS staining buffer	1% FCS, 1x PBS
FACS staining buffer (spleen)	0.5% BSA, 2 mM EDTA, 1x PBS
Formaldehyde solution	4% formaldehyde, pH 6.9
Giensa staining buffer	6.7 mM KH_2PO_4 $\text{Na}_2\text{HPO}_4 \times 2\text{H}_2\text{O}$, pH 7.1
Glycan array blocking solution	2% BSA 1x PBS
TCEP	Tris(2-carboxyethyl)phosphine

3.1.4 Antibodies

3.1.4.1 Glycan array

Antibody	Manufacturer (catalogue number)
Donkey anti-mouse IgM-AlexaFluor [®] 594	Dianova, Hamburg, Germany (715-585-020)
Goat anti-mouse IgG1-AlexaFluor [®] 594	Thermo Fischer, Darmstadt, Germany (A21125)
Goat anti-mouse IgG2-AlexaFluor [®] 647	Thermo Fischer, Darmstadt, Germany (A21241)
Goat anti-mouse IgG3-AlexaFluor [®] 488	Thermo Fischer, Darmstadt, Germany (A21151)
Goat anti-rabbit IgG-FITC	Dianova, Hamburg, Germany (ab6717)
Rabbit anti-mouse IgG-FITC	Sigma-Aldrich, Munich, Germany (F9137)

3.1.4.2 Flow cytometry

Antibody	Manufacturer (catalogue number)
Hamster anti-mouse CD11c-APC-Cy7	Fischer Scientific, Darmstadt, Germany (A18639)
Hamster anti-mouse CD3e-PerCP	BD Pharmingen, Heidelberg, Germany (553067)
Hamster anti-mouse CD69-PerCP-Cy5.5	eBioscience, Frankfurt Main, Germany (45-0691-80)
Hamster anti-mouse CD80-FITC	eBioscience, Frankfurt Main, Germany (11-0801-85)
Rat anti-mouse CD11b-APC	eBioscience, Frankfurt Main, Germany (17-0112-81)
Rat anti-mouse CD16/32	eBioscience, Frankfurt Main, Germany (14-0161-85)
Rat anti-mouse CD25-APC	BD Pharmingen, Heidelberg, Germany (558643)
Rat anti-mouse CD45-PerCP	Miltenyi, Bergisch Gladbach, Germany (130097964)
Rat anti-mouse CD4-FITC	Miltenyi, Bergisch Gladbach, Germany (130097958)
Rat anti-mouse CD62L-PE	Miltenyi, Bergisch Gladbach, Germany (130099218)
Rat anti-mouse CD62L-PE-Cy7	eBioscience, Frankfurt Main, Germany (25-0621-81)
Rat anti-mouse CD8-APC-Cy7	BD Pharmingen, Heidelberg, Germany (560182)
Rat anti-mouse FoxP3-PE	BD Pharmingen, Heidelberg, Germany (560408)
Rat-anti mouse CD4-APC-Cy7	eBioscience, Frankfurt Main, Germany (47-0042-82)
Rat-anti-mouse CD8a-APC	Miltenyi, Bergisch Gladbach, Germany (130097991)

3.1.4.3 ELISpot

Antibody	Manufacturer (catalogue number)
Hamster anti-mouse CD28	BD Pharmingen, Heidelberg, Germany (553294)
Hamster anti-mouse CD3e	BD Pharmingen, Heidelberg, Germany (550275)
IFN- γ capture and detection antibody	BD Pharmingen, Heidelberg, Germany (551881)

3.1.4.4 Cytometric bead array

Antibody	Manufacturer (catalogue number)
IL-12p70 capture and PE detection antibody	BD Pharmingen, Heidelberg, Germany (558303)
IL-6 capture and PE detection antibody	BD Pharmingen, Heidelberg, Germany (558301)
IFN- γ capture and PE detection antibody	BD Pharmingen, Heidelberg, Germany (558296)
IL-1 β capture and PE detection antibody	BD Pharmingen, Heidelberg, Germany (560232)
IL-4 capture and PE detection antibody	BD Pharmingen, Heidelberg, Germany (558298)
IL-10 capture and PE detection antibody	BD Pharmingen, Heidelberg, Germany (558300)
TNF- α capture and PE detection antibody	BD Pharmingen, Heidelberg, Germany (558299)

3.1.5 Kits, reagents and chemicals

Name	Manufacturer (catalogue number)
Aluminiumhydroxide, Alhydrogel®	Brenntag, Frederikssund, Denmark (21645512)
AEC substrate set	BD Pharmingen, Heidelberg, Germany (551951)
HRP-Streptavidin	BD Pharmingen, Heidelberg, Germany (557630)
CRM ₁₉₇ lyophilized	ReagentProteins, San Diego, CA, US (CRM-197)
Cytometric Bead Array master buffer kit (Flex sets IFN- γ , TNF- α , IL-1 β , IL-6, IL-12p70, IL-10, IL-4)	BD Pharmingen, Heidelberg, Germany (558266)
Mouse FoxP3 buffer set	BD Pharmingen, Heidelberg, Germany (560409)
RPMI 1640 (without L-glutamine and sodium pyruvate)	PAN Biotech, Aidenbach, Germany

3.1.6 GPI glycans

GPI #	Chemical structure	GPI-CRM ₁₉₇ glycoconjugate
GPI1		
GPI2		
GPI3		
GPI4		
GPI5		
GPI6		

The following synthetic GPI compounds were synthesized and generously provided by Ankita Malik and Maurice Grube from Dr. Daniel Varón Silva's group. Hereafter, the abbreviations GPI1 to GPI6 and GPI-CRM₁₉₇ glycoconjugate 1-6 are used to refer to the different GPI-CRM₁₉₇ glycoconjugates.

3.1.7 Mice and parasite strains

Strain	Origin
BALB/c	Max Planck Institute for Infection Biology, Berlin, Germany
C57BL/6JRj	Janvier Labs, Saint-Berthevin, France
Plasmodium berghei ANKA (MRA-671)	Malaria Research and Reference Reagent Resource Center, Manassas, VA, US

3.1.8 Software

Software	Provider
ChemBioDraw Ultra 12.0	CambridgeSoft Corporation, Waltham, MA, US
FACSDiva v 6.1.3	BD, Franklin Lakes, NJ, US
FCAP array software v 1.0.1	BD, Franklin Lakes, NJ, US
FlowJo	Tree Star Inc., Ashland, OR, US
GraphPad Prism 6	GraphPad Software Inc., La Jolla, CA, US
ImageJ 1.47	National Institutes of Health, Bethesda, Maryland, US

3.2 Methods

3.2.1 Study design

C57BL/6JRj mice were divided into seven groups each consisting of 15 animals: Mice were vaccinated intraperitoneally (i.p.) on days 0, 14 and 28.* Study groups were immunized with GPI-CRM₁₉₇ glycoconjugates **1-6** and control mice were immunized with CRM₁₉₇-Gal. Galactose-conjugated CRM₁₉₇ was used as a control to account for possible conformational changes of the glycan-loaded carrier protein, that has been described in literature before (113). Serum was obtained at 14-day intervals; prior to prime, 1st and 2nd booster-vaccination and *post* infection. All mice were challenged on day 42 with 1x10⁶ PbA-infected erythrocytes i.p. On day 6 *post* infection, 5 mice per group were sacrificed for a coherent immunological characterization (spleen cell composition, brain T cell sequestration, vaccine-specific T cell re-stimulation) by

* To improve legibility, numerical digits are used for number of animals and days.

CO₂ asphyxiation. The remaining 10 mice per group were used for survival studies, testing for vaccine efficacy (Fig. 5).

Group sizes of 10 mice for vaccine efficacy studies were based on the expected incidence of ECM in C57BL/6 mice between 80-100%. The dependent variable (survival) in this group was analysed using log-rank test. With respect to type I error ($\alpha \leq 0.05$), type II error ($\beta \leq 0.2$) and hazard ratio (0.3), group sizes of 10 mice were chosen. 5 mice per group were used for detailed immunological characterisation.

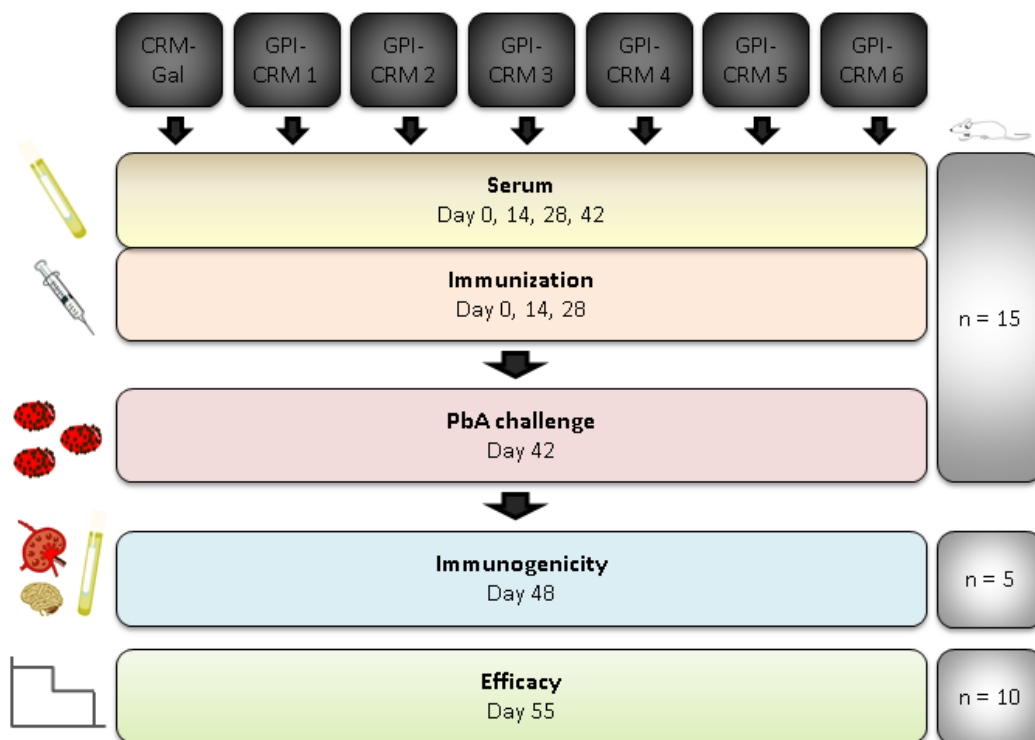


Figure 5: Study design for testing protective potential and immunogenicity of GPI-CRM₁₉₇ glycoconjugate vaccines 1-6 against CRM₁₉₇-Galactose in the murine model of cerebral malaria

C57BL/6JRj mice were divided into 7 groups each consisting of 15 animals. Serum was obtained at 14-day intervals; prior to prime, 1st and 2nd boost-vaccination and *post* infection. Control mice were immunized with galactose conjugated to CRM₁₉₇ (CRM₁₉₇-Gal), whereas study mice were immunized with GPI-CRM₁₉₇ glycoconjugates **1-6** on days 0, 14 and 28. Immunized mice were challenged on day 42 with 1×10^6 PbA-infected erythrocytes intraperitoneally. On day 6 *post* infection, 5 mice per group were sacrificed for a coherent immunological characterization (spleen cell composition, brain T cell sequestration, vaccine-specific T cell re-stimulation). The remaining 10 mice per group were used for survival studies, testing for vaccine efficacy.

3.2.2 GPI synthesis and conjugation

Synthesis of GPI1-6 was accomplished by Ankita Malik and Maurice Grube as previously described (114, 115). In general, glucosamine, mannose and inositol building blocks were synthesized and assembled individually for different GPI structures (see 3.1.6 and Fig. 6). The resulting carbohydrate backbone containing mannose, glucosamine and inositol (for GPI5 and 6) was deprotected and phosphorylation was performed for GPI2, 4, 5 and 6.

Next, GPI compounds were conjugated to the non-toxic mutant of diphtheria toxin CRM₁₉₇, to enable a T cell-dependent immune response leading to an immunological memory. Conjugation was performed by Ankita Malik, Dr. Maria Antonietta Carillo and Dr. Benjamin Schumann. Briefly, GPI glycans were reduced using Tris(2-carboxyethyl)phosphine (TCEP) and conjugated to succinimidyl 3-(bromoacetamido)propionate (SBAP) activated CRM₁₉₇. All glycoconjugates were quenched and subsequently characterized by matrix-assisted laser desorption/ionization (MALDI) and sodium dodecyl sulfate polyacrylamide gel electrophoresis (SDS-PAGE) (Fig. 7).

Further, glycoconjugates were separated by gel electrophoresis and directly stained against carrier protein with Coomassie Brilliant Blue R250 (CBB) (Sigma-Aldrich, Munich, Germany, 6104-59-2) or used for western blotting. For gel electrophoresis, glycoconjugates were diluted 1:10 in dH₂O, loading buffer was added, boiled for 5 minutes and loaded onto a 12% polyacrylamide gel. Gel electrophoresis was performed at 150 V, 150 mA for 60 minutes. Western blot transfer was accomplished at 100 V and 35 mA. The membrane was routinely tested for positive transfer with Ponceau S (Sigma-Aldrich, Munich, Germany, 6226-79-5), subsequently blocked for 2 h at RT with 5% BSA in PBS-T. Biotinylated Concanavalin-A (Vector Laboratories, Burlingame, California, B-1005) was diluted 1:500 in 1x PBS 5% BSA 0.01 mM Mn²⁺ 0.1 mM Ca²⁺ and incubated for 2 h shaking at RT. The membrane was then washed and streptavidin HRP (BD Pharmingen, Heidelberg, Germany, 557630) was added 1:500 in 1x PBS 5% BSA 0.01 mM Mn²⁺ 0.1 mM Ca²⁺ and incubated for 1 h shaking at RT. Finally, the membrane was washed again in 1x PBS 0.01 mM Mn²⁺ 0.1 mM Ca²⁺ and developed by enhanced luminol-based chemiluminescent according to manufacturer's instructions (Thermo Fisher Scientific, Darmstadt, Germany, 32109). Dual color precision protein standard (Bio-Rad Laboratories, Munich, Germany, 161-0374) was used as protein standard.

3.2.3 Animal experiments

Animals were treated strictly according to German (Tierschutz-Versuchstierverordnung) and European Law (Directive 2010/63/EU). Recommendations of the Society for Laboratory Animal Science (GV-SOLAS) and of the Federation of European Laboratory Animal Science Associations (FELASA) were followed. The Office for Health and Social Affairs Berlin (LAGeSo) approved the experiment conclusively (Permit Number: G0239/14). All efforts were made to minimize suffering.

All C57BL/6JRj mice used in this study were obtained from Janvier Labs (Saint-Berthevin, France). Mice were housed in individually-ventilated cages (IVCs) under specific-pathogen-free (SPF) conditions in the animal facility of the Federal Institute for Risk Assessment (BfR, Berlin, Germany). Mice were provided food and water *ad libitum*. Upon delivery (day -7), mice were allowed to rest for one week before the experimental setting was started (Fig. 5).

3.2.4 Immunization

On day 0, groups consisting of 15 C57BL/6JRj 5 week old female mice were prime-immunized i.p. with GPI-CRM₁₉₇ glycoconjugates **1-6** or CRM₁₉₇-Gal as a control. Two boost-immunizations were performed at 14-day intervals (day 14 and day 28).

Each mouse was injected with a total of 100 µL i.p. of either GPI-CRM₁₉₇ or CRM₁₉₇-Gal formulated with aluminum hydroxide (alum). Immunizations were performed with 5 µg GPI per vaccination. Due to diverging loadings of GPI on CRM₁₉₇, conjugates were diluted in sterile PBS accordingly. GPI-CRM₁₉₇ conjugates were formulated with aluminum hydroxide 1:2 (Alhydrogel®, Brenntag, Denmark) and rotated over night at 4°C before immunization.

In a previous unpublished study, the dose-dependent efficacy was tested for 5 µg and 9 µg GPI per immunization/mouse. As no correlation between protection and amount of immunized GPI was observed, mice were treated with 5 µg glycan per immunization in the present study.

3.2.5 Serum collection

Blood was taken from each mouse from the anterior facial vein before prime-immunization, first and second boosts and PbA infection (day 0, 14, 28, 42). Blood was allowed to coagulate for at least 30 minutes at RT and was then centrifuged at 2000 x g for 15 minutes. Then, serum was

isolated and stored at -80°C until further use. No more than 50 µL per mouse and event was withdrawn to guarantee best animal health and avoid unnecessary suffering.

3.2.6 *Plasmodium berghei* ANKA stabilates

Plasmodium berghei ANKA MRA-671 stocks were obtained from Malaria Research and Reference Reagent Resource Center (Manassas, VA, US). Stocks were used to infect female BALB/c mice. Mice were sacrificed at a parasitemia between 10-20%, cardiac bleeding was performed and pooled heparinized blood was used for the preparation of stabilates. Aliquots of 2×10^7 infected RBCs were stored in liquid nitrogen in a solution of 0.9% NaCl, 4.6% sorbitol, and 35% glycerol.

3.2.7 *Plasmodium berghei* ANKA infection

On day 42, mice were challenged i.p. with *Plasmodium berghei* ANKA MRA-671. Stabilates were quickly thawed by hand and carefully re-suspended in sterile PBS. 100 µL corresponding to 1×10^6 infected RBCs was injected intraperitoneally. 10 mice were infected with one stabilate in less than 5 minutes. Mice were randomized prior to infection, so that one mouse out of each group was infected per stabilate.

3.2.8 Parasitemia

Parasitemia was determined on days 5, 7, 9 and 12 *post* infection. Thin blood smears were taken from mouse tail veins, air-dried, fixed in 99% methanol and stained in 5% Giemsa in Giemsa staining buffer. Parasitemia was calculated by counting at least 1000 RBC, corresponding to 2-3 visual fields at 100 x magnification. Mice that did not develop parasitemia were excluded from the experiment.

3.2.9 Weight and score

It has consistently been shown that C57BL/6 mice infected with PbA develop neurological symptoms from day 6 and die between days 6 and 10 *post* infection. Hence, all mice were monitored from day 5 *post* infection for weight (days 5, 7, 10, 12 p.i.), and clinical scoring (days 5-12) according to Amante *et al.* (116). Successive points were added for respective symptoms

of infected mice: healthy (0), ruffled fur (1), hunching (2), wobbly gait (3), limb paralysis (4), convulsions (5) and coma (6). In accordance with the animal study proposal, mice scoring ≥ 3 points or a weight loss $\geq 20\%$ were euthanized. All surviving mice were euthanized 12 days *post* infection (day 54).

3.2.10 Glycan array printing and development

GPI glycans **1-6** were diluted to 1 mM and 0.2 mM in 0.1x sodium phosphate buffer (pH 7.4). Galactose, CRM₁₉₇, BSA-spacer, buffer and *S. pneumoniae* polysaccharide were further added as controls (printing pattern see Fig. 11). 25 mM and 5 mM TCEP (pH 8) was added to 1 mM and 0.2 mM glycans and proteins 20 minutes prior to printing, respectively. Glycans and proteins were printed on maleimide slides (PolyAn, Berlin, Germany) by SciFlexarrayer microarray printer (Scienion, Berlin, Germany) in triplicates in a 64-well format. Following 24 h incubation in a wet chamber at RT, slides were quenched with 0.1% (v/v) 2-mercaptoethanol in PBS 1 h at RT. Slides were washed with dH₂O, dried and stored in a desiccator until used.

Anti-GPI antibody levels in GPI-CRM₁₉₇ immunized and control mice were measured on days 0, 14, 28, 42 and on day 6 *post* infection. Printed slides were blocked with 1% BSA in 1x PBS for 1 h at RT and washed with dH₂O. Slides were dried, 1:50 serum dilutions were added per well and incubated at 4°C in a wet chamber overnight. Following incubation, serum was discarded and wells washed three times with 1x PBS 0.1% Tween. 23 μ L of the following anti-mouse IgG or IgM antibody dilutions were added and incubated for 1 h at RT in a dark wet chamber: rabbit anti-mouse IgG-FITC (diluted 1:400) (Sigma-Aldrich, Munich, Germany, F9137); donkey anti-mouse IgM-Alexa Fluor[®] 594 (1:200) (Dianova, Hamburg, Germany, 715-585-020); goat anti-mouse IgG1-AlexaFluor[®] 594 (1:400) (Thermo Fischer Scientific, Darmstadt, Germany, A21125); goat anti mouse IgG2-AlexaFluor[®] 647 (1:200) (Thermo Fischer Scientific, Darmstadt, Germany, A21241); goat anti-mouse IgG3-AlexaFluor[®] 488 (1:200) (Thermo Fischer Scientific, Darmstadt, Germany, A21151); goat anti rabbit IgG-FITC (1:400) (Dianova, Hamburg, Germany, ab6717). Slides were washed three times with PBS 0.1% Tween, rinsed carefully with dH₂O, dried and measured by Axon GenePix[®] 4300A fluorescent scanner (Molecular Devices, Sunnyvale, CA, US). The average of mean fluorescent intensities of triplicates was measured and background was subtracted for further analysis.

3.2.11 Flow cytometry

On day 6 *post* infection (day 48), 5 randomly chosen mice per group were sacrificed for the analysis of immunological parameters. For the characterization of spleen cell populations, flow cytometry analysis was performed. Spleen cells were isolated by flushing the spleen with complete RPMI medium. Next, erythrocyte lysis was performed in 90% 160 mM NH₄Cl and 10% 100 mM Tris, pH 7.4. Cells were washed twice with medium and were then kept on ice until further used. A total amount of $\sim 2 \times 10^7$ cells was obtained per spleen.

For lymphocyte staining, spleen cells were incubated with PE-Cy7-conjugated anti-CD62L Ab (eBioscience, Frankfurt am Main, Germany, 25-0621-81), PerCP-Cy5.5-conjugated anti-CD69 Ab (ebioscience, Frankfurt, Germany, 45-0691-80), FITC-conjugated anti-CD4 Ab (Miltenyi, Bergisch Gladbach, Germany, 130-097-958), APC-conjugated anti-CD8 Ab (Miltenyi, Bergisch Gladbach, Germany, 130-097-991).

Macrophages and DCs were stained with APC-conjugated anti-CD11b (eBioscience, Frankfurt am Main, Germany, 17-0112-81) and APC-Cy7-conjugated anti-CD11c (Thermo Fischer Scientific, Darmstadt, Germany, A18639), with FITC-conjugated anti-CD80 (eBioscience, Frankfurt am Main, Germany, 11-0801-85) as activation marker.

For analysis of T_{reg} cell frequencies (defined by the expression of Forkhead-Box-Protein P3), an intracellular staining was performed. First, spleen cells were incubated with APC-Cy7-conjugated anti-CD4 antibody (eBioscience, Frankfurt am Main, Germany, 47-0042-82) and APC-conjugated anti-CD25 antibody (BD Pharmingen, Heidelberg, Germany, 558643). Cells were then fixed, permeabilized and stained for FoxP3 with PE-conjugated anti-FoxP3 (BD Pharmingen, Heidelberg, Germany, 560408) according to manufacturer's instructions.

For flow cytometry of brain-sequestered T cell populations, mouse brains were homogenized in RPMI and filtered through a 40 μ m cell strainer (Corning, NY, US). Erythrocyte lysis was performed in 90% 160 mM NH₄Cl and 10% 100 mM Tris, pH 7.4. Cells were washed twice with medium and were then kept on ice. A total amount of $\sim 1 \times 10^7$ cells was obtained from one brain hemisphere. Cells were incubated with PerCP-conjugated anti-CD45 (Miltenyi, Bergisch Gladbach, Germany, 130-097-964), PE-conjugated anti-CD62L (Miletnyi, Bergisch Gladbach, Germany, 130-099-218) and APC-Cy7-conjugated anti-CD8 (BD Pharmingen, Heidelberg, Germany, 560182).

1×10^6 spleen cells and 2×10^6 brain cells were used for stainings. Fc block with anti CD16/CD32 (eBioscience, Frankfurt am Main, Germany, 14-0161-85) was performed for all cellular stainings for 15 minutes, 4°C . Cells were then incubated with specific antibody dilutions 1:200 for splenocytes and 1:100 for brain-sequestered T cells for 30 minutes at 4°C in the dark. Cells were subsequently washed twice in FACS staining buffer and measured by flow cytometry.

1×10^4 and 1×10^6 events were acquired with a FACSCanto™ II flow cytometer (BD, Franklin Lakes, NJ, US) for splenocytes and brain homogenates, respectively. Cells were gated on living cells. All data were analyzed with FlowJo software (Tree Star Inc., Ashland, OR, US).

3.2.12 ELISpot

MultiScreen® HTS ELISpot plate (Millipore, Bedford, MA, US) was pre-wetted with 20 μL 35% ethanol for one minute and then washed three times with PBS under aseptic conditions. Wells were coated with 50 μL 1:200 diluted anti-IFN- γ capture antibody in PBS (BD Pharmingen, Heidelberg, Germany, 551881) overnight at 4°C . Free binding sites were blocked with complete RPMI for 2 h at room temperature.

Spleen cells were isolated from randomly chosen mice of each group as previously described at day 6 *post* infection. 2×10^5 spleen cells were re-stimulated with 50 μL of 20 $\mu\text{g}/\text{mL}$ GPI-CRM₁₉₇ **1-6** (weight refers to weight of GPI conjugated to CRM₁₉₇) or with the corresponding concentration of CRM₁₉₇ for all compounds at 37°C for 18h. CRM₁₉₇-Gal immunized mice were re-stimulated with CRM₁₉₇-Gal. CD3/CD28 was employed as positive control (BD Pharmingen, Heidelberg, Germany, 553294 and 550275).

IFN- γ -producing cells were detected by using 50 μL of biotinylated anti-IFN- γ detection antibody diluted 1:250 (BD Pharmingen, Heidelberg, Germany, 551881) and horseradish peroxidase-conjugated avidin (1:200 dilution). The ELISpot plate was developed using 100 μL freshly prepared AEC substrate solution (BD Pharmingen, Heidelberg, Germany, 551951). The membrane was air-dried in the dark before numbers of spot forming units (sfu) were determined by Bioreader® 5000 E α (Bio-Sys, Karben, Germany). To account for cell clusters not detected by Bioreader® 5000 E α as single spot forming units (sfu), ImageJ (v. 1.47) was applied. An equivalent of 10 sfu was given for each 1% of the membrane area covered with cell clusters.

3.2.13 Cytometric bead array

Blood was taken from randomly chosen mice by cardiac puncture after CO₂ asphyxiation at day 6 *post* infection. Serum was obtained as previously described and stored at -80°C until cytokine measurement. Cytokine levels were quantified using the mouse soluble protein CBA kit (BD Pharmingen, Heidelberg, Germany, 558266). CBA was performed according to manufacturer's instructions. The following flex sets were used for cytokine quantification: IL-1β, IL-4, IL-6, IL-10, IL-12p70, TNF-α, and IFN-γ. Data was acquired with a FACSCanto™ II flow cytometer (BD, Franklin Lakes, NJ, US) and analyzed with CBA analysis FCAP array software v 1.0.1.

3.2.14 Statistical analysis

Statistical analysis was performed using GraphPad Prism software (GraphPad Software Inc., La Jolla, CA, US). Unpaired Student's *t* test was used to compare different sets of data, whereas two-way ANOVA was used to compare anti-GPI antibody levels over time between immunized and non-immunized groups. Log rank test was employed for analysis of survival between different groups. Statistical significance within figures is indicated by asterisks: * represents $p < 0.05$, ** $p < 0.01$, *** $p < 0.001$ and **** $p < 0.0001$.

4 Results

4.1 GPI synthesis, conjugation to CRM₁₉₇ and glycoconjugate characterization

Six structurally distinct GPI glycans were synthesized as described in 3.2.1 and conjugated to CRM₁₉₇ by Ankita Malik, Maurice Grube, Dr. Maria Antonietta Carillo and Dr. Benjamin Schumann. GPI1 and GPI2 were both synthesized with a Man₃-GlcN backbone, and PEthN attached to GPI2. GPI3 and GPI4 core structures were synthesized with Man₄-GlcN, and additionally PEthN attached to GPI4. GPI5 (Man₃-GlcN) and GPI6 (Man₄-GlcN) were both synthesized with attached PEthN and PI (see Fig. 6). Glycoconjugates were then tested for immunogenicity and efficacy in C57BL/6JRj mice susceptible to experimental cerebral malaria (ECM). Structurally divergent GPI-CRM₁₉₇ glycoconjugates are referred to as GPI1-GPI6 in the following (see 3.1.6 and Fig. 6).

To determine GPI loading onto CRM₁₉₇ after conjugation, matrix-assisted laser desorption/ionization (MALDI) mass spectrometry was performed by Ankita Malik (representative MALDI spectra see Fig. 7). SBAP-activated CRM₁₉₇ (CRM-AcBr) was measured as a baseline (Fig. 7 A) and change in mass of GPI-CRM₁₉₇ glycoconjugate (Fig. 7 B) was calculated for all compounds accordingly (see Table 1).

GPI-CRM	Batch	$\Delta m/z$	GPI molecular weight	Loading: GPI/CRM (% of mass)
GPI1	1	3835	781.82	4.92 (6.5% glycan)
	2	4778		6.12 (7.2% glycan)
GPI2	1	6972	904.87	7.4 (10.2% glycan)
	2	4329		5 (7% glycan)
GPI3	1	5668	943.96	5.7 (8.1% glycan)
	2	9299		9.8 (13% glycan)
GPI4	1	9865	1067.01	9.3 (14% glycan)
	2	9792		9.2 (13.7% glycan)
GPI5	1	5889	1146.99	5.2 (8.9% glycan)
	2	10240		8.9 (14.3% glycan)
GPI6	1	9322	1309.13	7.12 (13% glycan)
	2	8412		6.47 (12% glycan)

Table 1: Loading of GPI on CRM₁₉₇ determined by mass spectrometry

GPI conjugation to CRM₁₉₇ was performed in two batches. Glycan loading was determined by MALDI and expressed as GPI molecules per CRM and as percentage of weight. GPI-CRM₁₉₇ conjugates were diluted to 0.1 $\mu\text{g}/\mu\text{L}$ glycan in PBS and stored at 4°C until vaccination.

Further, CRM₁₉₇, activated CRM₁₉₇ (CRM₁₉₇-BrAc), conjugated GPI-CRM₁₉₇ (CRM₁₉₇-glycan), and the quenched GPI-CRM₁₉₇ (CRM₁₉₇-glycan-cys) were separated by gel electrophoresis (SDS-PAGE) and directly stained against protein with CBB (Fig. 7 C) or used for western blotting. Biotinylated concanavalin A was used in western blot analysis to stain against carbohydrate moieties of glycoconjugates by Ankita Malik and Dr. Maria Antonietta Carillo (Fig. 7 D). As

expected, unconjugated CRM₁₉₇ was detected at about 58kD, whereas activated CRM₁₉₇, conjugated and quenched CRM₁₉₇ glycan bands displayed a higher mass (Fig. 7 C). Carbohydrate moieties were only detected in GPI-CRM₁₉₇ conjugated samples (lane 2 and 3 Fig. 7 D)

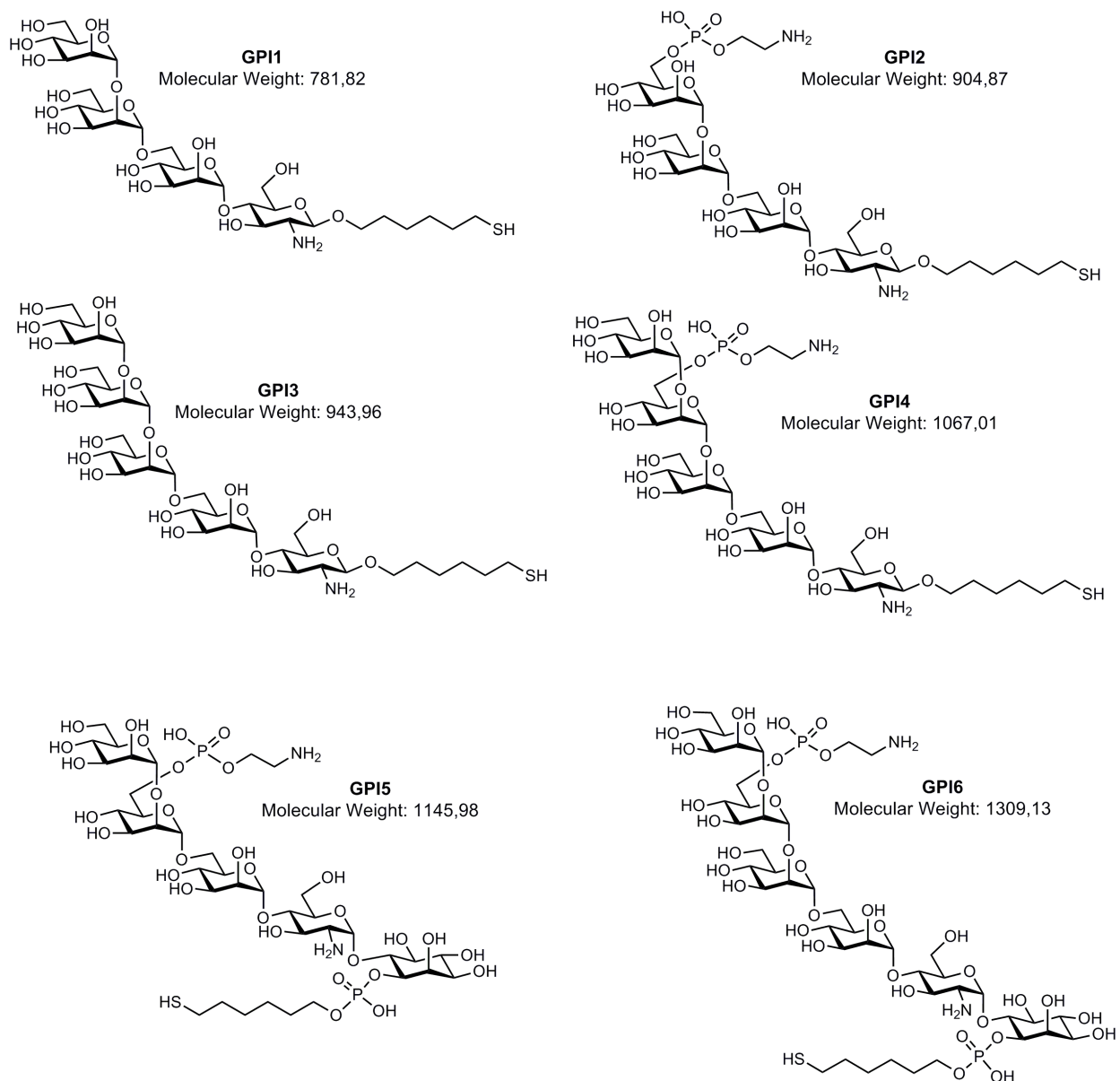


Figure 6: Six structurally different synthetic GPI glycans were conjugated to CRM₁₉₇

GPI1 and GPI2 were both synthesized with a Man₃-GlcN backbone, and PEthN attached to GPI2. GPI3 and GPI4 core structures were synthesized with Man₄-GlcN, and additionally PEthN attached to GPI4. GPI5 (Man₃-GlcN) and GPI6 (Man₄-GlcN) were both synthesized with attached PEthN and PI. Glycoconjugates were then tested in C57BL/6JRj mice susceptible to experimental cerebral malaria (ECM) for immunogenicity and efficacy. PEthN=phosphoethanolamine, GlcN=glucosamine, PI=phosphoinositol, Man₃=structure containing a three-mannose chain, Man₄=structure containing a four-mannose chain. Figure provided by Ankita Malik

All GPI-CRM₁₉₇ glycoconjugates were comprehensively characterized prior to immunization of mice. MALDI mass spectrometry of GPI-CRM₁₉₇ glycoconjugates revealed glycan loading between 4.92 (GPI1, batch 1) and 9.3 (GPI3, batch 2) on CRM₁₉₇. GPI-CRM₁₉₇ glycoconjugates were stable over time as determined by gel electrophoresis.

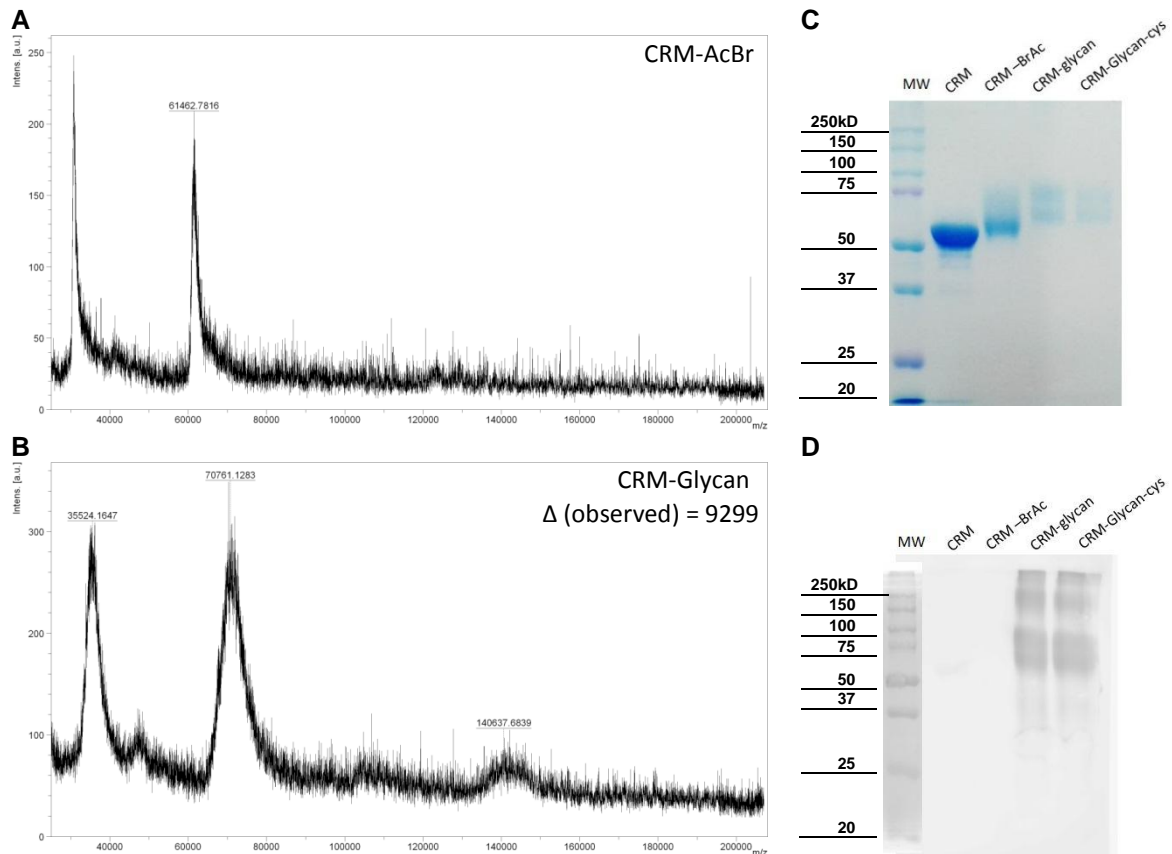


Figure 7: Representative matrix-assisted laser desorption/ionization (MALDI) mass spectrometry and gel electrophoresis (SDS-PAGE) of activated (CRM-AcBr) and conjugated CRM₁₉₇ (CRM-Glycan) of GPI-CRM₁₉₇ conjugate 3

CRM₁₉₇ loading of GPI glycoconjugates was determined by MALDI mass spectrometry. SBAP activated CRM (CRM-AcBr) was measured (A) as a baseline and change in mass of GPI-CRM₁₉₇ glycoconjugate (B) was calculated to define glycan loading onto carrier protein. The above spectra were measured for GPI-CRM₁₉₇ conjugate 3 and are representative of all glycoconjugates used. (C) CRM₁₉₇, activated CRM₁₉₇ (CRM-BrAc) and GPI-CRM₁₉₇ glycoconjugates (CRM-glycan) and quenched GPI-CRM₁₉₇ (CRM-glycan-cys) separated by gel electrophoresis (SDS-PAGE) and stained with Coomassie Brilliant Blue show bands at ~58kDa for CRM₁₉₇ and an increase in mass for GPI-conjugated CRM₁₉₇ (molecular mass CRM₁₉₇ = 58.4kDa). (D) Carbohydrate moieties detected by biotinylated Concanalin A are only visible for CRM-glycan and CRM-glycan-cys on Western blot with CRM, CRM-BrAc, CRM-glycan and CRM-glycan-cys. Glycoconjugate characterization was performed by Ankita Malik and Dr. Maria Antonietta Carillo

4.2 Immunogenicity of GPI-CRM₁₉₇ conjugates 1-6

C57BL/6 mice received one prime- and two boost-immunizations at 14-day intervals (see Fig. 5). GPI-CRM₁₉₇ treated mice received 5 µg of GPI glycan per dose, whereas CRM₁₉₇-Gal treated control mice received a corresponding dose adjusted to CRM₁₉₇ of GPI-CRM₁₉₇ treated mice. All compounds were administered with the adjuvant alum intraperitoneally. Serum samples were taken from mice for anti-GPI antibody analysis prior to immunizations, PbA challenge and on day 6 *post* infection. Anti-GPI antibody levels were determined by glycan microarray analysis and are shown for a 1:50 serum dilution.

In a previous study, GPI-KLH immunization of mice was reported to induce substantial anti-GPI antibody titers (110). In the present thesis, GPI-CRM₁₉₇ compounds **2**, **4**, **5** and **6** were highly immunogenic and mice immunized with the respective glycoconjugates developed a significant titer of anti-GPI antibodies compared to control mice (Fig. 8). In contrast, no induction of antibody response was observed against Man₃ GPI-CRM₁₉₇ conjugate **1** and only a slight increase (not significant) in Man₄ GPI-CRM₁₉₇ conjugate **3**, both glycans lacking phosphoethanolamine and inositol (Fig. 8). Interestingly, Man₃ GPI-CRM₁₉₇ conjugates with the phosphoethanolamine accessible at the end of the carbohydrate moiety (GPI**2** and **5**) induced a marked increase in anti-GPI antibodies straight after prime-immunization (day 14), whereas in Man₄ conjugates GPI-CRM₁₉₇ **4** and **6** significant anti-GPI antibody levels were observed only after 1st boost (day 28). The highest titer after 2nd boost-vaccination was observed in mice immunized with GPI-CRM₁₉₇ conjugate **5**. Antibody levels dropped for all but GPI-CRM₁₉₇ conjugate **6** immunized mice after infection, which can be explained either by malaria-induced immune suppression (see also 4.5) or a sufficient binding of anti-GPI antibodies to naturally occurring GPI after PbA infection.

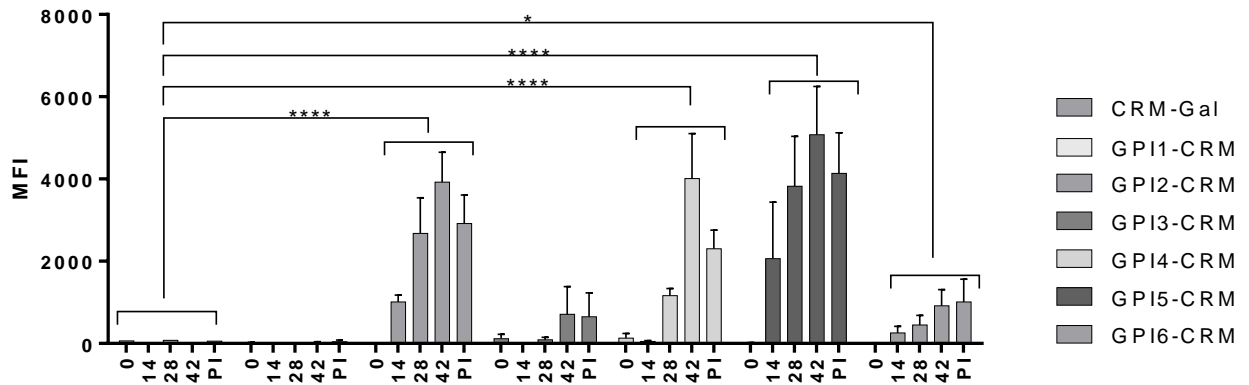


Figure 8: Anti-GPI antibody responses measured by glycan array in mice immunized with GPI-CRM₁₉₇ conjugates 1-6 over time

Serum IgG antibody level prior to immunization (day 0), after prime (day 14) and 1st and 2nd boost (day 28 and 42) as well as on day 6 post infection (PI) against CRM₁₉₇, Galactose and synthetic GPIs glycans 1-6 (from left to right). Serum was taken from CRM₁₉₇-Gal control and GPI-CRM₁₉₇ conjugates 1-6 immunized mice and diluted 1:50. Immunization with GPI-CRM₁₉₇ compounds 2, 4, 5 and 6 led to significant increase in antibody titers compared to CRM₁₉₇ control. Mean fluorescence intensity was calculated from 3 replicate values of 5 mice per group. Statistical significance was determined using two-way ANOVA to compare anti-GPI antibody levels between groups. Significance indicated by asterisks *(p<0.05) and *****(p<0.0001). MFI=mean fluorescence intensity; PI=post infection.

Endpoint anti-GPI IgG antibody level 14 days after 2nd boost (day 42) revealed a significant increase in antibodies against GPI-CRM₁₉₇ compounds 2, 4, 5 and 6 compared to CRM₁₉₇-Gal control (Fig. 9 B). No significant difference in IgM levels of GPI-CRM₁₉₇-immunized mice was detected at day 14 post 2nd boost-vaccination, which can be explained by a complete seroconversion of immunoglobulins from early IgM antibodies to IgG (Fig. 9 A).

Further, serum levels of IgG subclasses IgG1, IgG2 and IgG3 were determined at day 42 (Fig. 10). Pooled serum from 5 mice per group was serially diluted and measured in triplicates (1:50 dilution shown here). Binding of anti-GPI IgG1 and IgG2 antibodies to respective GPIs revealed patterns similar to those described above. In contrast, serum of mice immunized with GPI-CRM₁₉₇ compound 3 also displayed a significant increase in antibody binding compared to control mice (Fig. 10 A and B). Interestingly, anti-GPI IgG3 antibody levels that play an important role in anti-polysaccharide antibody responses in mice (117, 118) were highly increased for GPI-CRM₁₉₇ conjugate 5, and marginally increased for GPI-CRM₁₉₇ conjugates 2 and 4 (Fig. 10 C).

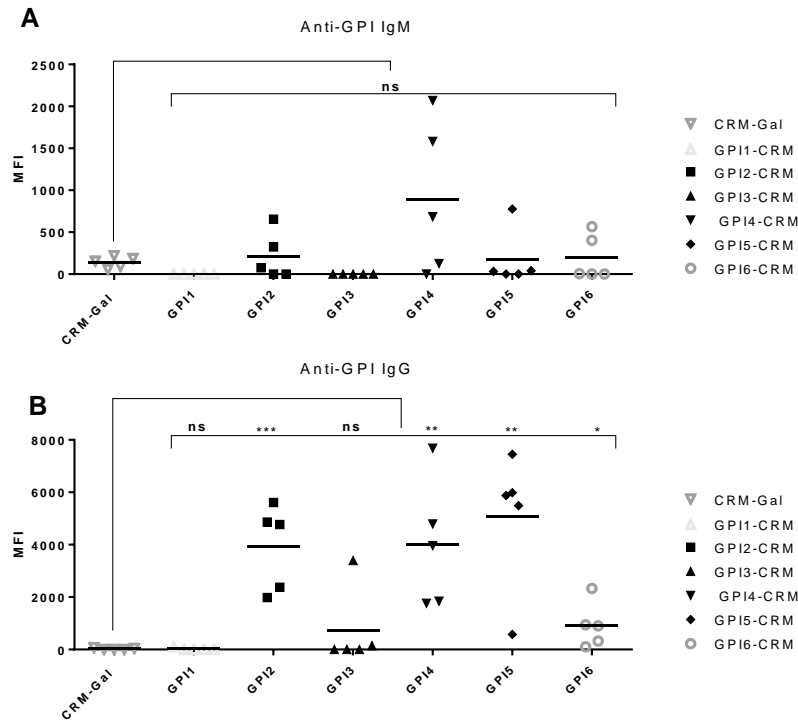


Figure 9: Endpoint anti-GPI IgG and IgM antibody titer measured by glycan array

Serum IgM (A) and IgG (B) antibodies after 2nd boost (day 42) against CRM₁₉₇ and synthetic GPI glycans 1-6 at day 42. Serum was taken from mice immunized with CRM₁₉₇-Gal and GPI-CRM₁₉₇ conjugates 1-6 and diluted 1:50. (A) Seroconversion was complete from IgM to IgG 14 days *post* 2nd boost-immunization with GPI-CRM₁₉₇ glycoconjugates. MFI calculated from 3 replicate values of 5 mice per group. (B) Immunization with GPI-CRM₁₉₇ compounds 2, 4, 5 and 6 led to significant increase in IgG antibody titers compared to CRM₁₉₇ control. Statistical significance was determined using Student's t-test, statistical significance indicated by asterisks, *(p<0.05), **(p<0.01), ns=not significant. MFI=mean fluorescence intensity.

Cross-reactivity of anti-GPI antibodies against synthetic GPI1-6 was observed across all compounds with distinct characteristics (Fig. 11 and 12). As expected, control mice immunized with CRM₁₉₇-Gal did not develop cross-reacting antibodies against GPI epitopes, but against galactose (Fig. 12; blue background). GPI-CRM₁₉₇ conjugates 1 and 3 (GPIs without phosphoethanolamine and inositol) induced cross-reacting antibodies that showed binding to GPI2, GPI3 and GPI4 glycans, whereas no reactivity was detected against inositol containing GPI5 and GPI6 (Fig. 12 A). Mice immunized with GPI-CRM₁₉₇ conjugates 2 and 4 (GPIs with phosphoethanolamine but without inositol) developed predominantly cross-reacting antibodies against PEthN containing GPIs, but notably less against the inositol containing GPI glycans 5 and 6 (also containing phosphoethanolamine) (Fig. 12 B). GPI-CRM₁₉₇ conjugates 5 and 6 (with phosphoethanolamine and inositol), by contrast, induced cross-reacting antibodies with high binding affinity to GPI5 and 6 itself, whereas binding to phosphoethanolamine containing GPI2 and GPI4 was moderate and against GPI1 and GPI3 not detectable (Fig. 12 C).

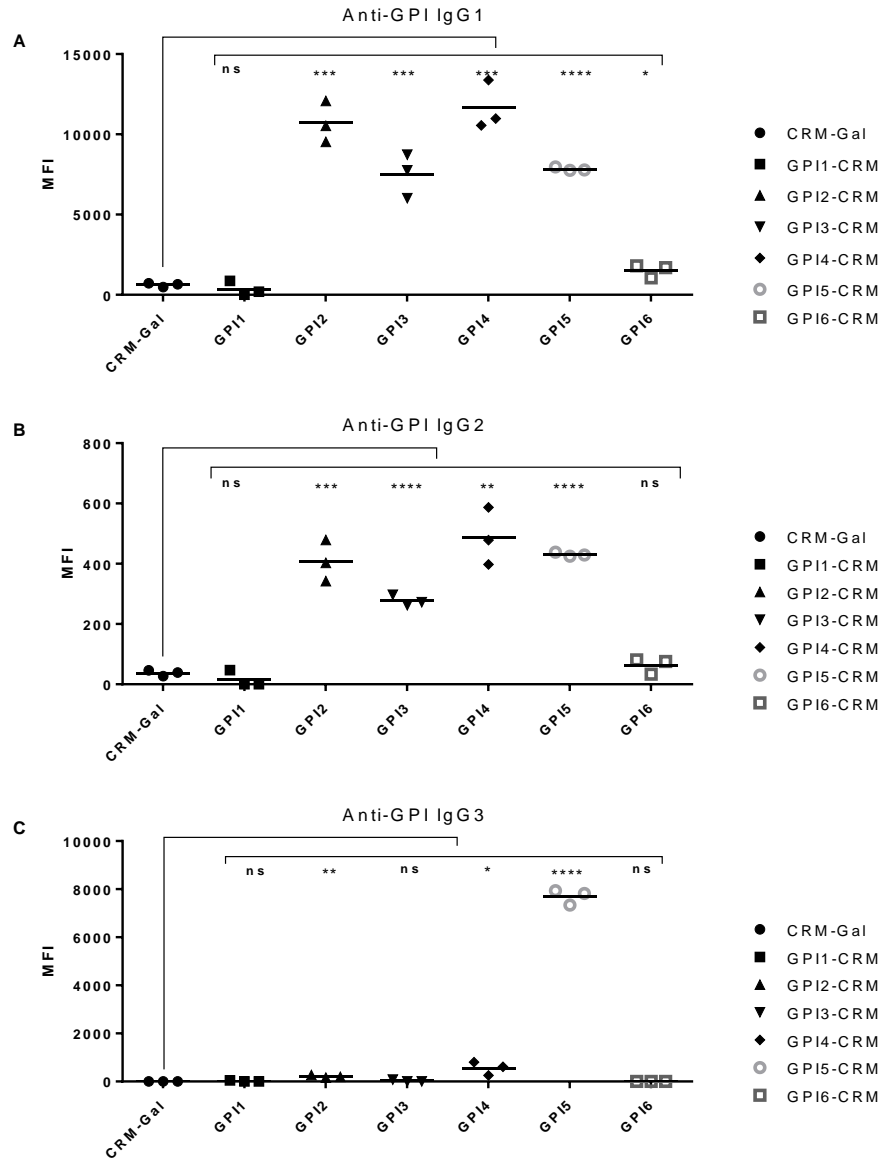


Figure 10: Endpoint anti-GPI antibody titer for IgG subclasses measured by glycan array for mice immunized with GPI-CRM₁₉₇ conjugates at day 42

Serum antibody levels at day 42 against CRM₁₉₇ and synthetic GPI glycans 1-6 in mice immunized with CRM₁₉₇-Gal and GPI-CRM₁₉₇ conjugates 1-6 for IgG subclasses IgG1 (A), IgG2 (B) and IgG3 (C). (A, B) IgG1 and IgG2 antibody levels against GPI1-6 were significantly increased in mice immunized with GPI-CRM₁₉₇ conjugates 2-5 (and -6 for IgG1) and revealed a similar pattern of antibody induction. Mice immunized with GPI-CRM₁₉₇ conjugate 1 showed only background binding, whereas GPI-CRM₁₉₇ conjugate 6 showed significantly reduced binding compared to compounds 2-5 (level of significance not shown). (C) IgG3 antibody levels were highly increased in mice immunized with GPI-CRM₁₉₇ conjugate 5, and marginally increased for GPI-CRM₁₉₇ conjugate 2 and 4. Data shown as triplicates with a mean of 1:50 diluted and pooled serum from 5 mice / group. Statistical significance was determined using Student's t-test, statistical significance indicated by asterisks *(p<0.05), *(p<0.01), *(p<0.001) and *(p<0.0001). MFI=mean fluorescence intensity

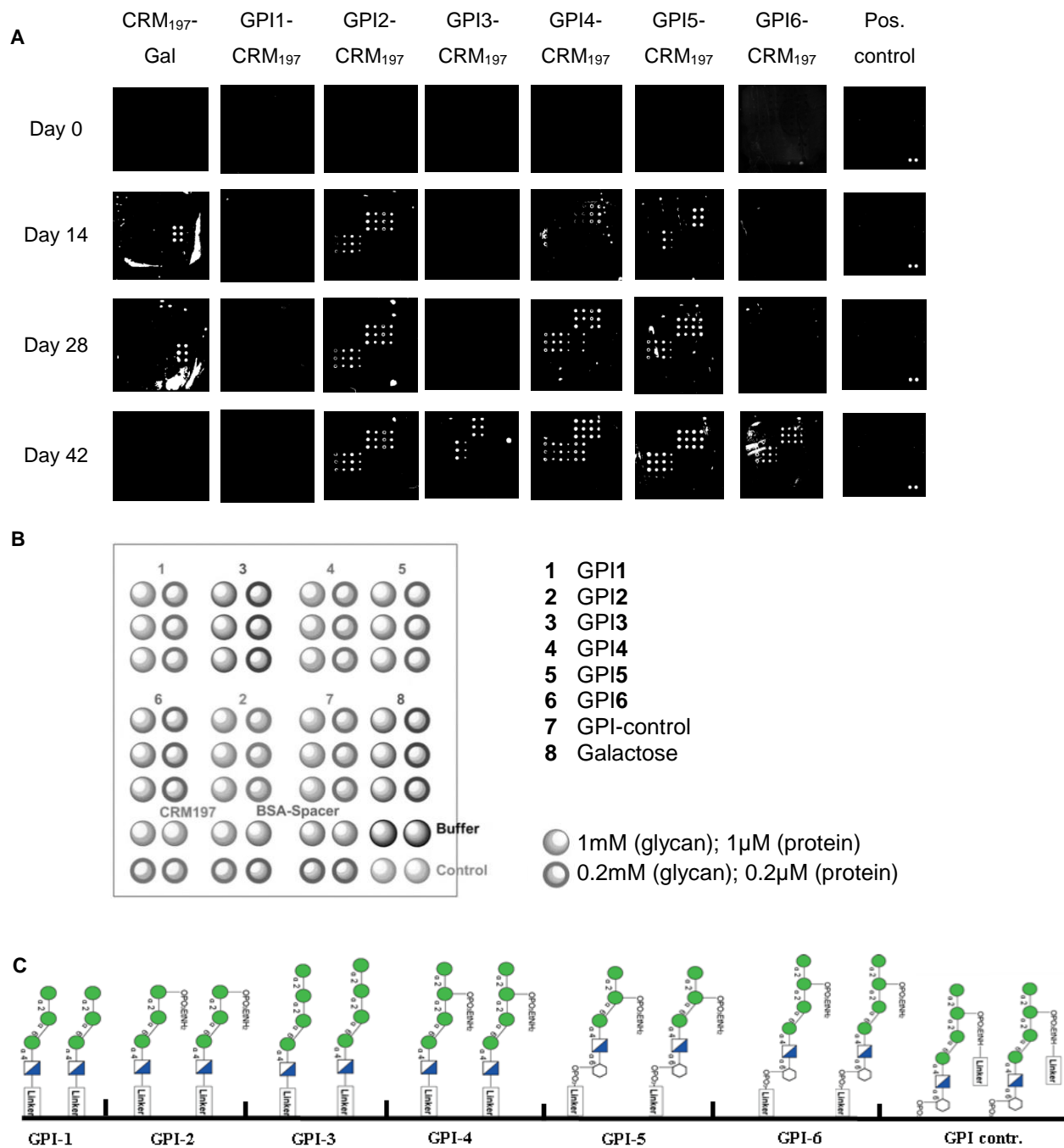


Figure 11: Anti-GPI IgG antibody were measured by glycan array in mice immunized with GPI-CRM₁₉₇ conjugates 1-6 and CRM₁₉₇-Gal

Serum antibody levels at day 42 against CRM₁₉₇, galactose, synthetic GPI glycans 1-6, GPI-control, SBAP-spacer and buffer in mice immunized with CRM₁₉₇-Gal and GPI-CRM₁₉₇ conjugates 1-6. (A) Representative microarray wells incubated with serum of mice immunized with GPI-CRM₁₉₇ conjugates 1-6 (days 0-42) and rabbit anti *S. pneumoniae* antibodies as positive control. (B) Microarray printing pattern of maleimide-treated glass slides (PolyAn, Berlin, Germany). (C) GPI glycans 1-6 were printed on maleimide slides (PolyAn, Berlin, Germany) by SciFlexarrayer microarray printer (Sciencion, Berlin, Germany) in triplicates in a 64 well format.

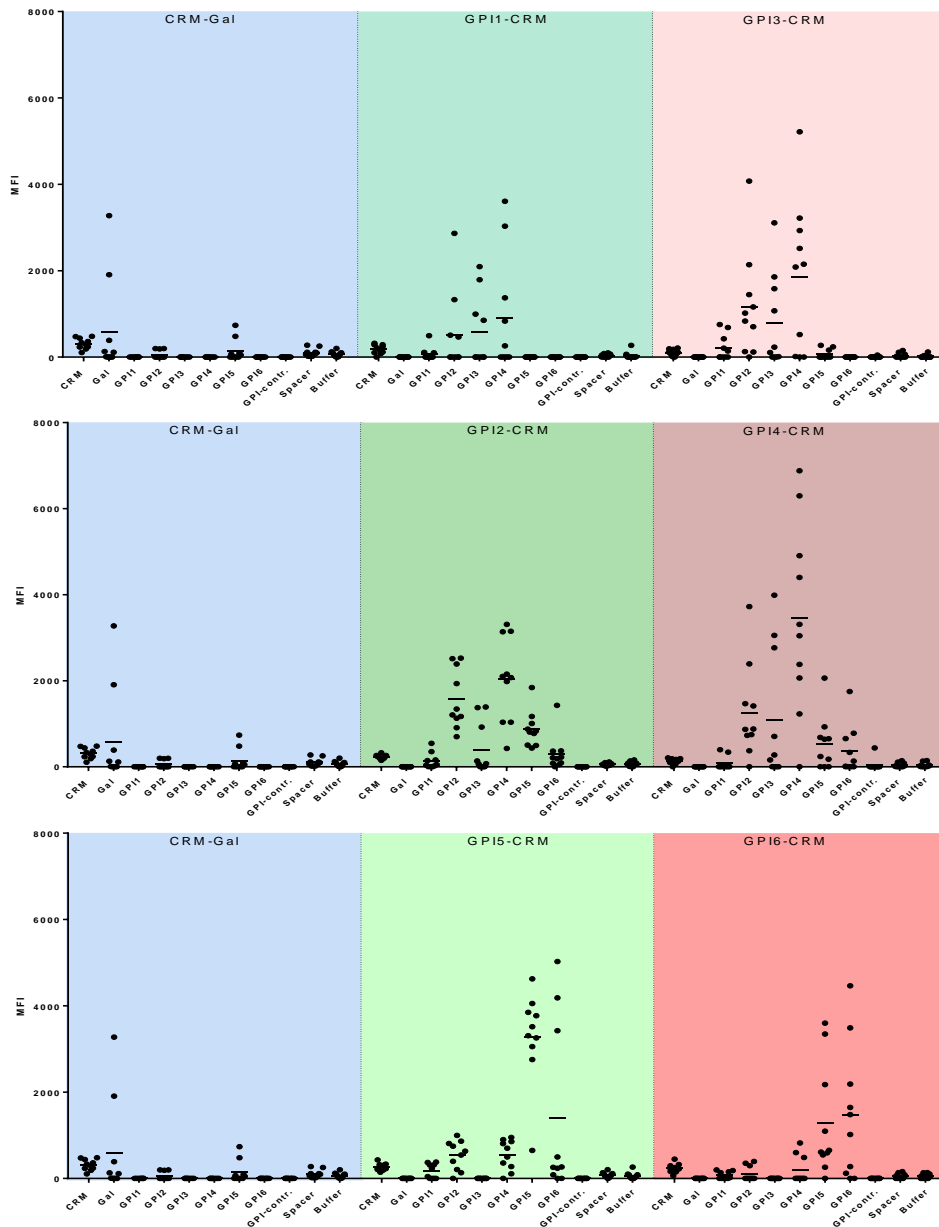


Figure 12: Cross-reactivity of anti-GPI IgG antibodies measured by glycan array in mice immunized with GPI-CRM₁₉₇ conjugates 1-6 and CRM₁₉₇-Gal after 2nd boost (day 42)

Serum antibody levels at day 42 against CRM₁₉₇, galactose, synthetic GPI glycans 1-6, GPI-control, SBAP-spacer and buffer in mice immunized with CRM₁₉₇-Gal and GPI-CRM₁₉₇ conjugates 1-6. Sera of 10 mice per group were analyzed. (A, B and C) Only 2 out of 10 mice immunized with CRM₁₉₇-Gal developed IgG antibodies against galactose. No cross-reactivity against synthetic GPI constructs 1-6 was detected (A) Serum of mice immunized with GPI1 did not contain self-recognizing IgG antibodies, but interacted with those synthetic GPIs not containing inositol (GPI2-4). Mice immunized with GPI2 developed IgG antibodies that exhibited distinct cross-reactivity against synthetic GPIs with phosphoethanolamine (GPI2, 4, 5 and 6), but also against GPI3 mannoses. (B) Serum of mice immunized with GPI3 showed IgG antibody cross-reactivity against all synthetic GPIs without inositol (GPI2, 3 and 4), however not against GPI1. GPI4 immunized mice developed IgG antibodies that cross-reacted with synthetic GPIs containing phosphoethanolamine (GPI2, 4, 5 and 6), and also against GPI3 core structure mannoses. (C) GPI5 glycoconjugates generated cross-reacting IgG antibodies markedly against GPIs containing inositol (GPI5 and 6) and also GPI2 and 4, both containing phosphoethanolamine in immunized mice. Just as GPI5, mice immunized with GPI6 developed cross-reacting IgG predominantly against inositol containing GPI5, and to a lower degree against GPIs containing phosphoethanolamine.

In conclusion, glycan array analysis revealed structure-activity relationships for different synthetic GPIs. Length (Man₃ vs. Man₄ in GPI1 and 3) as well as the presence of phosphoethanolamine and inositol had an impact on immunogenicity. Cross-reactivity analyses showed that inositol is immunodominant over phosphoethanolamine, which is again immunodominant over mannose moieties (Fig. 12). Finally, inositol seems to hinder cross-reactive antibodies to effectively bind to otherwise immunogenic GPI structures.

4.3 Protection of GPI-CRM₁₉₇ vaccinated mice from ECM

To evaluate vaccine efficacy, mice were challenged with 1×10^6 PbA-infected erythrocytes intraperitoneally on day 42 and monitored for weight, clinical scoring, parasitemia and survival from day 5 *post* infection. All mice developing symptoms of experimental cerebral malaria (scoring ≥ 3 points *i.e.* wobbly gait, paralysis, convulsions or coma) were immediately euthanized. Control mice vaccinated with CRM₁₉₇-Gal succumbed to experimental cerebral malaria in 100% of cases by day 9, demonstrating the high virulence of the PbA strain used. All mice immunized with GPI-CRM₁₉₇ showed an improved survival rate compared to control groups, ranging from 11% to 40% (groups of 9-10 mice) (Fig. 13). In particular, GPI-CRM₁₉₇ conjugate 5 treated mice were significantly protected against PbA-induced encephalopathy, with 40% survival (Fig. 13 F). Mice immunized with GPI conjugates 1-4, and 6 were not significantly protected compared to control mice, with survival rates ranging between 11% and 30%. In line with previously published observations, GPI-CRM₁₉₇ immunization did not impact the level of parasitemia compared to control mice (Fig. 14) (110). The high standard errors at day 12 reported for individual groups are a result of the low number of surviving mice in each group. Mice that did not develop parasitemia were excluded from the experiment (one each in GPI-CRM₁₉₇ conjugate 3 and 4 treated mice). In correlation with survival, clinical scores of PbA-challenged mice were highest for CRM₁₉₇-Gal control mice and lowest for mice immunized with GPI-CRM₁₉₇ conjugate 5, supporting the protective potential elicited by the glycoconjugate used in this group of mice (Fig. 15).

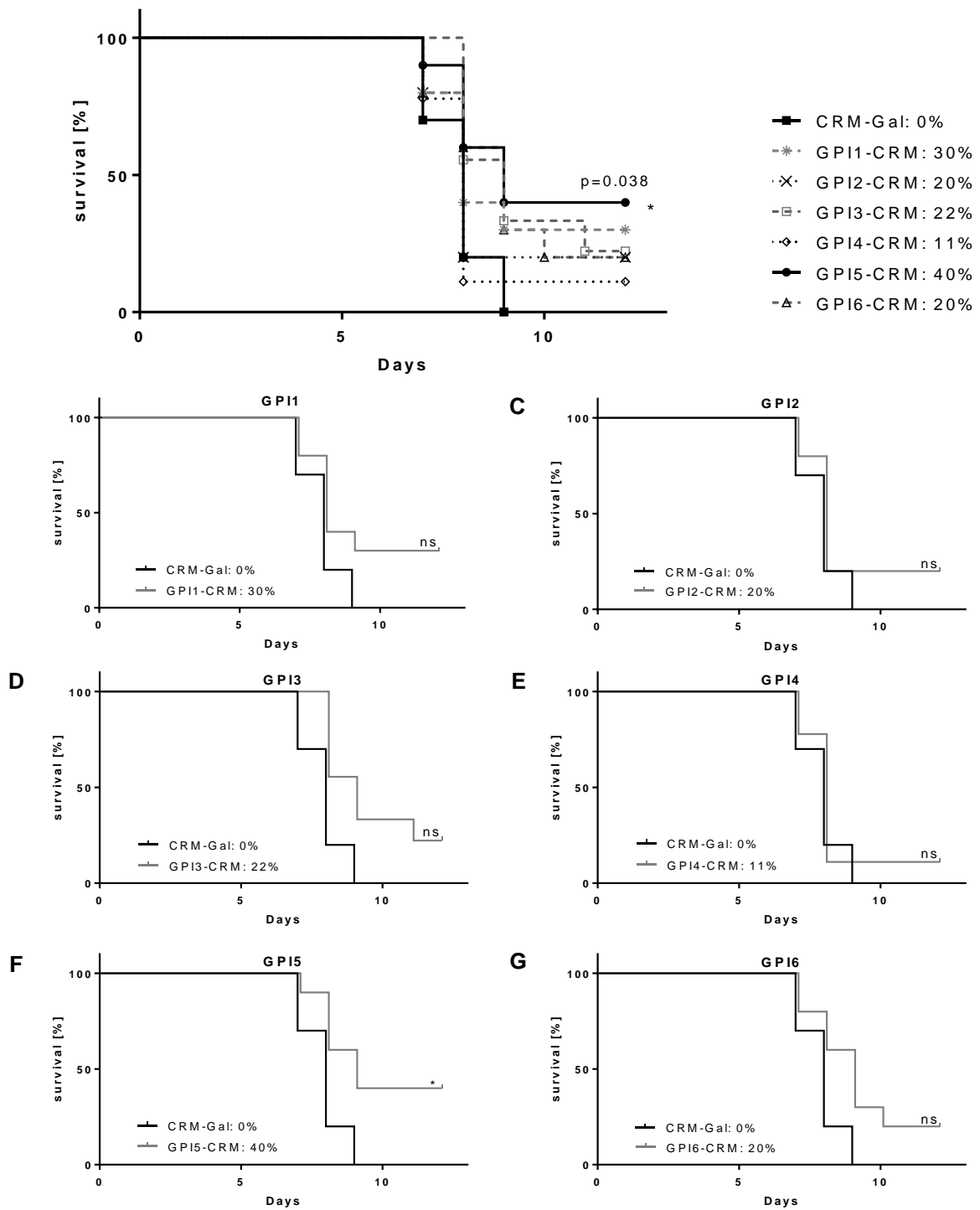


Figure 13: Protection against experimental cerebral malaria in mice immunized with GPI-CRM₁₉₇

(A) C57BL/6 mice immunized with GPI-CRM₁₉₇ conjugates displayed a higher survival rate compared to control mice immunized with CRM₁₉₇-Gal. (B-F) Survival of mice immunized with GPI-CRM₁₉₇ glycoconjugate 1-6 against CRM₁₉₇-Gal control mice: Survival was significantly higher in mice immunized with GPI-CRM₁₉₇ conjugate 5. Survival data based on 9-10 mice per group. Mice that did not develop parasitemia were excluded from the study (one mouse each in GPI-CRM₁₉₇ glycoconjugate 3 and 4 immunized groups). Log rank test was employed for analysis of survival. Statistical significance indicated by asterisks *(p<0.05)

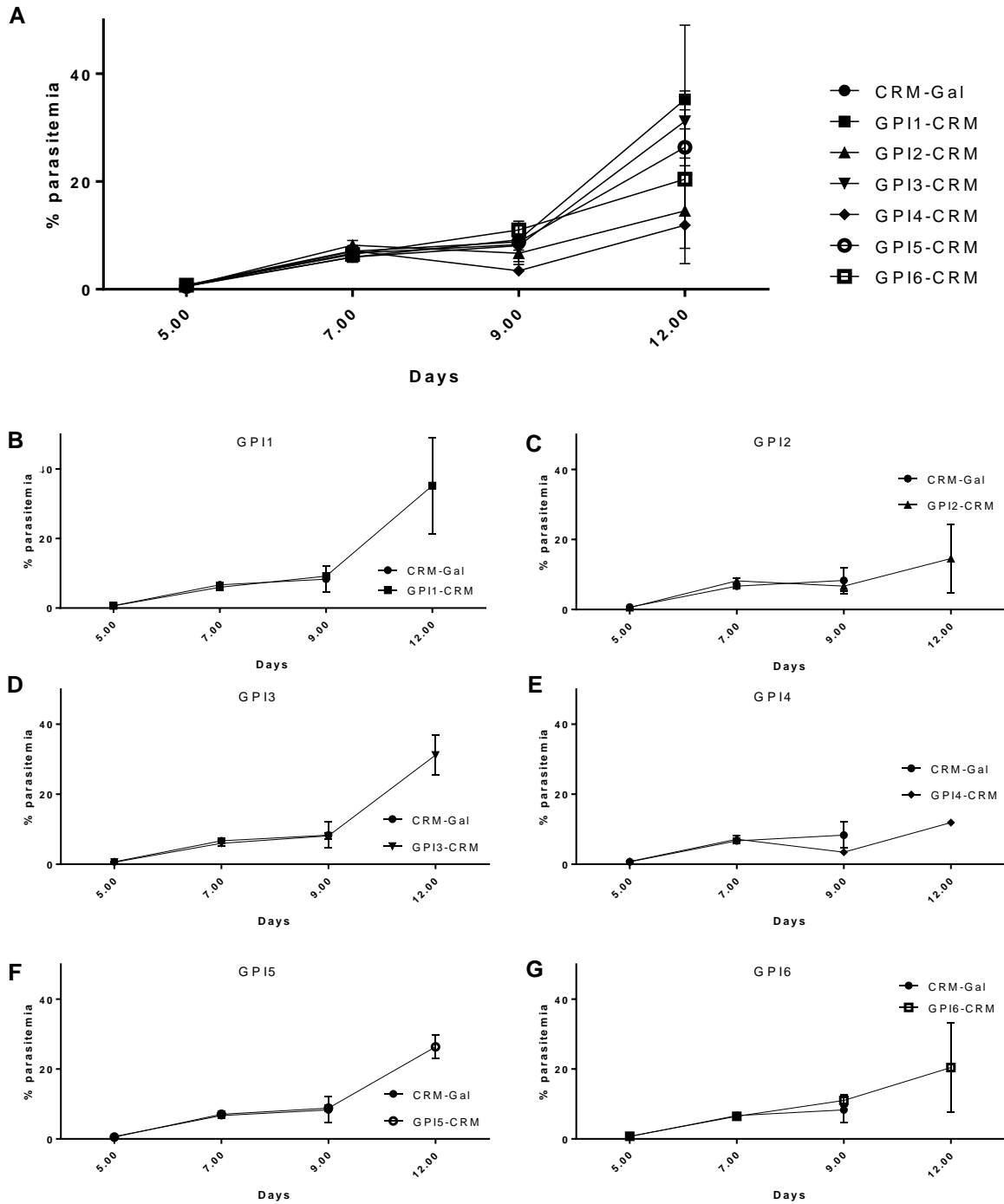


Figure 14: Parasitemia of mice immunized with GPI-CRM₁₉₇

(A) C57BL/6 mice displayed no significant difference in parasitemia between GPI-CRM₁₉₇ conjugate immunized and non-immunized mice. (B-F) Parasitemia of mice immunized with GPI-CRM₁₉₇ glycoconjugate 1-6 against CRM₁₉₇-Gal control mice: Numbers of pRBC increased in all mice after *P. berghei* ANKA challenge. Mice that did not develop parasitemia were excluded from the study (one mouse each in GPI-CRM₁₉₇ glycoconjugate 3 and 4 immunized groups). Parasitemia is shown as mean % \pm SEM for surviving mice (1-10 mice per group). Student's t-test was used to determine differences in parasitemia between study and control groups.

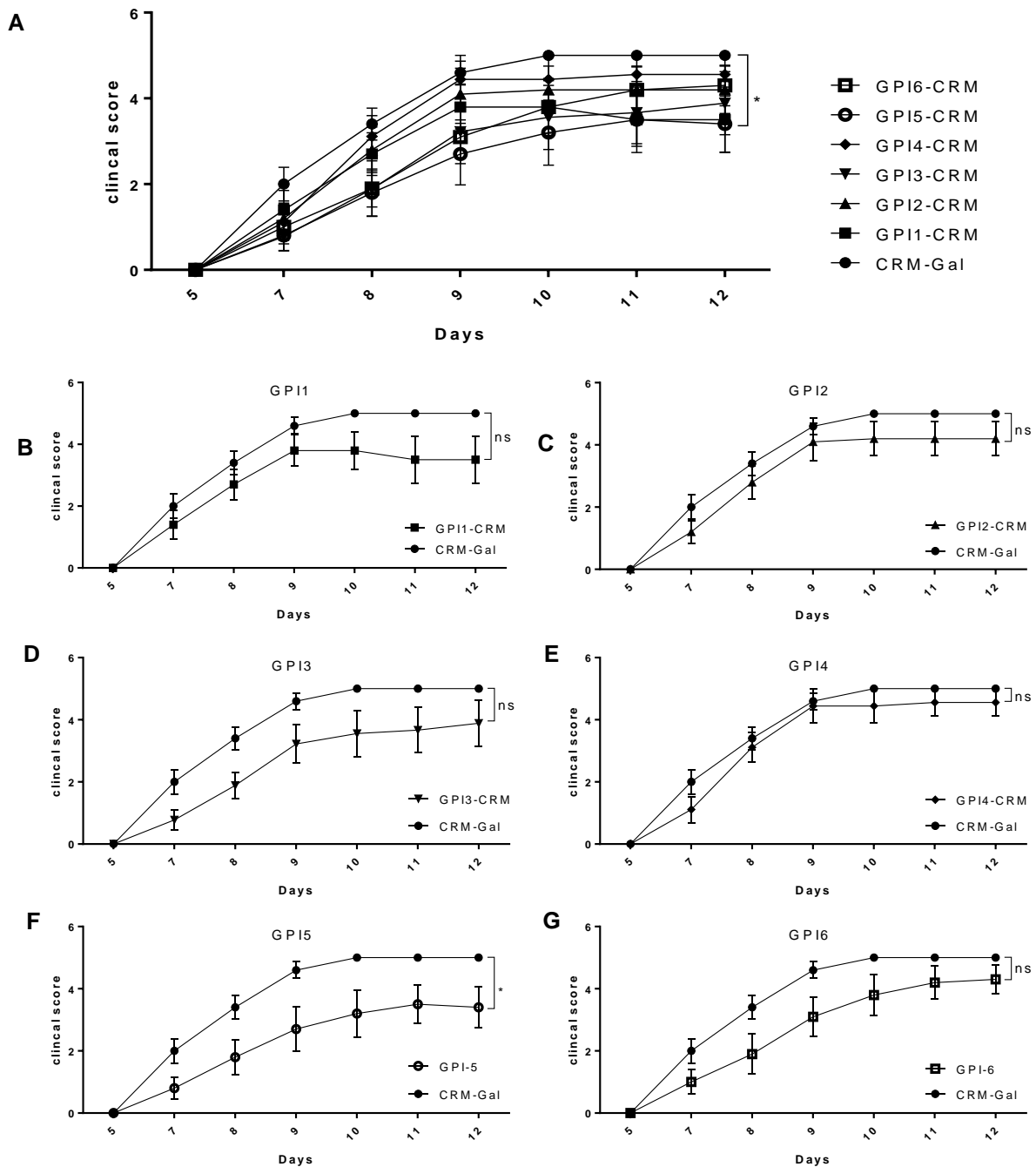


Figure 15: Clinical scoring of mice immunized with GPI-CRM₁₉₇

(A) All mice were monitored for clinical symptoms from day 5 *post* infection. Successive points were added for respective symptoms of infected mice: healthy (0), ruffled fur (1), hunching (2), wobbly gait (3), limb paralysis (4), convulsions (5) and coma (6). Mice scoring ≥ 3 points were euthanized, and dead mice were given a score of 5 points. (B-F) Clinical scoring of mice immunized with GPI-CRM₁₉₇ glycoconjugate 1-6 against CRM₁₉₇-Gal control mice: Mice immunized with GPI-CRM₁₉₇ conjugate 5 displayed significantly lower scores compared to control mice at day 12 *post* infection. Survival data are based on 9-10 mice per group. Mice that did not develop parasitemia were excluded from the study (one mouse each in GPI-CRM₁₉₇ glycoconjugate 3 and 4 immunized groups). Scores are shown as mean \pm SEM for surviving mice (1-10 mice per group). Student's t-test was used to determine differences in scoring between study and control groups. Statistical significance indicated by asterisks *($p < 0.05$)

4.4 Vaccine-specific T cell response

In carbohydrate-based vaccines, the hapten is covalently linked to an immunogenic carrier protein to enable MHC-II presentation, priming of carrier-peptide-specific CD4⁺ T cells and carbohydrate-specific B cell activation (83). This induces an immunological memory that unconjugated carbohydrates are incapable of eliciting. In this study, synthetic GPI compounds **1-6** were conjugated to CRM₁₉₇ (see 3.2.2).

In order to characterize immunized mice immunologically, 5 mice in each group were sacrificed on day 6 *post* infection for evaluation of spleen cell population, brain T cell sequestration and serum cytokine levels. CRM₁₉₇ and GPI glycoconjugate-specific T cell responses were determined using IFN- γ production of T cells upon re-stimulation of splenocytes with their immunized GPI-CRM₁₉₇ conjugate vaccine or CRM₁₉₇ alone by ELISpot analysis on day 6 *post* infection (Fig. 16). Previous results have shown that the number of IFN- γ -producing CRM₁₉₇-specific T cells was first observed after 2nd boost-vaccination (unpublished observations). In this study, a baseline of CRM₁₉₇-specific IFN- γ ⁺ T cells in all vaccinated but not in untreated animals was observed. A significant increase in T cell activation of GPI-CRM₁₉₇ re-stimulated splenocytes compared to CRM₁₉₇ alone was shown in all groups. Interestingly, this trend was also observed in mice immunized with CRM₁₉₇-Gal, illustrating that GPI glycoconjugates seem to be taken up more efficaciously compared to CRM₁₉₇ alone, hence leading to a higher INF- γ response (Fig. 16 A). As hypothesized by Avci *et. al* (2011), MHC-II presentation of GPI-CRM₁₉₇ glycoconjugates might be enhanced compared to carrier protein CRM₁₉₇ alone, therefore leading to a higher IFN- γ production of primed T cells. No difference in the number of IFN- γ spot forming units (sfu) was detected between mice immunized with either CRM₁₉₇-Gal or GPI-CRM₁₉₇ conjugate. Compared to untreated mice (NI), T cell stimulation was however significantly increased (Fig. 16 B). In conclusion, ELISpot analysis reinforces the notion previously observed that GPI-CRM₁₉₇ glycoconjugates effectively prime T cells and hence qualifies as a potential glycoconjugate vaccine candidate.

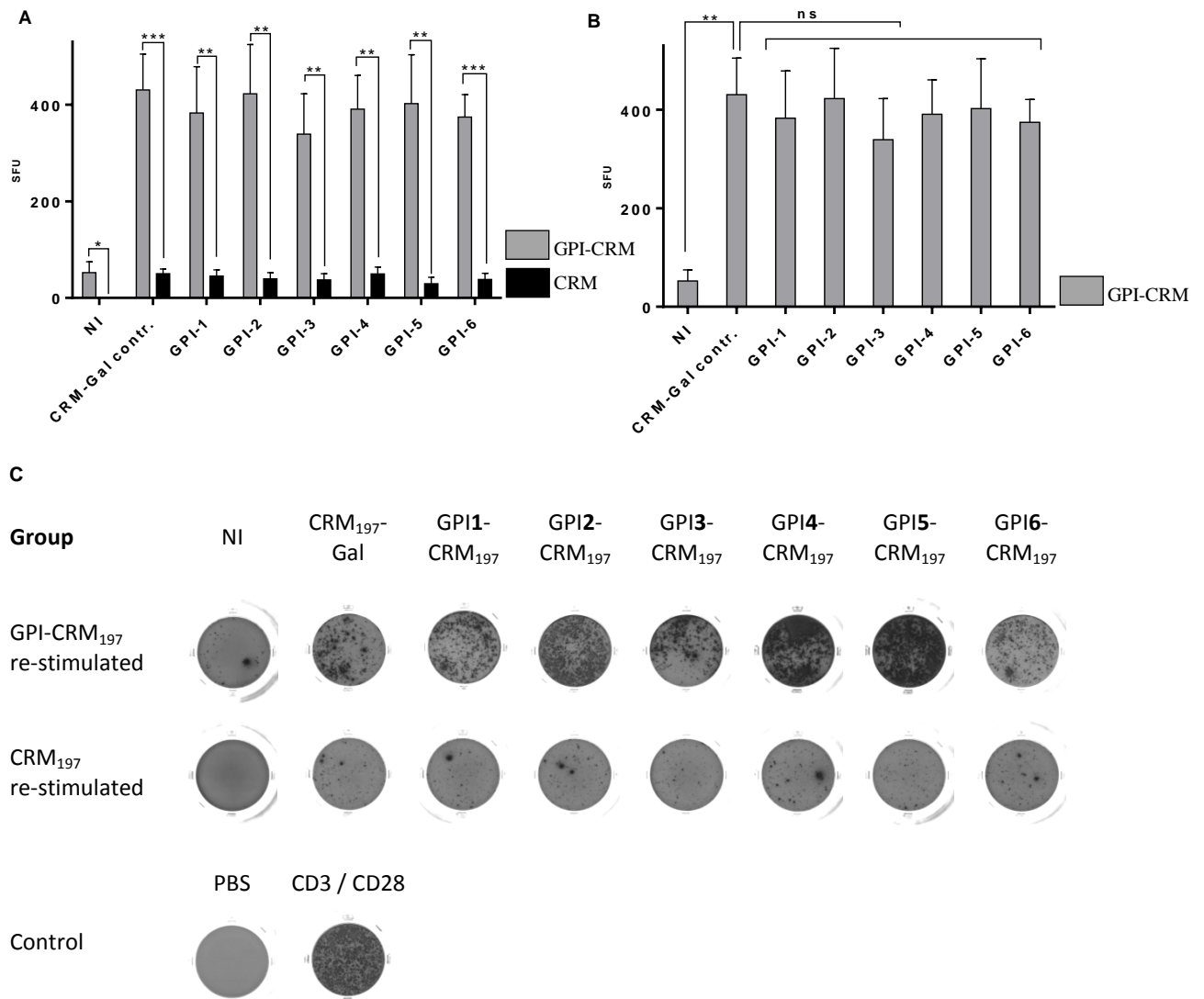


Figure 16: Vaccine-specific T cell response in mice immunized with GPI-CRM₁₉₇ post infection

(A) Mice were immunized with GPI-CRM₁₉₇ glycoconjugates and challenged with *P. berghei* ANKA. On day 6 *post* infection, 5 mice per group were sacrificed, spleen cells were isolated and re-stimulated with respective glycoconjugates or CRM₁₉₇ alone. CRM₁₉₇-specific IFN- γ ⁺ T cells were detected in all vaccinated but not in untreated animals (black bar). Activation of IFN- γ -producing T cells was significantly increased when re-stimulated with GPI-CRM₁₉₇ and CRM₁₉₇-Gal glycoconjugates (grey bars). (B) Re-stimulation with glycoconjugates led to a significant increase in T cell response compared to non-treated animals. (C) Representative ELISpot membranes of wells containing re-stimulated spleen cells. Spot forming units of IFN- γ -producing cells were developed, spots were detected and counted by ELISpot reader (Bioreader@5000- α , BioSys, Karben, Germany). Statistical significance was determined using Student's t-test, statistical significance is indicated by asterisks *(p<0.05), **(p<0.01) and ***(p<0.001). SFU=spot forming units.

4.5 Spleen cell composition

4.5.1 T cell frequency and activation

Spleen cells were isolated from PbA-infected mice treated with CRM₁₉₇-Gal or GPI-CRM₁₉₇ glycoconjugates on day 6 *post* infection. CD4⁺ and CD8⁺ T cell frequency and cellular activation was determined by flow cytometry to investigate a potential protective effect of GPI-CRM₁₉₇ immunization. It was previously shown that CD4⁺ T cell levels were slightly increased after 1st and 2nd boost-vaccination which can be explained by glycoconjugate vaccine activation of CD4⁺ T cells (data not shown). Generally, there were no significant alterations in splenic T cell populations or activation detected during vaccination, confirming that no unspecific side effects were elicited by GPI glycoconjugate vaccines (unpublished observations). Spleen T cell frequency and T cell activation in GPI-CRM₁₉₇ immunized and PbA-challenged mice were now investigated. Due to the acute inflammatory response during PbA infection, lymphopenia was observed in CD4⁺ T cells but not in CD8⁺ T cells (Fig. 17 B and E). This difference might be explained by CD4⁺ T cell depletion (*i.e.* crucial role of CD4⁺ T cells for parasite clearance) and also by the premature pre-ECM disease stage, where CD8⁺ T cells have not yet significantly contributed to disease pathology (*i.e.* no significant CD8⁺ T cell sequestration). Cellular activation, measured by the expression of the activation marker CD69, was however marked in both CD4⁺ and CD8⁺ T cells compared to non-infected controls (Fig. 17 C, F). Interestingly, CD4⁺ and CD8⁺ T cell activation was slightly decreased in mice immunized with GPI-CRM₁₉₇ conjugate **5** (and also GPI-CRM₁₉₇ conjugate **3**), which is consistent with the lower level of pro-inflammatory serum cytokines in this group as described in 4.6.

4.5.2 Regulatory T cells

A role for regulatory T cells (T_{reg}) contributing to ECM pathogenesis has been described previously (116). High levels of T_{reg} were also reported for *M. tuberculosis* vaccination and are a current challenge in anti-tumor vaccination, diminishing potential vaccine immunogenicity and efficacy (119, 120). The proportion of T_{reg} was measured by intracellular staining of the transcription factor forkhead-box-protein P3 (FoxP3). An increase in T_{reg} frequency has been detected after GPI glycoconjugate boost-vaccinations (unpublished observations) and on day 6 *post* infection. T_{reg} were significantly increased in all PbA-challenged groups compared to the non-infected control group (Fig. 18). No significant difference was observed between mice vaccinated with CRM₁₉₇-Gal and those with GPI-CRM₁₉₇, suggesting that GPI antitoxic

vaccination does not impact regulatory T cell frequency. High vaccine-induced T_{reg} levels after immunization however might have impacted vaccine efficacy.

4.5.3 Macrophage and dendritic cell frequency and cellular activation

Macrophages and dendritic cells play a crucial role during initial stages of malaria infection, establishing the link to the adaptive immune response against *Plasmodium* parasites. Downstream pro-inflammatory effects of macrophages and dendritic cells have been associated with experimental cerebral pathology and human cerebral malaria pathogenesis (121, 122). To test whether GPI glycoconjugate vaccination had an impact on macrophage and dendritic cell composition of the spleen, cells were stained against CD11b (macrophages), CD11c (dendritic cells) and CD80 (activation marker) and quantified by flow cytometry. Dendritic cell and macrophage proportions were decreased (not significantly) upon PbA infection in all challenged mice compared to non-infected controls (Fig. 19 B and E). A significant increase in macrophage and dendritic cell activation was detected in challenged mice, again with a slightly lower activation pattern for mice immunized with GPI-CRM₁₉₇ conjugates (most distinct for conjugate **5**) compared to CRM₁₉₇-Gal control mice (Fig. 19 C and F). Again, these results match previous findings of low cytokine levels and decreased T cell activation in mice immunized with GPI-CRM₁₉₇ conjugate **5** and **3** (as described in section 4.5.1 and 4.6).

4.6 Serum cytokine levels

Serum levels of pro- and anti-inflammatory cytokines (IL-1 β , IL-6, IL-12, TNF- α , IFN- γ , IL-10, IL-4) were measured by cytometric bead array (CBA) before and after PbA challenge (days 42 and 48) of 5 mice per group. GPI-CRM₁₉₇ glycoconjugate **1-6** immunized and control mice displayed low or only background levels of IFN- γ , TNF- α , IL-6 (Fig. 20 A, C, E) and IL-1 β , IL-12, IL-10, IL-4 (data not shown) after 2nd boost-vaccination, indicating that GPI-CRM₁₉₇ glycoconjugates did not induce an unspecific immune response. To investigate whether GPI-CRM₁₉₇ immunization modified the humoral immune responses to PbA infection, serum cytokines of mice were further measured on day 48 (day 6 p.i.).

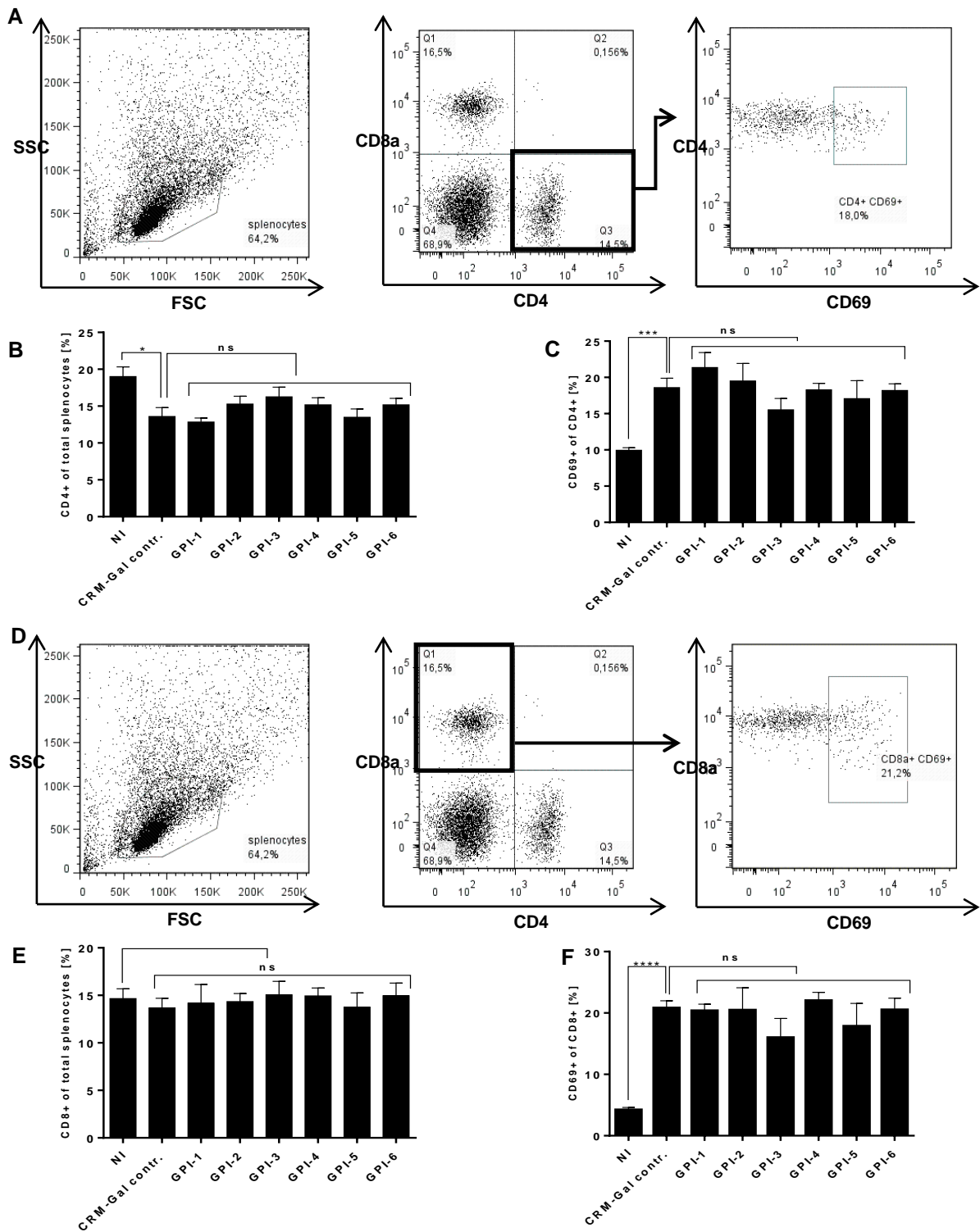


Figure 17: Spleen CD8⁺ and CD4⁺ T cell activation in immunized and *P. berghei* ANKA-challenged mice

(A, D) Representative gatings of activated CD4⁺ and CD8⁺ spleen T cells. Spleen cells were isolated from immunized and *P. berghei* ANKA-infected mice on day 6 *post* infection and quantified by flow cytometry. (B, E) Due to the acute inflammatory response, lymphopenia was observed with regard to CD4⁺ T cells but not to CD8⁺ T cells. (C, F) Cellular activation (measured by activation marker CD69) was marked in both CD4⁺ and CD8⁺ T cells compared to non-infected controls, with a slight non-significant decrease seen for mice immunized with GPI-CRM₁₉₇ conjugate 3 and 5. Statistical significance was determined using Student's t-test, statistical significance indicated by asterisks *(p<0.05), ***(p<0.001) and ****(p<0.0001).

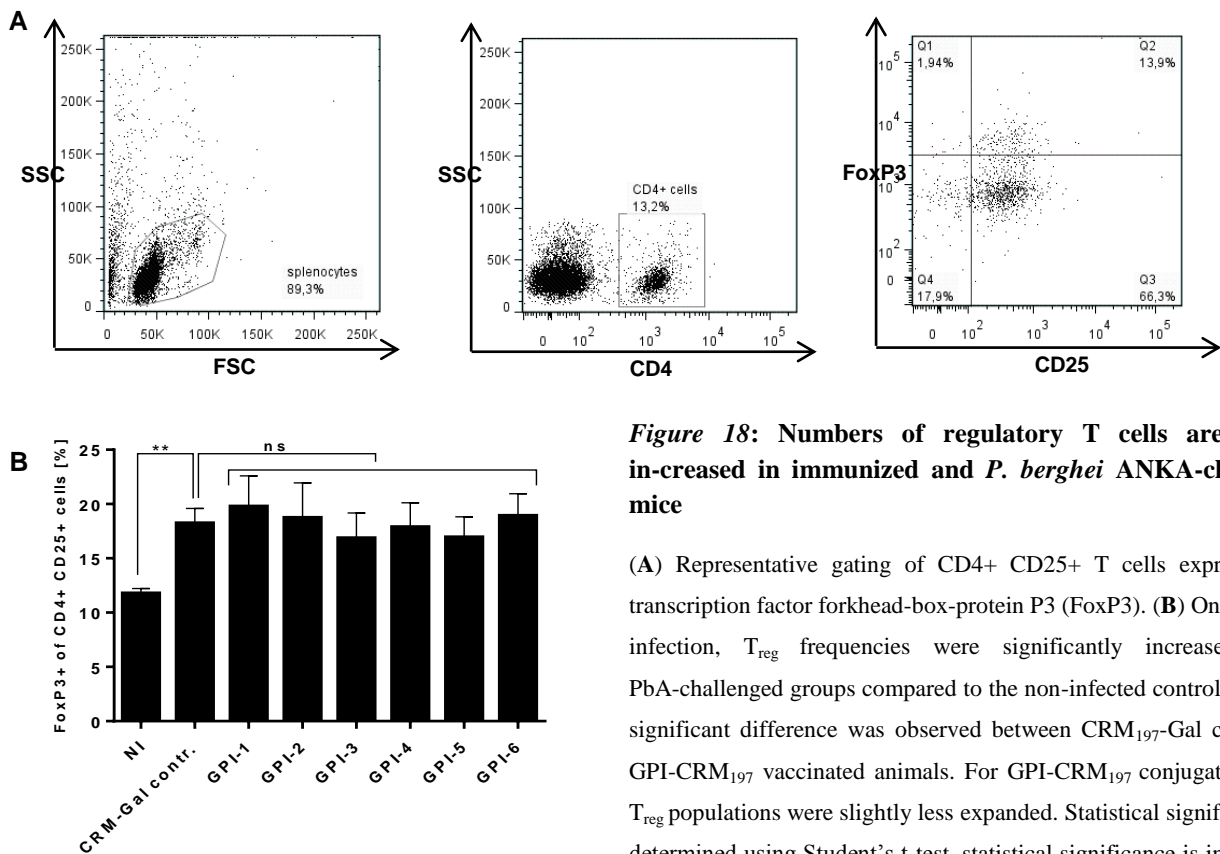


Figure 18: Numbers of regulatory T cells are equally in-creased in immunized and *P. berghei* ANKA-challenged mice

(A) Representative gating of CD4⁺ CD25⁺ T cells expressing the transcription factor forkhead-box-protein P3 (FoxP3). (B) On day 6 *post* infection, T_{reg} frequencies were significantly increased in all PbA-challenged groups compared to the non-infected control group. No significant difference was observed between CRM₁₉₇-Gal control and GPI-CRM₁₉₇ vaccinated animals. For GPI-CRM₁₉₇ conjugate 5 and 3, T_{reg} populations were slightly less expanded. Statistical significance was determined using Student's t-test, statistical significance is indicated by

Generally, PbA-infected groups showed significantly increased levels of IFN- γ , TNF- α and IL-6 compared to the non-challenged state (Fig. 20 A, C, E). TNF- α was not significantly increased in mice immunized with GPI-CRM₁₉₇ conjugate 1 and 5, and at a level comparable with that in conjugates 3 and 4 (Fig. 20 C). The level of pro-inflammatory cytokines *post* infection varied between GPI-CRM₁₉₇ vaccinated mice (Fig. 20, B, D, F). While mice immunized with GPI-CRM₁₉₇ compound 6 showed consistently increased levels of IFN- γ , TNF- α and IL-6, those were considerably reduced for mice immunized with compound 5. However, no significant difference in cytokine levels was seen in GPI-CRM₁₉₇ vaccinated versus CRM₁₉₇-Gal control mice (Fig 20, B, D, F). Levels of serum cytokines IL-1 β , IL-12, IL-10 and IL-4 were only marginally and inconsistently increased after PbA challenge (data not shown).

In summary, CBA analysis of serum cytokines revealed that GPI-CRM₁₉₇ did not induce an unspecific inflammatory response. Serum TNF- α and IFN- γ levels have been correlated with ECM and CM susceptibility. Interestingly, mice immunized with GPI-CRM₁₉₇ conjugate 5, that did not develop a significant increase in TNF- α *post* infection and also displayed a considerably lower level of serum IFN- γ , showed the highest survival rates amongst all vaccinated animals.

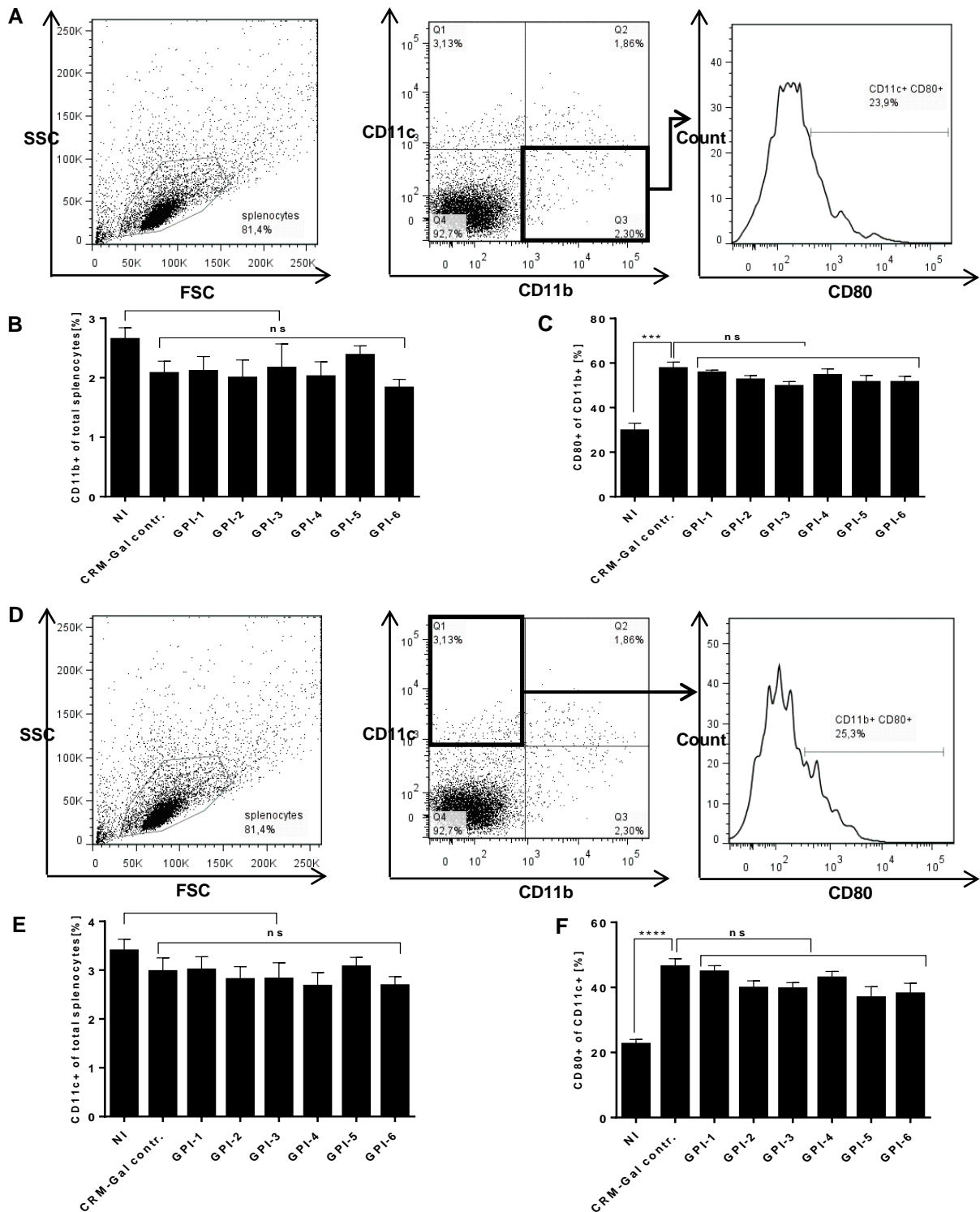


Figure 19: Macrophage and dendritic cell activation in immunized and *P. berghei* ANKA-challenged mice

(A, D) Representative gatings of activated macrophages (CD11b) and dendritic cells (CD11c). Spleen cells were isolated from immunized and *P. berghei* ANKA-infected mice on day 6 *post* infection and quantified by flow cytometry. (B, E) A non-significant decrease in relative numbers of macrophages and dendritic cells was observed in PbA-challenged mice. (C, F) Cellular activation (measured by activation marker CD80) was significantly increased in both macrophages and dendritic cells compared to non-infected controls upon PbA challenge. Only marginal differences in cellular activation were observed between immunized mice. Statistical significance was determined using Student's t-test, statistical significance is indicated by asterisks ***($p < 0.001$) and ****($p < 0.0001$).

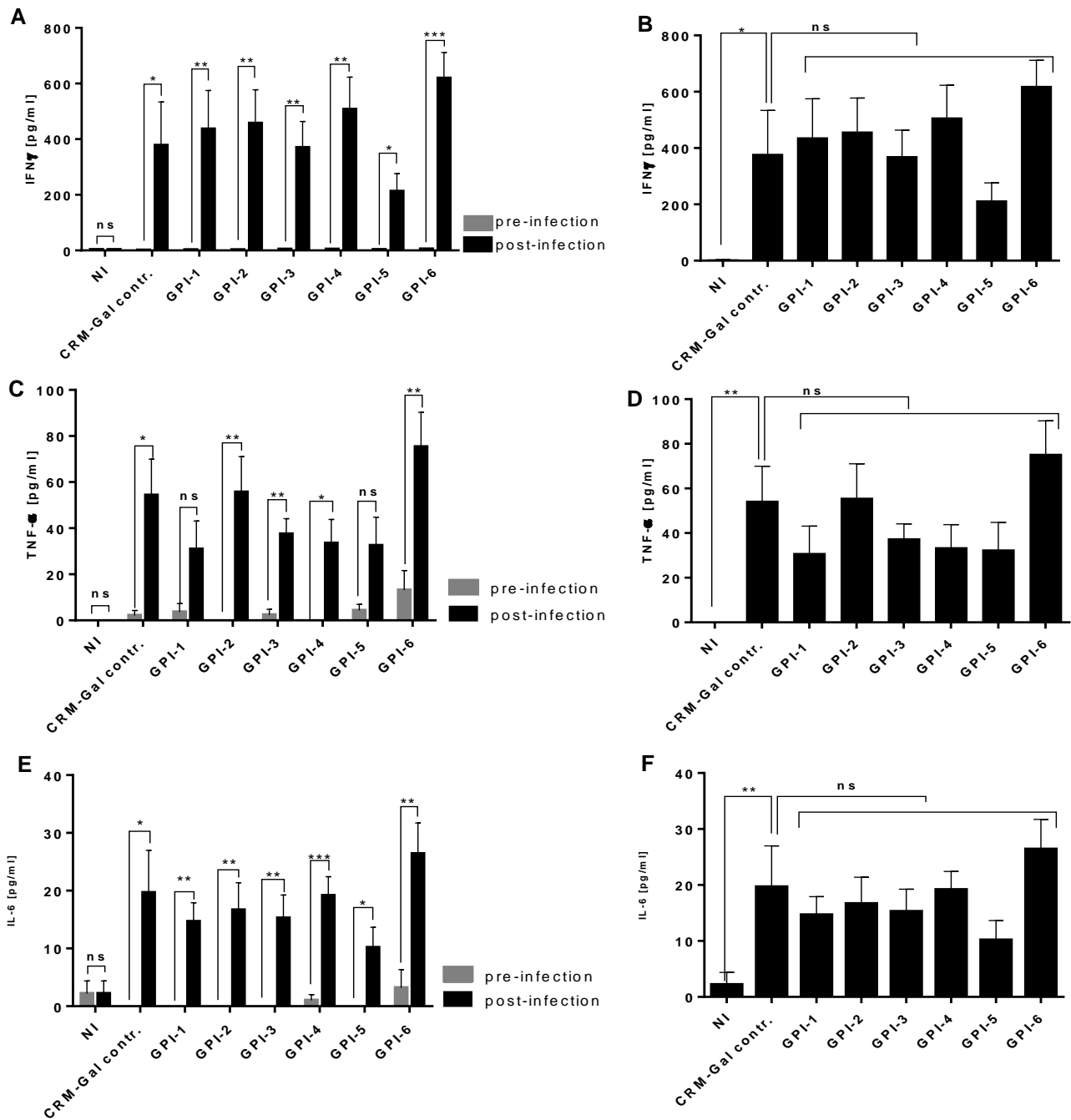


Figure 20: Pro-inflammatory cytokine level of PbA-infected mice varies between GPI-CRM₁₉₇ vaccinated mice but is consistently lower in GPI-CRM₁₉₇ compound 5 immunize mice

Serum cytokines were analyzed *pre* and *post* PbA infection (days 42 and 48) by cytometric bead array. (A, C, E) Prior to infection, GPI-CRM₁₉₇ conjugate 1-6 immunized and control mice displayed low or only background level of IFN- γ , TNF- α and IL-6, whereas upon infection, all PbA-challenged groups showed a significant increase in pro-inflammatory cytokine levels. No significant increase in serum TNF- α was seen in mice immunized with GPI-CRM₁₉₇ conjugate 1 and 5. (B, D, F) Serum levels of pro-inflammatory cytokines were significantly increased compared to non-infected mice, and varied between GPI-CRM₁₉₇ vaccinated mice. GPI-CRM₁₉₇ compound 6 showed consistently increased levels of IFN- γ , TNF- α and IL-6, whereas they were reduced for compound 5. Serum was taken from 5 mice per group. Data is shown as mean \pm SEM. Statistical significance was determined using Student's t-test, statistical significance is indicated by asterisks *($p < 0.05$), **($p < 0.01$), ***($p < 0.001$).

4.7 Brain CD8⁺ T cell sequestration

CD8⁺ T cell sequestration and subsequent accumulation of infected RBCs was ascribed a pivotal role in disease pathology in the murine model of cerebral malaria (see Fig. 21) (123, 124). To determine whether GPI-CRM₁₉₇ vaccination impacted CD8⁺ T cell sequestration, brain homogenates were stained for activated lymphocytes (CD45⁺ CD8⁺ CD62L^{low}) and measured by flow cytometry.

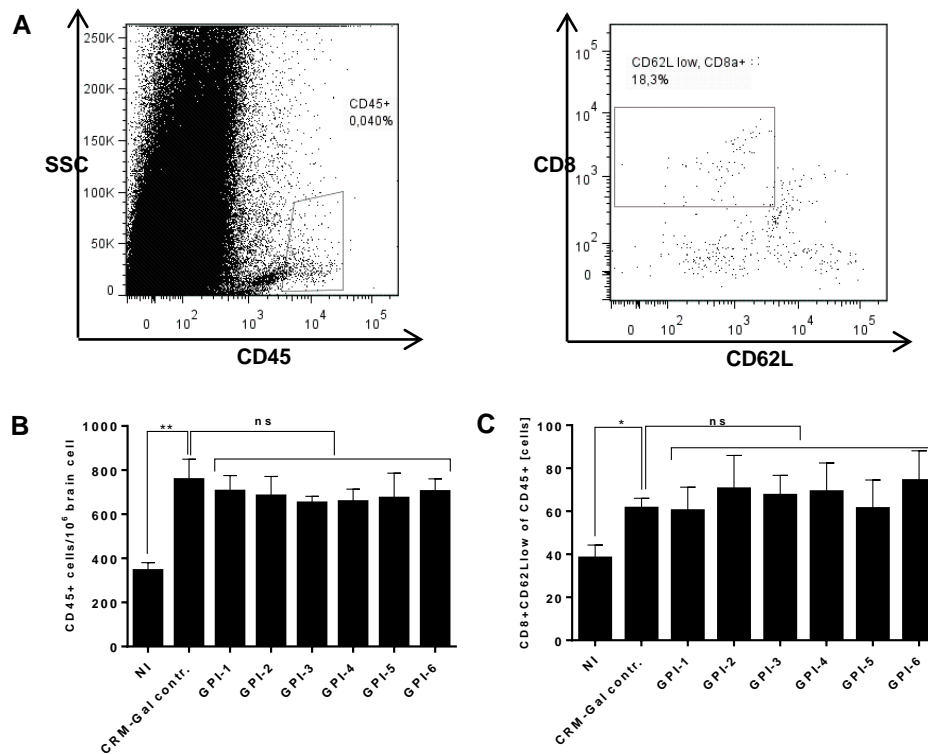


Figure 21: Brain CD8⁺ T cell sequestration

(A) Representative gating of brain homogenates from immunized and *P. berghei* ANKA-infected mice on day 6 *post* infection measuring activated CD8⁺ T cells by flow cytometry. In total, 1×10^6 events were recorded and gated on CD45^{hi} cells and CD62L^{low} CD8⁺ activated T cells. (B, C) Total numbers of CD45⁺ lymphocytes and activated CD62L^{low} CD8⁺ cytotoxic T cells significantly increased upon PbA infection of mice, but did not show any significant difference in challenged mice. Mice immunized with GPI-CRM₁₉₇ conjugate 5 displayed slightly lower level of CD8⁺ T cell sequestration compared to other GPI-CRM₁₉₇ immunized mice. Statistical significance was determined using Student's t-test, statistical significance is indicated by asterisks *($p < 0.05$) and **($p < 0.01$).

Total numbers of CD45⁺ lymphocytes and activated CD62L^{low} CD8⁺ cytotoxic T cells significantly increased upon PbA infection of mice, but did not show any significant difference in challenged mice (Fig. 21 B and C). The relatively similar level of CD8⁺ T cell sequestration might be a result of the early disease stage (pre-ECM), when neurological symptoms are still absent. Interestingly, mice immunized with GPI-CRM₁₉₇ conjugate 1 and 5 displayed slightly

lower levels of CD8⁺ T cell sequestration compared to other GPI-CRM₁₉₇ immunized mice. This observation might be partially explained by the protective potential of this conjugate vaccine and the lower serum cytokine response with respect to IFN- γ and TNF- α , both of which mediate CD8⁺ T cell sequestration (125).

5 Discussion

In this study, the efficacy and the mechanism of protection of an antitoxic GPI glycoconjugate vaccine was analyzed in the murine model of cerebral malaria. Despite more than 20 anti-malaria vaccines in the pipeline under current clinical investigation, the GPI antitoxic vaccine approach has not yet been investigated in detail nor has it undergone clinical trials (126). A first protective effect of a GPI glycoconjugate vaccine in ECM susceptible mice was demonstrated in 2002 (110). Based on *in vitro* studies, showing that *Plasmodium* GPI induces a pro-inflammatory signaling cascade that contributes to ECM pathogenesis, antitoxic GPI glycoconjugate vaccination was expected to protect from an overwhelming inflammatory response prohibiting ECM (40, 41, 74, 110). Unlike the extensively studied parasite subunit vaccines that are designed to prevent *Plasmodium* infection by inducing sterile immunity (liver stage vaccines), or by reducing parasitemia (blood stage vaccines), the GPI-antitoxic vaccine approach is thought to diminish the overwhelming immune response, thus preventing disease pathology (particularly with respect to cerebral malaria, severe malarial anemia and metabolic acidosis), but not impacting parasite development. This hypothesis is supported by various investigations concerning human anti-GPI antibody levels that correlate with resistance against CM developed in adolescence (111, 127, 128). Even more, anti-GPI antibodies were shown to be significantly reduced in patients with confirmed cerebral malaria (112). Additionally, *in vitro* studies verified that anti-GPI antibodies derived from individuals stemming from endemic regions suppressed GPI-induced activation of macrophages (129).

Within this thesis, the GPI glycoconjugate vaccine was adapted for the first time towards administration in humans. Synthetic GPII-6 was conjugated to the carrier protein CRM₁₉₇ and alum was used as adjuvant - both, carrier protein and adjuvant, being approved and widely applied in current vaccines. In a proof of concept study, GPI synthesized by Seeberger *et al.* was conjugated to KLH as carrier and Freund's adjuvant to enhance immunogenicity. Freund's adjuvant, a water-in-oil emulsion containing mycobacterium antigen (for Freund's Complete Adjuvant), is a highly efficacious immune-stimulator, however is not applicable in humans due to its toxicity. Further, Schofield *et al.* conjugated GPIs at ManIII to account for the presentation of protein-linked Man₄ GPIs, whereas the thiol linker was administered for conjugation at glucosamine or inositol of GPI structures in order to maintain the naturally occurring presentation in the cell membrane in this thesis. Besides that, six structurally distinct GPI glycans were synthesized to deepen our understanding of a structure-activity relationship (see Fig. 6). GPIs varied in length (Man₃ and Man₄) and addition of functional groups (PEthN and

PD). C57BL/6JRj mice were prime-vaccinated and twice boosted with GPI glycoconjugates **1-6** or CRM₁₉₇-Gal and finally challenged with 1×10^6 *P. berghei* ANKA-infected erythrocytes i.p. On day 6 *post* infection, (prior to onset of ECM), 5 mice per group were sacrificed for a coherent immunological characterization (spleen cell composition, brain T cell sequestration, vaccine-specific T cell re-stimulation). The remaining 10 mice per group were used for survival studies, to test vaccine efficacy.

Mice immunized with GPI**2**, **4**, **5** and **6** developed significantly increased anti-GPI antibody levels compared to control mice in this study. Only a non-significant increase was observed in titers against GPI**1** and GPI**3**, both glycans lacking functional phosphoethanolamine and inositol groups. Control mice succumbed to experimental cerebral malaria in 100% of cases by day 9, whereas all mice immunized with GPI-CRM₁₉₇ displayed an improved survival rate. In particular, GPI**5** vaccinated mice were significantly protected against PbA-induced encephalopathy, with 40% survival and a significantly improved clinical score. Immunological characterization of spleen cell population and serum cytokine levels did not reveal significant differences between GPI-CRM₁₉₇ vaccinated groups. However, distinct trends were observed with GPI**5** showing a decreased cellular activation and reduced level of serum cytokines (TNF- α , IFN- γ and IL-6).

With respect to the moderate protection from experimental cerebral malaria, more mice would be needed to refine the immunological outcomes of this study. Immunological results based on only 5 animals were unlikely to yield significant results with survival rates ranging between 10% and 40% (*i.e.* solely up to 2 mice per group). Further, investigating the immunological impact of GPI glycoconjugate vaccination in ECM-resistant mouse strains (*i.e.* BALB/c) or challenging with non-lethal or less virulent *Plasmodium* strains (*i.e.* *P. yoelii* 17NL, *P. chabaudi*) could reveal subtle differences that were not shown using lethal *P. berghei* ANKA in ECM-susceptible C57BL/6JRj mice. In general, having identified GPI**5** as the most protective glycoconjugate vaccine, desired methodological alterations should now include a dose-response relationship study, further structural optimizations of this GPI glycoconjugate and evaluation of different carrier proteins and adjuvant systems.

The results of this study will be discussed, put into context and compared to current literature in the following section.

5.1 Immunogenicity

Plasmodium parasites both synthesize and express Man₄-GPI that serve as protein anchors and free Man₃-GPI structures naturally occurring without protein attachment (130). Several studies suggest that *Plasmodium* GPIs contribute to CM pathogenesis by inducing an overwhelming pro-inflammatory response, and that malaria semi-immunity protecting from severe malaria conditions is partly explained by the formation of a robust anti-GPI antibody response in adulthood (6, 39-41, 71, 74, 108, 109, 111, 112, 127-129, 131). In this study, all GPI-CRM₁₉₇ conjugates were immunogenic, inducing varying degrees of antibody responses. Despite initial evidence that GPI-attached lipid moieties are necessary for GPI antibody recognition, synthetic GPIs lacking lipid moieties are also recognized by human antibodies (109, 128). In addition to Naik *et al.* (128), who stated that anti-GPI antibodies are mainly directed towards the conserved glycan structure of purified *Plasmodium* GPIs (Man₃) in humans, this study could further establish important structural correlations between GPI composition and epitope recognition in the murine model of cerebral malaria.

First, GPI glycoconjugates comprising only mannose and glucosamine (GPI1 and GPI3) were slightly immunogenic. Cross-reactivity revealed that the length of the mannose backbone is important for immune recognition. While solely Man₃ (GPI1) was not detected by antibodies, Man₄ GPI3 was more immunogenic and also detected by cross-reacting antibodies from mice immunized with GPI1. This is in line with previous findings on human anti-GPI antibody binding that did not recognize glycan fragments containing less than 5 carbohydrate units (109). Secondly, phosphoethanolamine was detected as an important immunogenic epitope in mice. Unlike in humans, where only a slight difference was seen in antibody response toward GPIs containing phosphoethanolamine and those that did not (109), a substantial differences between GPIs of similar composition with or without phosphoethanolamine was observed in this study (GPI1 vs. GPI2 and GPI3 vs. GPI4, Fig. 12). Interestingly, phosphoethanolamine bound to Man₃ GPIs (GPI2 and 5) led to a remarkable antibody response straight after prime-immunization (Fig. 8), which might be of interest for the rational design of potent glycoconjugate vaccines in the future. Finally, inositol was the immunodominant epitope when present in GPI5 and 6, which also has been described in literature before (71) (Fig. 12).

IgG subclass analysis further revealed unique findings for the most protective glycoconjugate vaccine in this study. Boutlis *et al.* previously described IgG₃ as the predominant immunoglobulin subclass against naturally occurring *Plasmodium* GPI (132). It was shown, that IgG₃ subclass is of major importance during acute phase *Plasmodium* infection and that after

parasite clearance, IgG₃ level decline and shift to IgG₁ in adults with naturally occurring CM resistance (132). In this study, IgG₃ subclass was highly abundant in mice immunized with GPI-CRM₁₉₇ conjugate **5**, but not in mice immunized with any other GPI glycoconjugate (shown in Fig. 10). As IgG₁ and IgG₃ share the highest affinity for Fc receptors on phagocytic cells, high titers of the respective IgG subclasses might have facilitated efficacious GPI clearance *post* infection. However, the reason for the sharp increase in IgG₃ for GPI-CRM₁₉₇ conjugate **5** needs to be further elucidated.

To improve our understanding of the effect of GPI conjugation to a carrier protein (*i.e.* the site of conjugation) and the respective spatial presentation of GPIs, immunogenicity studies of new glycoconjugates are essential. Hypothetically, conjugation to CRM₁₉₇ from glucosamine or phosphoinositol mimics natural GPI presentation in the cell wall, hence respective antibodies detect naturally occurring free Man₃ GPIs. On the contrary, conjugation as previously performed by Seeberger and Schofield *et al.* (2002) at ManIII might improve antibody affinity and avidity towards naturally occurring protein-linked Man₄ GPIs, as this glycoconjugate mimics the presentation of *Plasmodium* Man₄ GPI. Therefore, conjugating GPI**3**, **4** and **6** core structures at ManIII would be an essential next step in addressing this question. For further analysis of antibody-GPI binding kinetics, surface plasmon resonance (SPR) could help to characterize immunoglobulins induced by different synthetic GPI glycoconjugate vaccines. Opsonic phagocytosis assays of *Plasmodium* merozoites as recently performed by Faith *et al.* could additionally help to improve our understanding of the potential opsonic capacities induced by GPI glycoconjugate vaccines (133).

5.2 Immune cell modulation and cytokines

Key players involved in CM pathogenesis have been extensively studied and a role for lymphoid cells (CD8⁺ and CD4⁺ T cells) and myeloid cells (monocytes, dendritic cells), as well as pro-inflammatory cytokines (IL-1 β , IL6, IL-8, IL-12p70, TNF- α , IFN- γ) has been described (58, 121, 123, 125). Apart from long-term and specific humoral protection by plasma cells, protection from ECM pathology by GPI conjugate vaccination might also depend on cellular immunity (134). This mechanism might partially explain the protective potential of GPI conjugates that did not elicit a marked antibody response (*i.e.* GPI-CRM₁₉₇ conjugate **1** and **3**). T cell and APC populations in the spleen of immunized and PbA-challenged mice were therefore quantified by

flow cytometry. Serum cytokine levels were finally measured as a proxy for cellular activation by cytometric bead array.

Adoptive transfer studies recently revealed that INF- γ derived from CD4⁺ T cells can induce ECM pathology in usually resistant INF- γ ^{-/-} mice. Mechanistically, this is explained by INF- γ -induced upregulation of CXCL9 and CXCL10 that leads to CD8⁺ T cell migration to the brain (125). In further studies, the pathogenic role of CD8⁺ T cells in murine ECM was described, emphasizing the role of cell sequestration and cytotoxic response towards endothelial cells in PbA-infected mice (45, 56, 123). In the present thesis, mice immunized with GPI-CRM₁₉₇ conjugate **5** displayed slightly lower levels of activated CD4⁺ and CD8⁺ T cells (Fig. 17). This trend was also seen in mice immunized with less immunogenic GPI-CRM₁₉₇ conjugate **3** that still led to 22% improved survival of immunized mice compared to the CRM₁₉₇-Gal immunized control group. With respect to the role of T cells in the pathogenesis of cerebral malaria, those slight differences might have contributed to increased cerebral malaria resistance. Indeed, pro-inflammatory Th1 cytokine levels in the serum of immunized and PbA-challenged mice correlated with the aforementioned observations. To further elucidate this observation, intracellular cytokine staining of spleen T cells (such as IFN- γ) could clarify the decreased cellular activation in immunized vs. control mice. Adoptive transfer studies of T cells of immunized to non-immunized mice and subsequent challenge with PbA or non-lethal *Plasmodium* strains such as *P. yoelii* (17NL) could elucidate the role of vaccine-induced T cell suppression and cell-mediated protection.

The role of regulatory T cells (T_{reg}) in experimental cerebral malaria is paradoxical. T_{reg} cells regulate pro-inflammatory responses and limit tissue damage either directly by cell contact or indirectly through anti-inflammatory cytokines IL-10 and TGF- β (135, 136). IL-10 has been ascribed a protective role in the pathogenesis of ECM (137). However, Amante *et al.* showed that T_{reg}-depleted mice that were treated with an anti-CD25 monoclonal antibody showed reduced numbers of CD8⁺ T cells and sequestered parasites in the brain microvasculature. Effective parasite clearance and reduced numbers of sequestered parasites might explain these findings (116). In this study, the difference observed in regulatory T cell frequencies between GPI-CRM₁₉₇ immunized and control mice was marginal, with GPI-CRM₁₉₇ conjugate **3** and **5** displaying the lowest level of T_{regs}. However, this slight difference is unlikely to explain the protective potential of those glycoconjugates and a direct impact of glycoconjugate vaccination remains questionable.

Even though macrophages alone might not lead to cerebral pathology during malaria, as shown for instance by depletion studies of macrophages by Belnoue *et al.* (123), an important role has been ascribed to their downstream pro-inflammatory effects on cell activation and endothelial damage (121). In general, pRBC sequestration in the brain has been shown to attract macrophages that become arrested and lead to brain capillary obstruction (138). Macrophage activation *via* TLR and CD36 recognition of PAMPs mediates cytokine release (121). It was shown that subsequent release of platelet factor-4 and tissue factor leads to endothelial damage and blood coagulation in brain capillaries, contributing to cerebral pathology (139, 140). Dendritic cells have been assigned a critical role in ECM, with CD4⁺ priming, IFN- γ and granzyme B-expressing CD8⁺ T cells accumulation in brain microvasculature leading to disease pathogenesis (29, 141). Hypothetically, lower activation of macrophages and DCs might therefore contribute to decreased systemic release of TNF- α and IFN- γ through lower CD4⁺ T cell activation and subsequently less CD8⁺ T cell accumulation in the brain. However, in this study, mice immunized with GPI-CRM₁₉₇ conjugates showed only marginal differences of activated macrophages and DCs, which is unlikely to explain the improved survival of immunized mice.

In close correlation to activated lymphoid and myeloid cell populations, cytokine levels were shown to play a crucial role in the development of cerebral malaria in humans and mice (142). GPI-CRM₁₉₇ conjugate **5** was the compound that consistently led to reduced serum levels of IFN- γ , TNF- α and IL-6. As mentioned before, TNF- α and IFN- γ secreted by macrophages and Th1 cells, respectively, were shown to have a strong impact on ECM and CM severity.

Previous studies showed that mice treated with anti-IFN- γ monoclonal antibody, as well as IFN- γ ^{-/-} and IFN- γ receptor^{-/-} mice were protected from ECM (143-145). While IFN- γ is important for parasite clearance (*i.e.* priming of macrophages), its role in severe malaria and a protective potential of an IFN- γ receptor polymorphism was described in humans (146, 147). Anti-TNF- α antibodies were shown to prevent ECM development in mice, and a high serum level was associated with CM in humans (66, 148). No major role has been attributed to IL-6 in CM and ECM pathogenesis (149), however, IL-6 level has been shown to correlate with TNF- α (150). TNF- α and IL-6 can be induced by *Plasmodium* GPI through TLR signaling in macrophages and were reduced in TLR2, TLR4 and MyD88 knockout mice (39). Similarly, in this thesis, where the group of mice that showed the lowest level of IFN- γ and TNF- α also displayed lowest susceptibility to ECM (mice immunized with GPI-CRM₁₉₇ conjugate **5**). This finding might be explained by efficacious vaccine-induced antibody opsonization and clearance

of *Plasmodium* GPI with reduced TLR stimulation and decreased pro-inflammatory cytokine response. Opsonic phagocytosis assays and macrophage-based assays would be necessary however to confirm this hypothesis. *In vitro* macrophage-based assay as implemented by de Souza *et al.* could elucidate the role of macrophages in immunized and control mice. This group demonstrated that GPI-induced expression of both TNF- α and CD40 by macrophages was reduced upon GPI neutralization by anti-GPI IgG antibodies derived from malaria-exposed individuals (129). Finally, intracellular staining of IFN- γ and TNF- α would help to identify the cell populations responding to GPI glycoconjugate vaccination with decreased production of cytokines.

Taken together, these results suggest that protection from ECM by GPI-CRM₁₉₇ immunization might in part be explained by lower cellular activation and effector function of lymphoid and myeloid cell population. Whether GPI-CRM₁₉₇ induces a cellular immunity cannot be conclusively explained. As expected, IFN- γ , TNF- α and IL-6 cytokine levels in mice correlated with cellular activation of T cells, macrophages and DCs.

5.3 Brain CD8⁺ T cell sequestration

CD8⁺ T cell accumulation and sequestration in the brain contribute to CM and ECM pathogenesis. Howland *et al.* recently showed that *Plasmodium* antigens are cross-presented by endothelial cells, leading to an IFN- γ dependent cytotoxic response (45). Importantly, IFN- γ secreted by activated CD4⁺ T cells is necessary for CD8⁺ T cell migration to the brain (125). Previously, perforin and granzyme B expression have been described as a prerequisite for ECM induction by CD8⁺ cytotoxic T cells (56). In this study, total numbers of activated CD8⁺ T cells were only slightly decreased in GPI-CRM₁₉₇ conjugate **5** treated mice compared to other immunized mice. However, this difference might be explained in part by the lower serum cytokine response with respect to IFN- γ and TNF- α , that have been shown to mediate CD8⁺ T cell sequestration.

Methodologically, brain perfusion prior to homogenization and density gradient centrifugation with Percoll and Ficoll-Paque gradients to purify leukocytes as suggested by LaFrance-Corey (151) constitutes another possibility to quantify brain-sequestered T lymphocytes. Even though the method applied in this thesis is scientifically proven and frequently applied, following a different protocol might help to enhance the quality of sequestered cytotoxic T cells. The level of IFN- γ and granzyme B expression in CD8⁺-sequestered T cells in immunized mice by flow

cytometry would be another source of interest to assess a potential impact of antitoxic GPI vaccination. Further, immunohistochemical analysis of brain sections of immunized and PbA-challenged mice could help to verify results derived by flow cytometry. Brain histology as performed by Maglinao *et al.* (28) against sequestered leukocytes, endothelial activation and blood vessel hyalinization could additionally elucidate potential differences in ECM progression in immunized *versus* control mice.

5.4 GPI structure-activity relationship

With RTS,S (Mosquirix™) a start has been made towards malaria prevention and eradication in humans. However, efficacy of this vaccine needs to be improved, *exempli gratia* by multistage vaccination. Multistage vaccines have been successfully tested and might enhance protection and lower malaria transmission by merging antigens of different *Plasmodium* developmental stages within one vaccine formulation. For instance, combining conserved and immunogenic malarial pre-erythrocytic circumsporozoite protein (recombinant protein used in Mosquirix™) and GPI conjugated to recombinant MSP-1 or MSP-2 both highly abundant during blood stage infection, could therefore be envisioned in the future. Together, immunogenic protein-based vaccines combined with GPI carbohydrate-based vaccines might improve tolerance to parasite GPI during childhood and could additionally stop parasite replication and transmission.

In this thesis, mice immunized with Man₃ GPI-CRM₁₉₇ conjugate (GPI-CRM₁₉₇ conjugate **1**, **2** and **5**) showed higher resistance to ECM compared to their Man₄ counterparts (GPI-CRM₁₉₇ conjugate **3**, **4** and **6**). Whereas Man₄-GPIs anchor surface proteins in *P. falciparum* (MSP-1 and MSP-2), Man₃-GPIs exist protein-free (152) and are 4-5 times more abundant (71, 153). In this study, all synthetic GPI compounds were conjugated to carrier protein from glucosamine or phosphoinositol according to their orientation within the cell membrane.

Both the high abundance of free Man₃ GPI in *Plasmodium* and the naturally occurring presentation of synthetic GPI conjugated to CRM₁₉₇ from the bottom (glucosamine or phosphoinositol), might explain the higher protective potential of Man₃ GPI compounds compared to Man₄ GPI. Previously, mice immunized with Man₄-GPI-KLH were protected from cerebral pathology in ~80% of cases (110). However, a structurally related GPI conjugated from phosphoinositol in this thesis only protected mice in 20% of cases from ECM. This provides evidence for the first time that the site of conjugation, hence the structural representation in a vaccine of protein free Man₃ and protein bound Man₄ GPIs, might play an important role in

vaccine efficacy. Moderate protection of anti-toxic GPI glycoconjugate vaccines might also be explained by other parasite waste products that mediate disease pathology such as uric acid, hemozoin or other shizont micro particles (14, 154).

The results of this thesis confirm previous observations that a synthetic GPI glycoconjugate vaccine elicits a significant humoral antibody response in mice. Further, this study demonstrates that immunogenicity varies according to the composition of GPI structures. Mice immunized with GPI-CRM₁₉₇ conjugate **5** exhibited a slightly reduced activation of CD4⁺ and CD8⁺ T cells, macrophages and dendritic cells, which can be explained by a decreased expression of pro-inflammatory cytokines IFN- γ and TNF- α . Immunization with other GPI glycoconjugates did not lead to a coherent reduction in cellular or humoral immune response. Cytokine levels in fact might have influenced CD8⁺ T cell migration and accumulation in the brain, thereby reducing ECM occurrence. These observations very likely explain the improved survival rate of mice immunized with GPI-CRM₁₉₇ conjugate **5** in this study.

In summary, structural refinements combined with optimized vaccine formulation and a detailed immunological characterization would be needed for a definite mechanistic understanding of the protection provided by GPI conjugate vaccines. Taken together, these results encourage further research to eventually develop an antitoxic antimalarial vaccine.

6 Conclusion

In this study, it was shown for the first time that prime-boost-immunization with synthetic malaria GPI conjugated to the clinically approved carrier protein CRM₁₉₇ and administered with alum partially protects C57BL/6 mice from experimental cerebral malaria. This finding reinforces the notion that malaria GPI acts as a toxin, and that an antitoxic GPI glycoconjugate vaccine can reduce disease severity. From this study, it can be concluded that protection is in part dependent on humoral adaptive immunity (antibody levels) but also seems to evoke a cellular immune response that impacts ECM susceptibility. As a suggested mechanism of protection that needs to be experimentally elucidated, antibody-mediated opsonic phagocytosis *via* FcγR in immunized mice would lead to a reduction of systemic *Plasmodium* GPI and thus lower the pro-inflammatory response, with reduced severe malaria conditions such as cerebral malaria.

Indeed, GPI composition and site of conjugation need to be further investigated to improve our understanding of the mode of protection. In a previous study, a Man₄ GPI-KLH glycoconjugate vaccine was shown to be highly protective against ECM in the murine model of cerebral malaria. In that study, conjugation was established imitating spatial presentation of naturally occurring Man₄ GPIs, which might in part explain improved survival.

As expected, protection from cerebral pathology varied between GPI-CRM₁₉₇ glycoconjugates, and was highest for Man₃ GPI containing inositol and phosphoethanolamine at ManII (GPI5). The results of this thesis reveal for the first time a structure-activity relationship with regard to immunogenicity of GPI glycoconjugates. Further evidence with respect to the immunological response against *Plasmodium* GPI of immunized mice was generated and minor alterations in cellular activation of myeloid and lymphoid cells as well as the level of ECM inducing cytokines were shown. This is the first coherent immunological characterization of structurally different GPI-CRM₁₉₇ glycoconjugates in the murine model of cerebral malaria.

In conclusion, detailed studies in the murine model of cerebral malaria are necessary to improve the current understanding of GPI anti-toxic glycoconjugate vaccines. The correlation between GPI structure, site of conjugation and protection from cerebral pathology needs to be further elucidated to improve vaccine efficacy. If these steps are taken, a human antitoxic malaria GPI glycoconjugate vaccine may eventually become a reality.

7 Bibliography

1. Medzhitov R, Janeway C, Jr. Innate immunity. *The New England journal of medicine*. 2000;343(5):338-44.
2. Lacy P, Stow JL. Cytokine release from innate immune cells: association with diverse membrane trafficking pathways. *Blood*. 2011;118(1):9-18.
3. Litman GW, Rast JP, Fugmann SD. The origins of vertebrate adaptive immunity. *Nature reviews Immunology*. 2010;10(8):543-53.
4. Iwasaki A, Medzhitov R. Control of adaptive immunity by the innate immune system. *Nature immunology*. 2015;16(4):343-53.
5. Takeuchi O, Akira S. Pattern recognition receptors and inflammation. *Cell*. 2010;140(6):805-20.
6. Gowda DC. TLR-mediated cell signaling by malaria GPIs. *Trends in Parasitology*. 2007;23(12):596-604.
7. Verstak B, Nagpal K, Bottomley SP, Golenbock DT, Hertzog PJ, Mansell A. MyD88 adapter-like (Mal)/TIRAP interaction with TRAF6 is critical for TLR2- and TLR4-mediated NF-kappaB proinflammatory responses. *The Journal of biological chemistry*. 2009;284(36):24192-203.
8. Guermonprez P, Valladeau J, Zitvogel L, Thery C, Amigorena S. Antigen presentation and T cell stimulation by dendritic cells. *Annu Rev Immunol*. 2002;20:621-67.
9. Matzinger P. Tolerance, danger, and the extended family. *Annu Rev Immunol*. 1994;12:991-1045.
10. Haniffa M, Shin A, Bigley V, McGovern N, Teo P, See P, et al. Human tissues contain CD141hi cross-presenting dendritic cells with functional homology to mouse CD103+ nonlymphoid dendritic cells. *Immunity*. 2012;37(1):60-73.
11. Schlitzer A, McGovern N, Teo P, Zelante T, Atarashi K, Low D, et al. IRF4 transcription factor-dependent CD11b+ dendritic cells in human and mouse control mucosal IL-17 cytokine responses. *Immunity*. 2013;38(5):970-83.
12. Schofield L, Grau GE. Immunological processes in malaria pathogenesis. *Nature reviews Immunology*. 2005;5(9):722-35.
13. Detels R, Gulliford M, Karim QA, Tan CC. *Oxford Textbook of Global Public Health*. Oxford, UK: 'Oxford University Press'. 2015.
14. Gazzinelli RT, Kalantari P, Fitzgerald KA, Golenbock DT. Innate sensing of malaria parasites. *Nature reviews Immunology*. 2014;14(11):744-57.

15. Miller LH, Ackerman HC, Su XZ, Wellem TE. Malaria biology and disease pathogenesis: insights for new treatments. *Nature medicine*. 2013;19(2):156-67.
16. Miller LH, Baruch DI, Marsh K, Doumbo OK. The pathogenic basis of malaria. *Nature*. 2002;415(6872):673-9.
17. WHO. World Malaria Report 2013. 2013:284.
18. Murray CJ, Ortblad KF, Guinovart C, Lim SS, Wolock TM, Roberts DA, et al. Global, regional, and national incidence and mortality for HIV, tuberculosis, and malaria during 1990-2013: a systematic analysis for the Global Burden of Disease Study 2013. *Lancet*. 2014;384(9947):1005-70.
19. von Philipsborn P, Steinbeis F, Bender ME, Regmi S, Tinnemann P. Poverty-related and neglected diseases - an economic and epidemiological analysis of poverty relatedness and neglect in research and development. *Glob Health Action*. 2015;8:25818.
20. Langhorne J, Ndungu FM, Sponaas AM, Marsh K. Immunity to malaria: more questions than answers. *Nature immunology*. 2008;9(7):725-32.
21. Malaguarnera L, Musumeci S. The immune response to Plasmodium falciparum malaria. *Lancet Infect Dis*. 2002;2(8):472-8.
22. Stevenson MM, Riley EM. Innate immunity to malaria. *Nature reviews Immunology*. 2004;4(3):169-80.
23. Baird JK. Host age as a determinant of naturally acquired immunity to Plasmodium falciparum. *Parasitology today (Personal ed)*. 1995;11(3):105-11.
24. White NJ, Turner GD, Day NP, Dondorp AM. Lethal malaria: Marchiafava and Bignami were right. *J Infect Dis*. 2013;208(2):192-8.
25. Hendriksen IC, Mwanga-Amumpaire J, von Seidlein L, Mtove G, White LJ, Olaosebikan R, et al. Diagnosing severe falciparum malaria in parasitaemic African children: a prospective evaluation of plasma PfHRP2 measurement. *PLoS medicine*. 2012;9(8):e1001297.
26. Severe falciparum malaria. World Health Organization, Communicable Diseases Cluster. *Transactions of the Royal Society of Tropical Medicine and Hygiene*. 2000;94 Suppl 1:S1-90.
27. Severe Malaria. *Tropical Medicine & International Health*. 2014;19:7-131.
28. Maglinao M, Klopffleisch R, Seeberger PH, Lepenies B. The C-type lectin receptor DCIR is crucial for the development of experimental cerebral malaria. *Journal of immunology (Baltimore, Md : 1950)*. 2013;191(5):2551-9.

29. Piva L, Tetlak P, Claser C, Karjalainen K, Renia L, Ruedl C. Cutting edge: Clec9A+ dendritic cells mediate the development of experimental cerebral malaria. *Journal of immunology (Baltimore, Md : 1950)*. 2012;189(3):1128-32.
30. Perry JA, Rush A, Wilson RJ, Olver CS, Avery AC. Dendritic cells from malaria-infected mice are fully functional APC. *Journal of Immunology*. 2004;172(1):475-82.
31. Wilson NS, Behrens GM, Lundie RJ, Smith CM, Waithman J, Young L, et al. Systemic activation of dendritic cells by Toll-like receptor ligands or malaria infection impairs cross-presentation and antiviral immunity. *Nature immunology*. 2006;7(2):165-72.
32. Wykes MN, Good MF. What really happens to dendritic cells during malaria? *Nat Rev Microbiol*. 2008;6(11):864-70.
33. Riley EM, Stewart VA. Immune mechanisms in malaria: new insights in vaccine development. *Nature medicine*. 2013;19(2):168-78.
34. Teasdale G, Jennett B. Assessment of coma and impaired consciousness. A practical scale. *Lancet*. 1974;2(7872):81-4.
35. Reappraisal of known malaria resistance loci in a large multicenter study. *Nat Genet*. 2014;46(11):1197-204.
36. Birbeck GL, Molyneux ME, Kaplan PW, Seydel KB, Chimalizeni YF, Kawaza K, et al. Blantyre Malaria Project Epilepsy Study (BMPEs) of neurological outcomes in retinopathy-positive paediatric cerebral malaria survivors: a prospective cohort study. *Lancet Neurol*. 2010;9(12):1173-81.
37. Dondorp AM, Fanello CI, Hendriksen ICE, Gomes E, Seni A, Chhaganlal KD, et al. Artesunate versus quinine in the treatment of severe falciparum malaria in African children (AQUAMAT): an open-label, randomised trial. *The Lancet*. 376(9753):1647-57.
38. Liu L, Oza S, Hogan D, Perin J, Rudan I, Lawn JE, et al. Global, regional, and national causes of child mortality in 2000-13, with projections to inform post-2015 priorities: an updated systematic analysis. *Lancet*. 2015;385(9966):430-40.
39. Krishnegowda G, Hajjar AM, Zhu J, Douglass EJ, Uematsu S, Akira S, et al. Induction of proinflammatory responses in macrophages by the glycosylphosphatidylinositols of *Plasmodium falciparum*: cell signaling receptors, glycosylphosphatidylinositol (GPI) structural requirement, and regulation of GPI activity. *The Journal of biological chemistry*. 2005;280(9):8606-16.
40. Schofield L, Novakovic S, Gerold P, Schwarz RT, McConville MJ, Tachado SD. Glycosylphosphatidylinositol toxin of *Plasmodium* up-regulates intercellular adhesion molecule-1, vascular cell adhesion molecule-1, and E-selectin expression in vascular

- endothelial cells and increases leukocyte and parasite cytoadherence via tyrosine kinase-dependent signal transduction. *Journal of immunology* (Baltimore, Md : 1950). 1996;156(5):1886-96.
41. Tachado SD, Gerold P, McConville MJ, Baldwin T, Quilici D, Schwarz RT, et al. Glycosylphosphatidylinositol toxin of *Plasmodium* induces nitric oxide synthase expression in macrophages and vascular endothelial cells by a protein tyrosine kinase-dependent and protein kinase C-dependent signaling pathway. *Journal of immunology* (Baltimore, Md : 1950). 1996;156(5):1897-907.
 42. Zhu J, Krishnegowda G, Gowda DC. Induction of proinflammatory responses in macrophages by the glycosylphosphatidylinositols of *Plasmodium falciparum*: the requirement of extracellular signal-regulated kinase, p38, c-Jun N-terminal kinase and NF-kappaB pathways for the expression of proinflammatory cytokines and nitric oxide. *The Journal of biological chemistry*. 2005;280(9):8617-27.
 43. Storm J, Craig AG. Pathogenesis of Cerebral Malaria: a combination of inflammation and cytoadherence? *Frontiers in Cellular and Infection Microbiology*. 2014;4.
 44. Dorovini-Zis K, Schmidt K, Huynh H, Fu W, Whitten RO, Milner D, et al. The neuropathology of fatal cerebral malaria in malawian children. *The American journal of pathology*. 2011;178(5):2146-58.
 45. Howland SW, Poh CM, Renia L. Activated Brain Endothelial Cells Cross-Present Malaria Antigen. *PLoS Pathog*. 2015;11(6):e1004963.
 46. Turner GD, Morrison H, Jones M, Davis TM, Looareesuwan S, Buley ID, et al. An immunohistochemical study of the pathology of fatal malaria. Evidence for widespread endothelial activation and a potential role for intercellular adhesion molecule-1 in cerebral sequestration. *The American journal of pathology*. 1994;145(5):1057-69.
 47. Fried M, Duffy PE. Adherence of *Plasmodium falciparum* to chondroitin sulfate A in the human placenta. *Science*. 1996;272(5267):1502-4.
 48. Jenkins N, Wu Y, Chakravorty S, Kai O, Marsh K, Craig A. *Plasmodium falciparum* intercellular adhesion molecule-1-based cytoadherence-related signaling in human endothelial cells. *J Infect Dis*. 2007;196(2):321-7.
 49. Rogerson SJ, Tembenu R, Dobano C, Plitt S, Taylor TE, Molyneux ME. Cytoadherence characteristics of *Plasmodium falciparum*-infected erythrocytes from Malawian children with severe and uncomplicated malaria. *American Journal of Tropical Medicine and Hygiene*. 1999;61(3):467-72.

50. Treutiger CJ, Heddini A, Fernandez V, Muller WA, Wahlgren M. PECAM-1/CD31, an endothelial receptor for binding Plasmodium falciparum-infected erythrocytes. *Nature medicine*. 1997;3(12):1405-8.
51. Chakravorty SJ, Craig A. The role of ICAM-1 in Plasmodium falciparum cytoadherence. *Eur J Cell Biol*. 2005;84(1):15-27.
52. Newbold C, Craig A, Kyes S, Rowe A, Fernandez-Reyes D, Fagan T. Cytoadherence, pathogenesis and the infected red cell surface in Plasmodium falciparum. *International journal for parasitology*. 1999;29(6):927-37.
53. Ponsford MJ, Medana IM, Prapansilp P, Hien TT, Lee SJ, Dondorp AM, et al. Sequestration and Microvascular Congestion Are Associated With Coma in Human Cerebral Malaria. *Journal of Infectious Diseases*. 2012;205(4):663-71.
54. Seydel KB, Kampondeni SD, Valim C, Potchen MJ, Milner DA, Muwalo FW, et al. Brain swelling and death in children with cerebral malaria. *The New England journal of medicine*. 2015;372(12):1126-37.
55. Howland SW, Claser C, Poh CM, Gun SY, Renia L. Pathogenic CD8(+) T cells in experimental cerebral malaria. *Semin Immunopathol*. 2015;37(3):221-31.
56. Haque A, Best SE, Unosson K, Amante FH, de Labastida F, Anstey NM, et al. Granzyme B expression by CD8+ T cells is required for the development of experimental cerebral malaria. *Journal of immunology (Baltimore, Md : 1950)*. 2011;186(11):6148-56.
57. Riley EM. Is T-cell priming required for initiation of pathology in malaria infections? *Immunol Today*. 1999;20(5):228-33.
58. Lyke KE, Burges R, Cissoko Y, Sangare L, Dao M, Diarra I, et al. Serum Levels of the Proinflammatory Cytokines Interleukin-1 Beta (IL-1 β), IL-6, IL-8, IL-10, Tumor Necrosis Factor Alpha, and IL-12(p70) in Malian Children with Severe Plasmodium falciparum Malaria and Matched Uncomplicated Malaria or Healthy Controls. *Infection and immunity*. 2004;72(10):5630-7.
59. White NJ, Turner GDH, Medana IM, Dondorp AM, Day NPJ. The murine cerebral malaria phenomenon. *Trends in Parasitology*. 2010;26(1):11-5.
60. Medana IM, Chaudhri G, Chan-Ling T, Hunt NH. Central nervous system in cerebral malaria: 'Innocent bystander' or active participant in the induction of immunopathology? *Immunol Cell Biol*. 2001;79(2):101-20.
61. de Souza JB, Riley EM. Cerebral malaria: the contribution of studies in animal models to our understanding of immunopathogenesis. *Microbes and infection / Institut Pasteur*. 2002;4(3):291-300.

62. Favre N, Da Laperousaz C, Ryffel B, Weiss NA, Imhof BA, Rudin W, et al. Role of ICAM-1 (CD54) in the development of murine cerebral malaria. *Microbes and Infection*. 1999;1(12):961-8.
63. Good MF, Xu HJ, Wykes M, Engwerda CR. Development and regulation of cell-mediated immuneresponses to the blood stages of malaria: Implications for vaccine research. *Annu Rev Immunol*. 2005;23:69-99.
64. Li J, Chang WL, Sun G, Chen HL, Specian RD, Berney SM, et al. Intercellular adhesion molecule 1 is important for the development of severe experimental malaria but is not required for leukocyte adhesion in the brain. *J Invest Med*. 2003;51(3):128-40.
65. Finley RW, Mackey LJ, Lambert PH. Virulent P-Berghei Malaria - Prolonged Survival and Decreased Cerebral Pathology in Cell-Deficient Nude-Mice. *Journal of Immunology*. 1982;129(5):2213-8.
66. Grau GE, Fajardo LF, Piguet PF, Allet B, Lambert PH, Vassalli P. Tumor-Necrosis-Factor (Cachectin) as an Essential Mediator in Murine Cerebral Malaria. *Science*. 1987;237(4819):1210-2.
67. Grau GE, Heremans H, Piguet PF, Pointaire P, Lambert PH, Billiau A, et al. Monoclonal-Antibody against Interferon-Gamma Can Prevent Experimental Cerebral Malaria and Its Associated Overproduction of Tumor Necrosis Factor. *Proceedings of the National Academy of Sciences of the United States of America*. 1989;86(14):5572-4.
68. Hansen DS, Siomos MA, Buckingham L, Scalzo AA, Schofield L. Regulation of murine cerebral malaria pathogenesis by CD1d-restricted NKT cells and the natural killer complex. *Immunity*. 2003;18(3):391-402.
69. Debierre-Grockiego F. Glycolipids are potential targets for protozoan parasite diseases. *Trends in Parasitology*. 2010;26(8):404-11.
70. Gowda DC, Davidson EA. Protein glycosylation in the malaria parasite. *Parasitology today (Personal ed)*. 1999;15(4):147-52.
71. Naik RS, Branch OLH, Woods AS, Vijaykumar M, Perkins DJ, Nahlen BL, et al. Glycosylphosphatidylinositol Anchors of *Plasmodium falciparum*: Molecular Characterization and Naturally Elicited Antibody Response That May Provide Immunity to Malaria Pathogenesis. *The Journal of experimental medicine*. 2000;192(11):1563-76.
72. Kinoshita T, Fujita M, Maeda Y. Biosynthesis, remodelling and functions of mammalian GPI-anchored proteins: recent progress. *Journal of biochemistry*. 2008;144(3):287-94.

73. Tsai Y-H, Grube M, Seeberger PH, Varon Silva D, Varón Silva D. Glycosylphosphatidylinositols of protozoan parasites. *Trends in Glycoscience and Glycotechnology*. 2012;24(140):231 - 43.
74. Schofield L, Hackett F. Signal transduction in host cells by a glycosylphosphatidylinositol toxin of malaria parasites. *The Journal of experimental medicine*. 1993;177(1):145-53.
75. Khor CC, Chapman SJ, Vannberg FO, Dunne A, Murphy C, Ling EY, et al. A Mal functional variant is associated with protection against invasive pneumococcal disease, bacteremia, malaria and tuberculosis. *Nature Genetics*. 2007;39(4):523-8.
76. Mockenhaupt FP, Cramer JP, Hamann L, Stegemann MS, Eckert J, Oh NR, et al. Toll-like receptor (TLR) polymorphisms in African children: Common TLR-4 variants predispose to severe malaria. *Proceedings of the National Academy of Sciences of the United States of America*. 2006;103(1):177-82.
77. Mockenhaupt FP, Hamann L, von Gaertner C, Bedu-Addo G, von Kleinsorgen C, Schumann RR, et al. Common polymorphisms of Toll-like receptors 4 and 9 are associated with the clinical manifestation of malaria during pregnancy. *Journal of Infectious Diseases*. 2006;194(2):184-8.
78. Hilleman MR. Vaccines in historic evolution and perspective: a narrative of vaccine discoveries. *J Hum Virol*. 2000;3(2):63-76.
79. Pulendran B, Ahmed R. Immunological mechanisms of vaccination. *Nature immunology*. 2011;12(6):509-17.
80. Siegrist C-A. *Vaccine immunology*. Vaccines Saunders. 2008.
81. Rappuoli R, Mandl CW, Black S, De Gregorio E. Vaccines for the twenty-first century society. *Nature reviews Immunology*. 2011;11(12):865-72.
82. Marty-Roix R, Vladimer GI, Pouliot K, Weng D, Buglione-Corbett R, West K, et al. Identification of QS-21 as an Inflammasome-activating Molecular Component of Saponin Adjuvants. *The Journal of biological chemistry*. 2016;291(3):1123-36.
83. Avci FY, Li X, Tsuji M, Kasper DL. A mechanism for glycoconjugate vaccine activation of the adaptive immune system and its implications for vaccine design. *Nature medicine*. 2011;17(12):1602-9.
84. WHO. *Global Technical Strategy for Malaria 2016–2030*. 2015.
85. Partnership RBM. *Action and investment to defeat malaria 2016-2030*. 2015.
86. The mal ERACGoV. *A Research Agenda for Malaria Eradication: Vaccines*. *PLoS medicine*. 2011;8(1):e1000398.

87. Quinones ML, Norris DE, Conn JE, Moreno M, Burkot TR, Bugoro H, et al. Insecticide Resistance in Areas Under Investigation by the International Centers of Excellence for Malaria Research: A Challenge for Malaria Control and Elimination. *The American journal of tropical medicine and hygiene*. 2015;93(3 Suppl):69-78.
88. WHO U. *Malaria Medicines Landscape*. 2015.
89. Ashley EA, Dhorda M, Fairhurst RM, Amaratunga C, Lim P, Suon S, et al. Spread of artemisinin resistance in *Plasmodium falciparum* malaria. *The New England journal of medicine*. 2014;371(5):411-23.
90. Cui L, Mharakurwa S, Ndiaye D, Rathod PK, Rosenthal PJ. Antimalarial Drug Resistance: Literature Review and Activities and Findings of the ICEMR Network. *The American journal of tropical medicine and hygiene*. 2015;93(3 Suppl):57-68.
91. Efficacy and safety of the RTS,S/AS01 malaria vaccine during 18 months after vaccination: a phase 3 randomized, controlled trial in children and young infants at 11 African sites. *PLoS medicine*. 2014;11(7):e1001685.
92. Agnandji ST, Lell B, Soulanoudjingar SS, Fernandes JF, Abossolo BP, Conzelmann C, et al. First results of phase 3 trial of RTS,S/AS01 malaria vaccine in African children. *The New England journal of medicine*. 2011;365(20):1863-75.
93. Tinto H, D'Alessandro U, Sorgho H, Valea I, Tahita MC, Kabore W, et al. Efficacy and safety of RTS,S/AS01 malaria vaccine with or without a booster dose in infants and children in Africa: final results of a phase 3, individually randomised, controlled trial. *Lancet*. 2015;386(9988):31-45.
94. Wu Y, Ellis RD, Shaffer D, Fontes E, Malkin EM, Mahanty S, et al. Phase 1 trial of malaria transmission blocking vaccine candidates Pfs25 and Pvs25 formulated with montanide ISA 51. *PloS one*. 2008;3(7):e2636.
95. Hu J, Chen Z, Gu J, Wan M, Shen Q, Kieny MP, et al. Safety and immunogenicity of a malaria vaccine, *Plasmodium falciparum* AMA-1/MSP-1 chimeric protein formulated in montanide ISA 720 in healthy adults. *PloS one*. 2008;3(4):e1952.
96. Butler NS, Vaughan AM, Harty JT, Kappe SH. Whole parasite vaccination approaches for prevention of malaria infection. *Trends in immunology*. 2012;33(5):247-54.
97. Mueller AK, Labaied M, Kappe SH, Matuschewski K. Genetically modified *Plasmodium* parasites as a protective experimental malaria vaccine. *Nature*. 2005;433(7022):164-7.
98. Sheehy SH, Duncan CJ, Elias SC, Choudhary P, Biswas S, Halstead FD, et al. ChAd63-MVA-vectored blood-stage malaria vaccines targeting MSP1 and AMA1: assessment of

- efficacy against mosquito bite challenge in humans. *Molecular therapy : the journal of the American Society of Gene Therapy*. 2012;20(12):2355-68.
99. Olotu A, Fegan G, Wambua J, Nyangweso G, Awuondo KO, Leach A, et al. Four-Year Efficacy of RTS,S/AS01E and Its Interaction with Malaria Exposure. *New England Journal of Medicine*. 2013;368(12):1111-20.
 100. Neafsey DE, Juraska M, Bedford T, Benkeser D, Valim C, Griggs A, et al. Genetic Diversity and Protective Efficacy of the RTS,S/AS01 Malaria Vaccine. *New England Journal of Medicine*. 2015;373(21):2025-37.
 101. Heidelberger M, Avery OT. The soluble specific substance of pneumococcus. *Journal of Experimental Medicine*. 1923;38(1):0073-9.
 102. Hutter J, Lepenies B. Carbohydrate-Based Vaccines: An Overview. *Methods Mol Biol*. 2015;1331:1-10.
 103. Landsteiner K. Über heterogenetisches antigen und haptene XV Mitteilung über antigene. *Biochem Zeitschrift*. 1921 119:294–306.
 104. Adamo R, Nilo A, Castagner B, Boutureira O, Berti F, Bernardes GJL. Synthetically defined glycoprotein vaccines: current status and future directions. *Chemical Science*. 2013;4(8):2995-3008.
 105. Ada G, Isaacs D. Carbohydrate-protein conjugate vaccines. *Clin Microbiol Infect*. 2003;9(2):79-85.
 106. Verez-Bencomo V, Fernandez-Santana V, Hardy E, Toledo ME, Rodriguez MC, Heynngnezz L, et al. A synthetic conjugate polysaccharide vaccine against *Haemophilus influenzae* type b. *Science*. 2004;305(5683):522-5.
 107. Benaissa-Trouw B, Lefeber DJ, Kamerling JP, Vliegenthart JFG, Kraaijeveld K, Snippe H. Synthetic polysaccharide type 3-related di-, tri-, and tetrasaccharide-CRM197 conjugates induce protection against *Streptococcus pneumoniae* type 3 in mice. *Infection and immunity*. 2001;69(7):4698-701.
 108. Tamborrini M, Liu X, Mugasa JP, Kwon YU, Kamena F, Seeberger PH, et al. Synthetic glycosylphosphatidylinositol microarray reveals differential antibody levels and fine specificities in children with mild and severe malaria. *Bioorg Med Chem*. 2010;18(11):3747-52.
 109. Kamena F, Tamborrini M, Liu X, Kwon YU, Thompson F, Pluschke G, et al. Synthetic GPI array to study antitoxic malaria response. *Nat Chem Biol*. 2008;4(4):238-40.
 110. Schofield L, Hewitt MC, Evans K, Siomos MA, Seeberger PH. Synthetic GPI as a candidate anti-toxic vaccine in a model of malaria. *Nature*. 2002;418(6899):785-9.

111. Boutlis CS, Gowda DC, Naik RS, Maguire GP, Mgone CS, Bockarie MJ, et al. Antibodies to *Plasmodium falciparum* glycosylphosphatidylinositols: inverse association with tolerance of parasitemia in Papua New Guinean children and adults. *Infection and immunity*. 2002;70(9):5052-7.
112. Perraut R, Diatta B, Marrama L, Garraud O, Jambou R, Longacre S, et al. Differential antibody responses to *Plasmodium falciparum* glycosylphosphatidylinositol anchors in patients with cerebral and mild malaria. *Microbes and infection / Institut Pasteur*. 2005;7(4):682-7.
113. Crotti S, Zhai H, Zhou J, Allan M, Proietti D, Pansegrau W, et al. Defined conjugation of glycans to the lysines of CRM197 guided by their reactivity mapping. *Chembiochem : a European journal of chemical biology*. 2014;15(6):836-43.
114. Liu X, Kwon Y-U, Seeberger PH. Convergent Synthesis of a Fully Lipidated Glycosylphosphatidylinositol Anchor of *Plasmodium falciparum*. *Journal of the American Chemical Society*. 2005;127(14):5004-5.
115. Tsai Y-H, Götze S, Vilotijevic I, Grube M, Silva DV, Seeberger PH. A general and convergent synthesis of diverse glycosylphosphatidylinositol glycolipids. *Chemical Science*. 2013;4(1):468-81.
116. Amante FH, Stanley AC, Randall LM, Zhou Y, Haque A, McSweeney K, et al. A Role for Natural Regulatory T Cells in the Pathogenesis of Experimental Cerebral Malaria. *The American journal of pathology*. 2007;171(2):548-59.
117. Perlmutter RM, Hansburg D, Briles DE, Nicolotti RA, Davie JM. Subclass restriction of murine anti-carbohydrate antibodies. *Journal of immunology (Baltimore, Md : 1950)*. 1978;121(2):566-72.
118. Snapper CM, McIntyre TM, Mandler R, Pecanha LM, Finkelman FD, Lees A, et al. Induction of IgG3 secretion by interferon gamma: a model for T cell-independent class switching in response to T cell-independent type 2 antigens. *The Journal of experimental medicine*. 1992;175(5):1367-71.
119. Joosten SA, Ottenhoff TH. Human CD4 and CD8 regulatory T cells in infectious diseases and vaccination. *Hum Immunol*. 2008;69(11):760-70.
120. Shevach EM. CD4+ CD25+ suppressor T cells: more questions than answers. *Nature reviews Immunology*. 2002;2(6):389-400.
121. Chua CLL, Brown G, Hamilton JA, Rogerson S, Boeuf P. Monocytes and macrophages in malaria: protection or pathology? *Trends in Parasitology*. 2013;29(1):26-34.

122. Wykes MN, Good MF. OPINION What really happens to dendritic cells during malaria? *Nat Rev Microbiol.* 2008;6(11):864-70.
123. Belnoue E, Kayibanda M, Vigario AM, Deschemin JC, van Rooijen N, Viguiet M, et al. On the pathogenic role of brain-sequestered alpha beta CD8(+) T cells in experimental cerebral malarial. *Journal of Immunology.* 2002;169(11):6369-75.
124. Claser C, Malleret B, Gun SY, Wong AYW, Chang ZW, Teo P, et al. CD8(+) T Cells and IFN-gamma Mediate the Time-Dependent Accumulation of Infected Red Blood Cells in Deep Organs during Experimental Cerebral Malaria. *PloS one.* 2011;6(4).
125. Villegas-Mendez A, Greig R, Shaw TN, de Souza JB, Findlay EG, Stumhofer JS, et al. IFN-gamma-Producing CD4(+) T Cells Promote Experimental Cerebral Malaria by Modulating CD8(+) T Cell Accumulation within the Brain. *Journal of Immunology.* 2012;189(2):968-79.
126. WHO Tables of malaria vaccine projects globally: "The Rainbow Tables" [Internet]. 2015. Available from: http://www.who.int/immunization/research/development/Rainbow_tables/en/.
127. de Souza JB, Todd J, Krishegowda G, Gowda DC, Kwiatkowski D, Riley EM. Prevalence and boosting of antibodies to Plasmodium falciparum glycosylphosphatidylinositols and evaluation of their association with protection from mild and severe clinical malaria. *Infection and immunity.* 2002;70(9):5045-51.
128. Naik RS, Krishnegowda G, Ockenhouse CF, Gowda DC. Naturally Elicited Antibodies to Glycosylphosphatidylinositols (GPIs) of Plasmodium falciparum Require Intact GPI Structures for Binding and Are Directed Primarily against the Conserved Glycan Moiety. *Infection and immunity.* 2006;74(2):1412-5.
129. de Souza JB, Runglall M, Corran PH, Okell LC, Kumar S, Gowda DC, et al. Neutralization of malaria glycosylphosphatidylinositol in vitro by serum IgG from malaria-exposed individuals. *Infection and immunity.* 2010;78(9):3920-9.
130. Gerold P, Dieckmannschuppert A, Schwarz RT. Glycosylphosphatidylinositols Synthesized by Asexual Erythrocytic Stages of the Malarial Parasite, Plasmodium-Falciparum - Candidates for Plasmodial Glycosylphosphatidylinositol Membrane Anchor Precursors and Pathogenicity Factors. *Journal of Biological Chemistry.* 1994;269(4):2597-606.
131. Brattig NW, Kowalsky K, Liu X, Burchard GD, Kamena F, Seeberger PH. Plasmodium falciparum glycosylphosphatidylinositol toxin interacts with the membrane of non-

- parasitized red blood cells: a putative mechanism contributing to malaria anemia. *Microbes and Infection*. 2008;10(8):885-91.
132. Boutlis CS, Fagan PK, Gowda DC, Lagog M, Mgone CS, Bockarie MJ, et al. Immunoglobulin G (IgG) Responses to Plasmodium falciparum Glycosylphosphatidylinositols Are Short-Lived and Predominantly of the IgG3 Subclass. *Journal of Infectious Diseases*. 2003;187(5):862-5.
 133. Osier FH, Feng G, Boyle MJ, Langer C, Zhou J, Richards JS, et al. Opsonic phagocytosis of Plasmodium falciparum merozoites: mechanism in human immunity and a correlate of protection against malaria. *BMC medicine*. 2014;12(1):1-15.
 134. Seder RA, Hill AVS. Vaccines against intracellular infections requiring cellular immunity. *Nature*. 2000;406(6797):793-8.
 135. Joosten SA, Ottenhoff TH. Human CD4 and CD8 regulatory T cells in infectious diseases and vaccination. *Human immunology*. 2008;69(11):760-70.
 136. Mills KHG. Regulatory T cells: Friend or foe in immunity to infection? *Nature Reviews Immunology*. 2004;4(11):841-55.
 137. Kossodo S, Monso C, Juillard P, Velu T, Goldman M, Grau GE. Interleukin-10 modulates susceptibility in experimental cerebral malaria. *Immunology*. 1997;91(4):536-40.
 138. Dorovini-Zis K, Schmidt K, Huynh H, Fu WJ, Whitten RO, Milner D, et al. The Neuropathology of Fatal Cerebral Malaria in Malawian Children. *American Journal of Pathology*. 2011;178(5):2146-58.
 139. Francischetti IMB. Does activation of the blood coagulation cascade have a role in malaria pathogenesis? *Trends in Parasitology*. 2008;24(6):258-63.
 140. Srivastava K, Field DJ, Aggrey A, Yamakuchi M, Morrell CN. Platelet Factor 4 Regulation of Monocyte KLF4 in Experimental Cerebral Malaria. *PloS one*. 2010;5(5).
 141. deWalick S, Amante FH, McSweeney KA, Randall LM, Stanley AC, Haque A, et al. Cutting edge: conventional dendritic cells are the critical APC required for the induction of experimental cerebral malaria. *Journal of immunology (Baltimore, Md : 1950)*. 2007;178(10):6033-7.
 142. Hunt NH, Grau GE. Cytokines: accelerators and brakes in the pathogenesis of cerebral malaria. *Trends in immunology*. 2003;24(9):491-9.
 143. Amani V, Vigarario AM, Belnoue E, Marussig M, Fonseca L, Mazier D, et al. Involvement of IFN-gamma receptor-mediated signaling in pathology and anti-malarial immunity induced by Plasmodium berghei infection. *European journal of immunology*. 2000;30(6):1646-55.

144. Grau GE, Heremans H, Piguet P-F, Pointaire P, Lambert P-H, Billiau A, et al. Monoclonal antibody against interferon gamma can prevent experimental cerebral malaria and its associated overproduction of tumor necrosis factor. *Proceedings of the National Academy of Sciences*. 1989;86(14):5572-4.
145. Yanez DM, Manning DD, Cooley AJ, Weidanz WP, van der Heyde HC. Participation of lymphocyte subpopulations in the pathogenesis of experimental murine cerebral malaria. *Journal of immunology (Baltimore, Md : 1950)*. 1996;157(4):1620-4.
146. Koch O, Awomoyi A, Usen S, Jallow M, Richardson A, Hull J, et al. IFNGR1 gene promoter polymorphisms and susceptibility to cerebral malaria. *Journal of Infectious Diseases*. 2002;185(11):1684-7.
147. Ringwald P, Peyron F, Vuillez JP, Touze JE, Lebras J, Deloron P. Levels of Cytokines in Plasma during Plasmodium-Falciparum Malaria Attacks. *J Clin Microbiol*. 1991;29(9):2076-8.
148. Grau GE, Taylor TE, Molyneux ME, Wirima JJ, Vassalli P, Hommel M, et al. Tumor Necrosis Factor and Disease Severity in Children with Falciparum-Malaria. *New England Journal of Medicine*. 1989;320(24):1586-91.
149. Grau GE, Frei K, Piguet P-F, Fontana A, Heremans H, Billiau A, et al. Interleukin 6 production in experimental cerebral malaria: modulation by anticytokine antibodies and possible role in hypergammaglobulinemia. *The Journal of experimental medicine*. 1990;172(5):1505-8.
150. Urquhart AD. Putative Pathophysiological Interactions of Cytokines and Phagocytic Cells in Severe Human Falciparum Malaria. *Clinical Infectious Diseases*. 1994;19(1):117-31.
151. LaFrance-Corey RG, Howe CL. Isolation of brain-infiltrating leukocytes. *Journal of visualized experiments : JoVE*. 2011(52).
152. Gerold P, Dieckmann-Schuppert A, Schwarz RT. Glycosylphosphatidylinositols synthesized by asexual erythrocytic stages of the malarial parasite, Plasmodium falciparum. Candidates for plasmodial glycosylphosphatidylinositol membrane anchor precursors and pathogenicity factors. *The Journal of biological chemistry*. 1994;269(4):2597-606.
153. Singh N, Liang LN, Tykocinski ML, Tartakoff AM. A novel class of cell surface glycolipids of mammalian cells. Free glycosyl phosphatidylinositols. *The Journal of biological chemistry*. 1996;271(22):12879-84.
154. Neumann K, Ruland J. Immune sensing by activating and inhibitory C-type lectin receptors. *LaboratoriumsMedizin*. 2014;291.

Curriculum vitae

Declaration of academic honesty

Eidesstattliche Versicherung

„Ich, Fridolin Steinbeis, versichere an Eides statt durch meine eigenhändige Unterschrift, dass ich die vorgelegte Dissertation mit dem Thema: „Protective potential and immunological evaluation of synthetic *Plasmodium* GPI glycoconjugate vaccines against experimental cerebral malaria“ selbstständig und ohne nicht offengelegte Hilfe Dritter verfasst und keine anderen als die angegebenen Quellen und Hilfsmittel genutzt habe.

Alle Stellen, die wörtlich oder dem Sinne nach auf Publikationen oder Vorträgen anderer Autoren beruhen, sind als solche in korrekter Zitierung (siehe „Uniform Requirements for Manuscripts (URM)“ des ICMJE -www.icmje.org) kenntlich gemacht. Die Abschnitte zu Methodik (insbesondere praktische Arbeiten, Laborbestimmungen, statistische Aufarbeitung) und Resultaten (insbesondere Abbildungen, Graphiken und Tabellen) entsprechen den URM (s.o) und werden von mir verantwortet.

Meine Anteile an etwaigen Publikationen zu dieser Dissertation entsprechen denen, die in der untenstehenden gemeinsamen Erklärung mit dem/der Betreuer/in, angegeben sind. Sämtliche Publikationen, die aus dieser Dissertation hervorgegangen sind und bei denen ich Autor bin, entsprechen den URM (s.o) und werden von mir verantwortet.

Die Bedeutung dieser eidesstattlichen Versicherung und die strafrechtlichen Folgen einer unwahren eidesstattlichen Versicherung (§156,161 des Strafgesetzbuches) sind mir bekannt und bewusst.“

Berlin, 30.06.2016